APPLIED TECHNOLOGIES OF FMCW RADIO ALTIMETERS FOR NEXT-GENERATION AVIATION AND AUTOMOTIVE SYSTEMS

Pavol Kurdel - Marek Češkovič - Anton Panda

RAM-Verlag
2026

Title:

Applied Technologies of FMCW Radio Altimeters for Next-Generation Aviation and Automotive Systems

Authors:

prof. Ing. Pavol Kurdel, PhD.

assoc. prof. Ing. Marek Češkovič, PhD.

Dr.h.c. prof. Ing. Anton Panda, PhD.

Reviewers:

prof. Ing. František Adamčík, CSc.

assoc. prof. Ing. Raul Mateos Gil, PhD.

prof. Ing. Sergii Boichenko, DrSc.

prof. Dr. Hab. Dr.h.c. inž. Tadeusz Zaborowski

Publisher:

©RAM-Verlag

Stüttinghauser Ringstr. 44

58515 Lüdenscheid

Germany

Mail: RAM-Verlag@t-online.de

Website: https://www.ram-verlag.eu

ISBN 978-3-96595-057-3

Abstract

The field of Frequency Modulated Continuous Wave (FMCW) radar represents a significant area of modern intelligent transportation systems. Owing to their ability to simultaneously determine the distance and relative velocity of objects through the exploitation of the Doppler effect, FMCW radars have found widespread application, particularly in automotive Advanced Driver Assistance Systems (ADAS) and autonomous driving technologies. Building upon these technological advances, the presented monograph extends their application to aviation by investigating the use of onboard FMCW radio altimeters as cost-effective terrain collision avoidance systems for small aircraft and helicopters. The monograph provides a comprehensive theoretical and experimental analysis of the Doppler component contained in the beat signal for predicting the time to terrain collision, experimentally validates the proposed concepts under real flight conditions, and introduces novel methods for improving measurement accuracy. The proposed solutions extend the functionality of existing radio altimeters by incorporating active Controlled Flight Into Terrain (CFIT) warning capabilities without the need for expensive onboard terrain awareness systems, thereby contributing significantly to the enhancement of flight safety.

Keywords:

FMCW radio altimeter, Doppler effect, Terrain collision avoidance, Controlled Flight into Terrain (CFIT), Helicopter flight safety, Radio altimeter signal processing, Mathematical modelling, Terrain awareness, Low-altitude helicopter operations

Vote of thanks:

The authors express their sincere gratitude to the reviewers for their valuable comments and constructive suggestions, whose substantive and formal observations significantly improved the overall quality of this monograph.

CONTENTS

Preface

The presented monograph aims to address the need for cost-effective terrain collision avoidance systems for small aircraft and helicopters. The rapid advancement of aviation technology and the increasing volume of air traffic have highlighted the necessity for affordable anti-collision systems for these aircraft, which are not required by current regulations to be equipped with complex systems such as TCAS/ACAS or EGPWS. Building upon the monograph Applied Technologies for the Use of FMCW Radio Altimeter, this work explores the possibilities of extending the functionality of onboard low-range frequency-modulated continuous wave (FMCW) radio altimeters to create simple terrain collision avoidance and warning systems. The monograph provides a comprehensive theoretical and experimental analysis of FMCW altimeter operation, with a special focus on utilizing the Doppler component in the difference frequency signal. Through mathematical modeling, error analysis, and stabilization of the altimeter constant, the authors demonstrate that the existing altimeter hardware can be effectively used not only for precise altitude measurement but also for predicting the time to potential collision with rising terrain. The monograph experimentally verifies the Doppler effect during flights over ascending terrain, presents dual-channel altimeter configurations, and introduces a patented measurement method using a depolarization plate, which significantly improves the resolution of methodological errors. It proposes supplementary solutions based on the research, which generate timely warnings of approaching terrain based on the ratio of altitude to vertical velocity, and integrates altimeter outputs with aircraft dynamic models to enhance the crew's situational awareness. The proposed solutions offer a practical and economically accessible way to improve flight safety for small aircraft and helicopters, particularly in operations where expensive advanced systems are not available. They may also help reduce the risk of controlled flight into terrain (CFIT).

LIST OF USED SYMBOLS AND ABBREVIATIONS

a	- terrain approach angle
c	- propagation speed of light (electromagnetic waves)
Δf	- frequency deviation
Δh	- absolute height measurement error
ΔH	- methodological error of the frequency method
ΔHS	- measurement error due to aircraft pitch or bank angle
ΔU	- error signal voltage
S0	- elementary reflecting surface of the Earth's surface
ρ	- random error
f_v	- frequency of the transmitted signal
f_0	- mean value of the carrier signal frequency
f_p	- instantaneous frequency of the received signal
f_M	- modulation frequency
f_D	- Doppler frequency
f_{rD}	- difference frequency including the Doppler effect
f_r	- difference frequency
f_{r0}	- difference frequency corresponding to the oblique (slant) distance
φ(t)	- phase of the low-frequency difference signal
φ_0	- initial phase of the difference signal
φ_M	- variable phase of the difference signal,
G_0	- energy spectrum of the signal reflected from an elementary surface
G	- energy spectrum of the composite (summary) signal
γ	- aircraft bank angle
H	- flight altitude
H_{abs}	- absolute height
H_{et}	- standard (reference) height
H_m	- flight altitude measurement result
H_{min}	- minimum measured flight altitude

H_n	- measured altitude during aircraft pitch or roll
H_{rel}	- relative height
H_a	- actual (true) flight altitude
IPS	- direct signal current
iC	- mean value of the integrating capacitor current
C	- radio altimeter constant
λ	- wavelength
ν	- systematic error
RA	- radio altimeter
T_M	- modulation frequency period
T_i	- measured part of the modulation frequency period
τ	- time delay of the reflected signal
τ_{ref}	- time delay of the reference coaxial line
U_{ref}	- reference voltage
U_v	- amplitude of the transmitted signal
U_p	- amplitude of the received signal
U_{dif}	- voltage proportional to the difference frequency
U_f	- difference frequency signal
ξ	- coaxial cable shortening (velocity) factor
ζ	- relative height measurement error
FMCW	- Frequency Modulated Continuous Wave
HAGL	- Height Above Ground Level
ACAS	- Airborne Collision Avoidance System
TCAS	- Traffic Collision Avoidance System
TAWS	- Terrain Awareness and Warning System
EGPWS	- Enhanced Ground Proximity Warning System
GPWS	- Ground Proximity Warning System
CFIT	- Controlled Flight Into Terrain
ADS-B	- Automatic Dependent Surveillance–Broadcast
UAS	- Unmanned Aerial System
UAV	- Unmanned Aerial Vehicle

EASA	- European Union Aviation Safety Agency
FAA	- Federal Aviation Administration
ICAO	- International Civil Aviation Organization
VFR	- Visual Flight Rules
IFR	- Instrument Flight Rules
GPS	- Global Positioning System
FFT	- Fast Fourier Transform
DAQ	- Data Acquisition
AFCS	- Automatic Flight Control System
AGL	- Above Ground Level
QNH	- altimeter setting to indicate altitude above mean sea level
QFE	- altimeter setting to indicate altitude above a specified datum
RWY	- runway
FDR	- Flight Data Recorder
HEMS	- Helicopter Emergency Medical Service
CTR	- Control Zone

1 INTRODUCTION

The rapid development of aviation and rocket technology continuously imposes increasingly demanding requirements on control and navigation systems. Modern systems must deliver a high degree of autonomy, accuracy at the meter level, reliability, and fault tolerance. Key components include autonomous radio-technical sensors that measure essential motion parameters such as true altitude above terrain (Height Above Terrain), vertical speed, true airspeed, drift angle, and distance traveled. Accurate measurement of true altitude above the ground has been critical since the early days of aviation, particularly for safe flights in mountainous and hilly terrain and during landing maneuvers. Historical development progressed from optical methods (dependent on visibility and weather) and acoustic methods (limited by the speed of sound) to electrical principles. While capacitive methods remained largely theoretical, early pulse-based radio altimeters faced technological barriers in generating nanosecond pulses. Phase-based methods proved too complex for practical deployment at the time. Contemporary avionics employs a wide range of physical principles for altitude measurement and terrain collision protection:

- Radiometric and laser methods (RADAR, LIDAR) – based on measuring the propagation time of electromagnetic waves.
- Barometric systems – measurement of static air pressure.
- Inertial systems (IMU) – double integration of vertical acceleration using accelerometers and gyroscopes.
- Specialized methods such as radioisotope or corona discharge techniques (used in specific historical applications).

The current trend in avionics is toward multi-sensor fusion, integrating data from multiple sources (radar, GPS, IMU, and digital terrain databases) to eliminate the weaknesses of individual methods. This approach is particularly important for small aircraft and helicopters, where legislation (e.g., FAA/EASA) has not strictly required advanced TAWS/EGPWS systems until recently. However, increasing air traffic density and accident statistics now demand their adoption.

Significant examples of technologies combining two principles include:

1. Radar-Inertial Fusion in Terrain Awareness and Warning Systems (TAWS/EGPWS). Modern systems (e.g., Honeywell) combine data from radio altimeters (direct measurement above the terrain) with inertial measurement units (IMU) and GPS. While the radio altimeter provides precise instantaneous height, the inertial system enables trajectory prediction and filters out noise caused by terrain irregularities.
2. Dual-principle signal processing in low-altitude radio altimeters (FMCW + Doppler). This monograph focuses on utilizing aircraft radio altimeters not only as distance-measuring devices but also as active collision-avoidance elements. It employs Frequency Modulated Continuous Wave (FMCW) for altitude measurement and exploits the Doppler shift present in the beat frequency to provide immediate information about the rate of closure to obstacles. This transforms a passive sensor into an active warning system. The growth in air traffic volume requires the introduction of collision-avoidance systems even into categories of aircraft and helicopters where they were not previously mandatory. This monograph analyzes and classifies existing warning and anti-collision systems and proposes operating modes optimized for the specific flight characteristics of helicopters. The main contribution lies in exploring practical applications of available technologies—specifically, using a radio altimeter as a simple yet effective collision-avoidance system. By utilizing the Doppler component in the radio altimeter signal, early detection of dangerous proximity to the ground or obstacles can be achieved. This is critical for safe operations at low altitudes and during search-and-rescue missions.

Flights into mountainous and hilly areas rank among the highest-risk operations in aviation. Even with a fully functional aircraft and pilot in control, unintentional collision with terrain (CFIT) can occur, historically causing thousands of fatalities. CFIT accidents frequently happen in conditions of reduced visibility (IMC), at night, or during approach and departure, when pilots underestimate rising terrain or misinterpret barometric altitude readings. Helicopters and general aviation aircraft engaged in search-and-rescue, firefighting, or VFR flights in mountainous regions face elevated risk due to low flight levels, turbulence, and rapidly changing terrain, where traditional barometric altimeters are often insufficient. Statistics show that the introduction of GPWS in 1974 and later TAWS/EGPWS dramatically reduced CFIT accidents in commercial air transport (nearly eliminating them among large jets in the USA). However, in general aviation and helicopter operations, CFIT still accounts for a significant proportion of fatal accidents. Key contributing factors include loss of situational awareness, incorrect altimeter settings, pilot fatigue, and the absence of look-ahead terrain warning functions in older systems. These highlight the need for Doppler-based detection and multi-sensor fusion even in smaller aircraft.

2 THEORETICAL FOUNDATIONS AND OPERATING PRINCIPLES OF RADIO ALTIMETERS

The flight altitude is currently determined by evaluating various physical phenomena in which altitude is related to measurable physical parameters. The following methods of measuring flight altitude are known [39]:

- ***Radio and laser*** methods based on measuring the propagation time of electromagnetic waves between the aircraft and the ground,
- ***Radioisotope system***, which measures the intensity of backscattered radioactive particles,
- ***Barometric system*** measuring atmospheric pressure using a membranous aneroid box,
- ***Stratospheric system*** measuring the dependence of corona discharge current on air density,
- ***Inertial accelerometer*** mounted on a gyrostabilized platform of the inertial system; it evaluates vertical acceleration with subsequent double integration.

Radio, laser, and radioisotope methods of altitude measurement are based on active sensing of the Earth’s surface. In other methods, energy is not radiated, i.e. they can be considered autonomous. Radio height measurement is currently used not only for measuring the altitude of aircraft, but also in other applications. For example, radio altimeters are used for:

- cartographic representation of the Earth's surface (GEOS-C, USA),
- soft landing of space probes on other planets (RADVS, USA),
- measurement of orbital trajectories of space rockets (EREP, ERS-1, USA).
- height (distance) measurement for industrial applications, e.g., devices for determining the height of bulk material, etc.

Since the early development of aviation radio altimeters, the main design requirements have included simplicity, low weight, compact dimensions, and low power consumption. The radio engineering method using frequency modulation proved to be the most advantageous method, meeting the above requirements. The beginnings of its development date back to the 30s, when the theoretical foundations were developed and the first types of low-altitude radio altimeters were constructed. These studies, together with the work of D. Bentley and R. V. Gart in the United States in 1935, enabled the development of a low-altitude radio altimeter in 1938 that operated with continuous transmission of a high-frequency, frequency-modulated signal. In 1947, the book AN/APN-1 Radio Altimeter, Theoretical Justification and Principle of Operation was published, which contains the theory and practical design of a low-altitude radio altimeter with frequency modulation.

In the following period, there was an extensive development of low-altitude radio altimeters, which brought improvements in their properties and expanded their possibilities of use. The development was mainly focused on improving their quality and reducing height measurement errors using a modern component base and new technologies. However, the basic principle of height measurement has not changed in radio altimeters with frequency modulation. Recently, after mastering technology and solutions for circuits working with very short pulses, low-altitude radio altimeters operating in pulse mode have been produced. For example, the Russian radio altimeter RV-21, or the AN/APN-194 radio altimeter manufactured in the USA. However, low-altitude radio altimeters operating with frequency modulation continue to play an important role on board aircraft.

2.1 Classification of aircraft radio altimeters

The term aircraft radio altimeter refers to a device that uses the propagation of electromagnetic waves to measure the altitude of an aircraft above the Earth's surface. The radio altimeter measures the actual altitude of the aircraft H_{AGL} above the Earth's surface, which changes due to changes in terrain relief at a constant flight level. A barometric altimeter determines aircraft altitude from atmospheric pressure. Depending on the pressure setting, it may indicate altitude above mean sea level or height relative to a selected aerodrome reference level, such as the departure or landing airport. It measures either referenced to mean sea level H_{QNH} relative to sea level or the relative altitude to height above aerodrome $H_{rel}\ QFE$ relative to the altitude of the airport of departure or landing (Fig. 1).

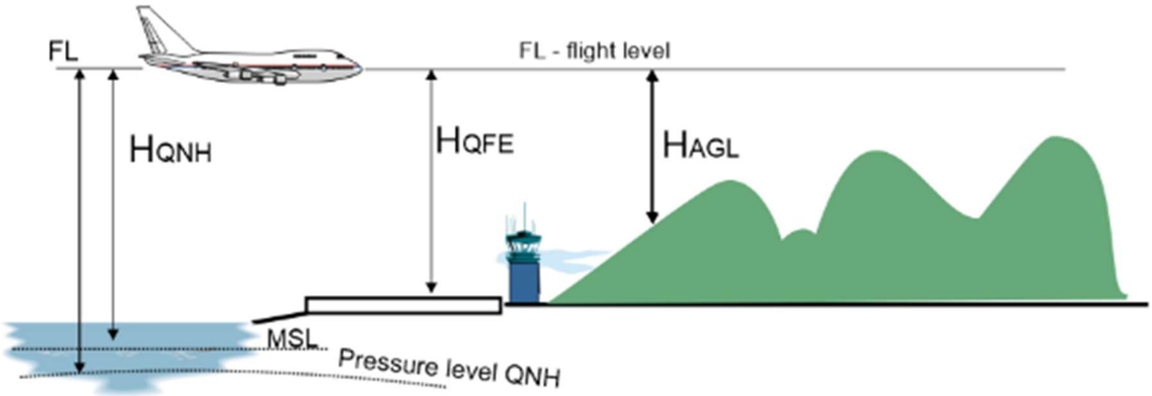

Fig. 1 Measured flight altitudes onboard the aircraft

Currently, two basic radio-technical principles of altitude measurement are used in aviation, which use the propagation of electromagnetic waves, with active location of the Earth's surface.

These are:

- *aviation radio altimeters operating in pulse mode,*
- *aviation radio altimeters operating with frequency modulation.*

Until recently, pulse-mode radio altimeters were used mainly for high-altitude measurements. Nowadays, after mastering the technology and solution of circuits operating with very short pulses, they are also used in measuring low altitudes. For better orientation in the above problem, a brief classification of these radio altimeters is given.

1. Pulse radio altimeters are divided into:

a) high-altitude pulse radio altimeters,

b) low-altitude pulse radio altimeters,

c) low- and high-altitude pulse radio altimeters.

2. High-altitude pulse radio altimeters are divided into:

a) pulse radio altimeters with direct altitude readout, *b) pulse radio altimeters with compensatory altitude readout.*

3. Low-altitude pulse radio altimeters are divided into:

a) coherent-altitude pulse radio altimeters,

b) non-coherent-altitude pulse radio altimeters.

Pulse radio altimeters for both low and high altitudes operate with pulse length switching at an operating altitude of around 500 to 600 m.

4. Radio altimeters operating with frequency modulation are exclusively low-altitude altimeters, and they can be divided into:

a) narrowband radio altimeters.

b) wideband radio altimeters,

5. Narrowband radio altimeters represent an automatic control system that maintains the difference frequency at a constant value by changing the length of the modulation period.

6. Broadband low-altitude radio altimeters can be divided into:

a) radio altimeters with direct measurement of the difference frequency,

b) radio altimeters with frequency locking to the difference frequency.

Broadband low-altitude radio altimeters with frequency modulation and direct measurement of the difference frequency are among the simplest radio-technical devices used to measure aircraft altitude.

2.2 A brief overview of aircraft radio-altimeter types and manufacturers

The beginning of mass production of aviation radio altimeters occurred during World War II. Currently, a large number of radio altimeters of various types, different purposes and different accuracy classes are produced in several countries.

The main directions of development are aimed at increasing accuracy and reliability, reducing weight and dimensions. Increasing accuracy is achieved by using new methods of processing the signal carrying information about the height. Increasing reliability and reducing weight and dimensions are achieved by using semi-conductors and integrated circuits. In addition, in current radio altimeters, to increase their reliability, circuits for automatic control of the immediate state of most high-frequency and low-frequency circuits are implemented. At the same time, it is possible to implement automated control of the accuracy of the radio altimeter height measurement (even in flight) using a standard delay line, which improves the reliability of the apparatus and guarantees (in time) the accuracy of the height measurement.

Currently, we distinguish radio altimeters for:

- *low altitudes in the range from 0 m to 300–750 m,*
- *medium altitudes in the range from 0 m to 1000–1500 m,*
- *high altitudes in the range from 0 m to 10–15 km.*

A brief overview of companies producing radio altimeters.

- In the United States, companies involved in the manufacture of radio altimeters include: Bendix/King, Honeywell, Sperry, ITT, Collins Radio Co., Litton Industries, Bonzer, LFE Electronics, Ryan Aeronautical Co., Texas Instruments, Teledyne Ryan Electronics, and others.
- In the United Kingdom, companies include: STC and Smiths Sons Ltd., GEC-Marconi, Smiths Industries Aerospace.
- In France, companies include: TRT and Thomson-CSF CNI Division.
- In Canada, the main manufacturer was Canadian Marconi.

In recent years, many types of radio altimeters have been produced for various kinds of aircraft and helicopters.

A brief overview of the types of radio altimeters produced in the world

a) ***Low- and medium-altitude radio altimeters operating with continuous transmission***

USA:	AN/APN-22, AN/APN-94, AN/APN-117, AN/APN - 150, AN/APN-156, ALA - 51A, ALT - 55, ALT - 200, KRA -10A, KRA - 405.
UK:	STR - 51A, STR - 52, STR - 53A, STR - 54A, STR - 70H, STR - 74A, RA 3000, RA 3002, RA 3003.
France:	AHV - 3, AHV - 4, AHV - 5, AHV - 6, AHV - 8, AHV - 9T, AHV - 16, AHV - 17, AHV - 18, AHV - 530, AHV - 540, AHV - 550, AHV - 2100, AHV - 2500, AHV - 2900.

Canada: CMA - 521, CMA - 709.

Russia: RV - UM, RV - 2, RV - 3, RV - 4, RV - 5, RV - 5M (A - 037), RV - 15 (A - 031).

Germany: DRA - 100.

b) ***Low and medium-altitude radio altimeters operating in pulse mode***

Recently, pulsed radio altimeters have been used to measure low and medium altitudes, which was made possible by the adoption of the technique of generating, amplifying and processing nanosecond-long pulse signals.

USA: HG - 151, HG - 7091A, HG -7091B, HG - 7092, HG - 7095, HG - 7181B, HG - 7500, HG - 7700, HG - 8500, HG - 9010, HG - 9050, HG - 9500, HG - YG 784, AN/APN - 141, AN/APN - 167, AN/APN - 171, AN/APN - 184, AN/APN - 194, AN/APN -198, AN/APN - 201, AN/APN - 209, AN/APN - 224.

UK: AD 1990, PSV1712.

Russia: RV1711, RV-21.

France: ERT-011

c) ***High-altitude radio altimeters operating in pulse mode***

USA: AN/APN - 222, AN/APN - 224, HG - 7197.

France: AHV - 12.

Russia: RV - 17, RV - 18, RV - 19, RV - 21 (A - 035), RV - 25 (A - 038), RV - 72, RV – 76, RV - 86.

3 CHARACTERISTICS OF FREQUENCY MODULATED RADIO ALTIMETER

The term frequency-modulated radio altimeter refers to a radio altimeter that uses a harmonic frequency-modulated radio signal to measure an aircraft's altitude above the Earth's surface. The measured altitude range is typically 0 to 1,500 m, depending on the aircraft type and the altimeter model. Onboard radio altimeters are used mainly at low altitudes and in the final stages of flight during approach and landing of the aircraft. They ensure the measurement and indication of the actual height of the aircraft above ground. The output signal of the radio altimeter, carrying information about the actual height, can also be used in the on-board automatic aircraft control system for continuous correction of the control subsystem during approach and for shaping the alignment trajectory during landing. In addition, radio altimeters acoustically and optically signal the descent of the aircraft below the selected so-called *"dangerous height"*.

3.1 Operating principle of frequency modulated radio altimeters

The aircraft radio altimeter operates in such a way that its transmitter generates a high-frequency frequency-modulated signal, which is radiated toward the earth's surface through the transmitting antenna (Fig. 2). One of three functions is used as the modulation function, the waveforms of which are shown in (Fig. 4). It is evident that the waveform of the signal reflected from the ground is identical to the waveform of the transmitted signal (Fig. 3), only delayed in time by a certain period.

$$\tau = \frac{2H}{c} \tag{1}$$

in which:

τ - time delay of the received signal,

H – flight altitude,

c - speed of propagation of light,

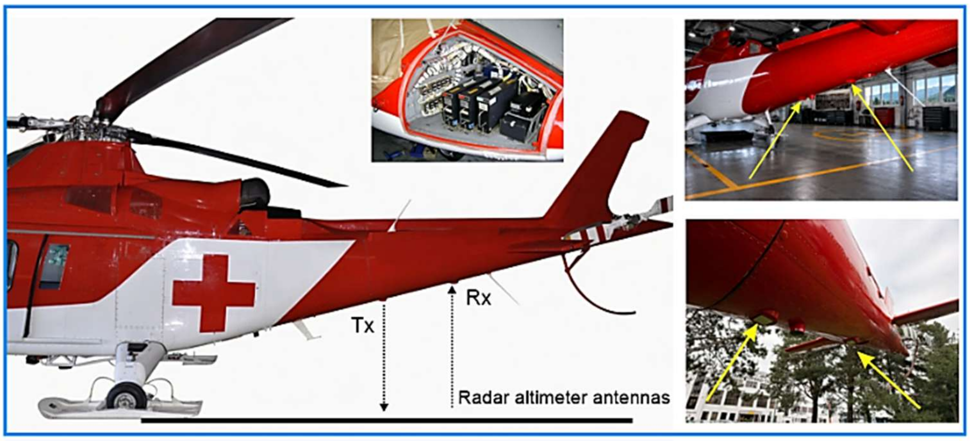

Fig. 2 Placement of the radio altimeter in the aircraft and its antenna system

The reflected signal from the ground,$u_p(t)$ received by the receiving antenna, is fed into a balanced mixer together with the so-called direct signal,$u_v(t)$ from the transmitter. Because the reflected signal is time-delayed, the frequency of the direct signal at any given moment is already different from that of the reflected signal. At the output of the balanced mixer, after unwanted components are removed, a difference (beat) signal, is generated, whose frequency f_d is:

$$f_r(t) = \left| f_v(t) - f_p(t) \right| \qquad (2)$$

In which:

f_T(t) – frequency of the transmitted signal,

f_r (t) – frequency of the received signal, (reflected).

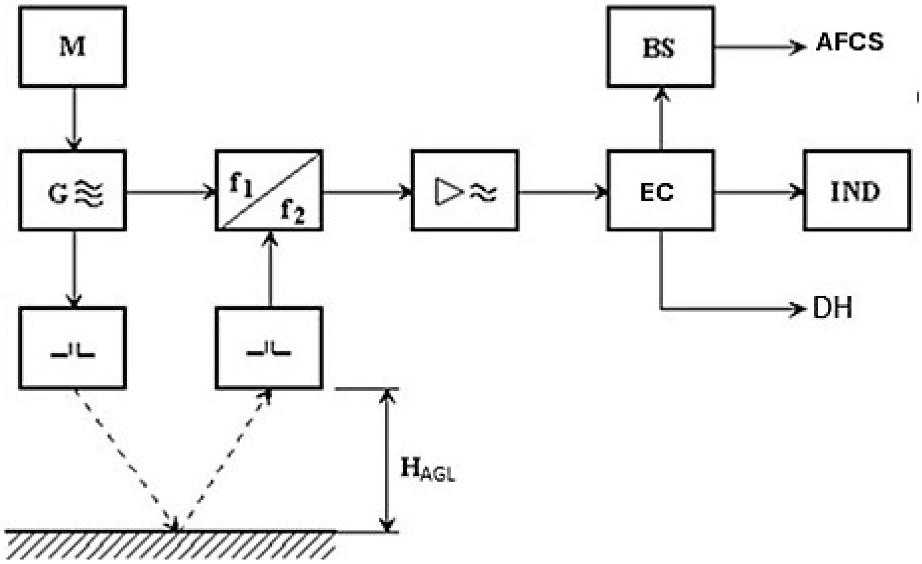

Fig. 3 Functional block diagram of a frequency-modulated radio altimeter

M - modulator, G - generator, EC - evaluation circuit, IND - altitude indicator, AFCS – Automatic Flight Control System, BS – Block signal, DH - dangerous height, H_{AGL} *– altitude ground level*

In relation (2), the absolute value is used because, physically, frequency is always positive. From the time waveforms in Fig. 4a and Fig. 4b, we can see that the magnitude of the difference frequency, which depends on the time delay of the reflected signal, is constant over most of the modulation period at a constant altitude and can be expressed by the relation:

$$f_d = \frac{8\,\Delta f\, f_M}{c}\, H \tag{3}$$

In which:

f_d - difference frequency,

Δf - frequency deviation.

f_M - modulation frequency.

The time interval τ during which the frequency f_d is not constant is called the phase-reversal band, because at the midpoint of this band the function f_d (t) equals zero (Fig. 4b). Equation (3) is called the fundamental equation of the frequency-modulated radio altimeter with a constant modulation period.

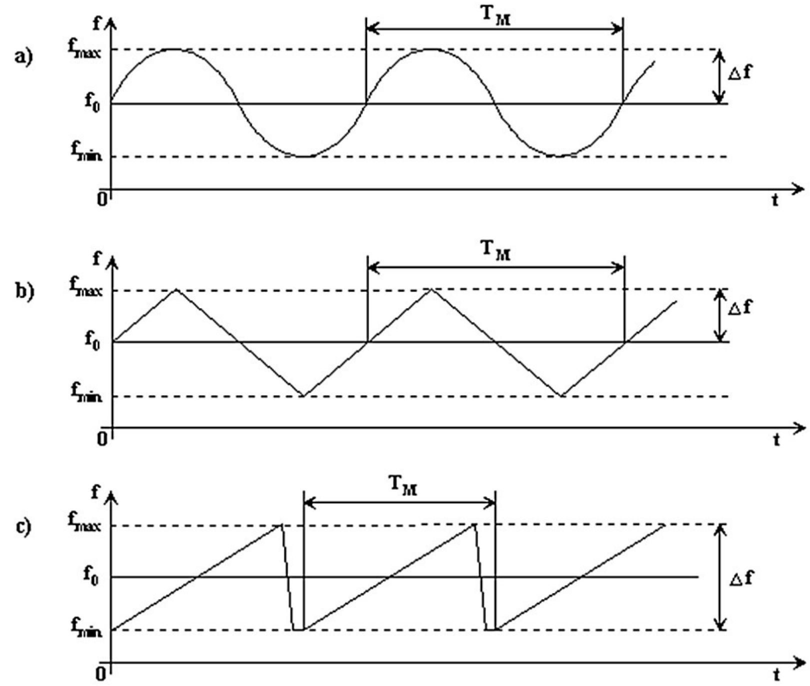

Fig. 4 Waveforms of modulation functions

a) - harmonic function, b) - symmetric sawtooth, c) - asymmetric sawtooth.

However, this equation is valid only in the case when T_M>> τ i.e. only in the case when we can neglect the influence of the phase rotation bands of the difference signal u_r(t) and when we can consider that:

$$f_d = const. \qquad (4)$$

during the entire modulation period (Fig. 5 b, c). This condition is practically satisfied only at relatively low altitudes, up to approximately 2,000 m. Therefore, these radio altimeters are called low-altitude radio altimeters. The signal from the balanced mixer u_{BM}(t) is further amplified using a differential signal amplifier and fed to the evaluation circuit, where the magnitude of the difference frequency, which corresponds to the actual flight altitude of the aircraft, is evaluated.

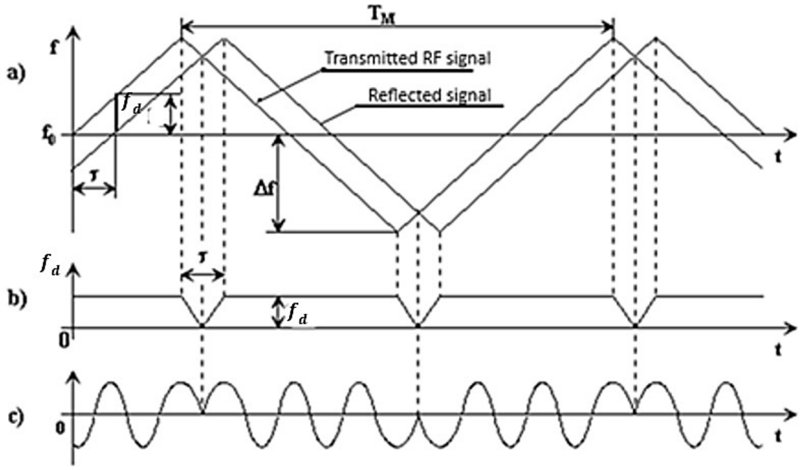

Fig. 5 Generation of the difference signal

a) - course of the difference signal, b) - value of the difference signal frequency,

c) - time waveform of the difference signal

In modern radio altimeters, various frequency meters are used as evaluation circuits, implemented either as spectrum analyzers or as analogue and digital meters with direct or indirect measurement of the difference frequency. Due to technical simplicity and operational reliability, evaluation circuits with direct measurement of the difference frequency have found the widest application in frequency-modulated radio altimeters. The principle of these evaluation circuits is based on counting pulses that are shaped from the difference signal u_d(t) over the entire duration of the modulation period T_M (Fig. 6). The low-frequency difference signal $u_{ds}(t)$ after filtering and the necessary amplification, is fed into a bilateral limiter. Bilateral limiting provides greater resistance to interference. The limiting thresholds u_1,u_2 are usually chosen as shown in Fig. 6b. The bilaterally limited signal, in the form of voltage pulses u_{lim}(t) (Fig. 6c), is then passed into a differentiating circuit. The voltage spikes (Fig. 6d) obtained at its output are fed into a half-wave rectifier. Its task is to clip the negative voltage spikes. The resulting positive derivative pulses u_{dif}(t) (Fig. 6e) have the same frequency as the difference signal. These voltage pulses are then applied either to a conventional integrating element, as in older types of radio altimeters with an analogue output, or to a decimal digital counter, as in more modern radio altimeters. The output is a direct voltage u_{dc}(t) (Fig.6f) (Fig. 6f) proportional to the number of voltage pulses (N). In addition to the circuit forming the altitude measurement channel, the radio altimeter also includes other auxiliary circuits, such as the dangerous altitude warning circuit, the radio altimeter self-check circuit, the radio altimeter testing circuit, and others. However, these circuits do not affect the actual altitude measurement and will therefore not be discussed further.

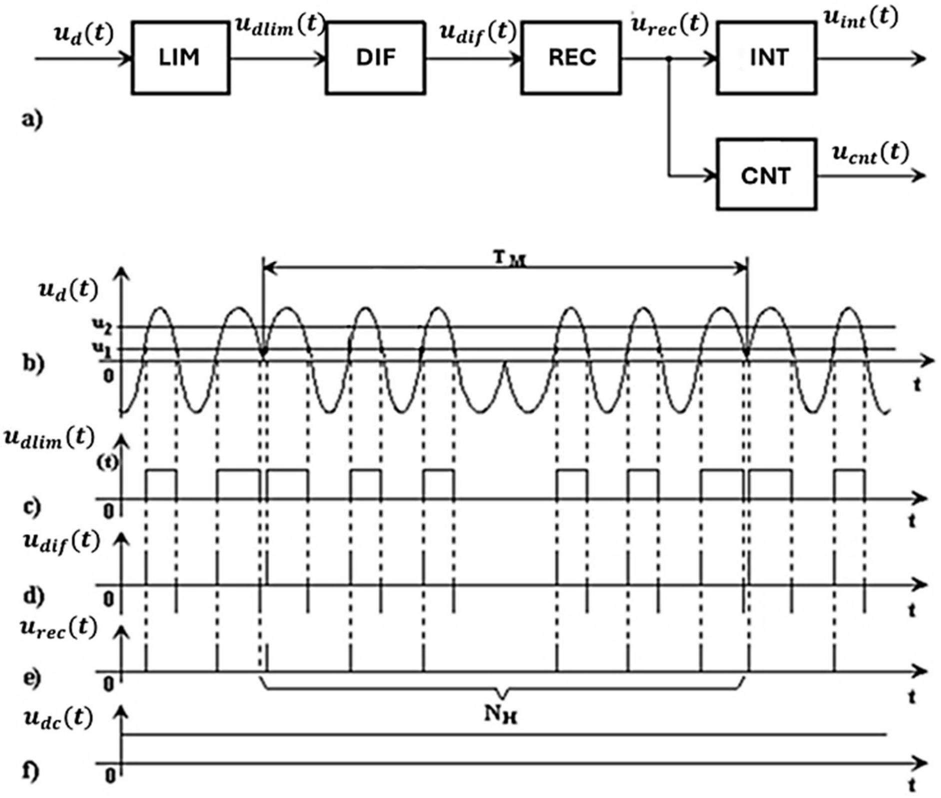

Fig. 6 Functional diagram and time waveforms of signals processed by the evaluation circuit with direct measurement of the difference signal

LIM - limiter, DIF - differentiating circuit, REC - rectifier, INT - integrating element, CNT -counter.

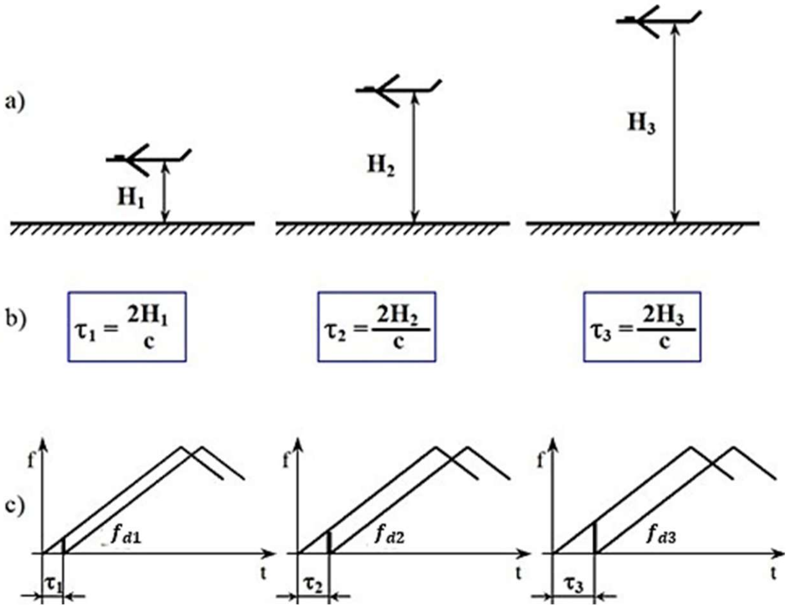

Fig. 7 Relationship between aircraft flight altitude and the generation of the difference frequency

Figure 7 illustrates the relationship between the aircraft flight altitude H and the generation of the difference frequency f_d. Fig. 7a shows three different flight altitudes (H_1, H_2, H_3), where H_1 represents the lowest altitude and H_3 the highest. In Fig. 7b, three different time delays (τ_1, τ_2, τ_3) corresponding to these altitudes are shown. The radio altimeter generates three different values of the difference frequency (f_{d1}, f_{d2}, f_{d3}) for these time delays as shown in Fig.7c. In Fig. 7a, the relationships indicate that the lowest altitude H_1 corresponds to the shortest time delay, which in turn corresponds to the smallest difference frequency f_{d1}. Similarly, the highest altitude H_3 corresponds to the largest difference in frequency. From this, it is evident that in altitude measurement, an indirect method is used to measure the very short time interval that elapses between the transmitted and received signals, through the evaluation of the difference frequency.

3.2 Operating modes of frequency modulated radio altimeters

3.2.1 Narrowband frequency-modulated radio altimeters

Narrowband radio altimeters are currently used as precise altitude measuring instruments, for example, in automatic landing systems. In narrowband radio altimeters, the frequency band for processing the difference signal is equal to the spectrum width of the difference signal Δf_{d}r. They use a tracking circuit that adjusts the average value of the difference signal frequency f_d to the frequency f_0 of the tuned circuit. Such radio altimeters provide relatively high measurement accuracy, even at low signal-to-noise ratios at the receiver input. This is due both to the reduction of noise levels at the input as a result of narrowing the processed signal's frequency band and to the suppression of the systematic error of the radio altimeter.

The radio altimeter operates successively in the measurement mode, the check mode, and the calibration mode of the radio altimeter constant (Fig. 8).

The measurement mode is implemented by the circuits:

a) controlled generator CG, b) modulator M, c) frequency-modulated generator FMG, d) directional coupler DCPL, e) transmitting and receiving antennas, f) balanced mixer BM, g) narrowband filter NBF, h) limiter amplifier LM, i) frequency discriminator FD-1, j) frequency-modulated signal control circuit FMC-1. The functional diagram of the radio altimeter represents a closed loop tracking system, whose sensitive element is a frequency discriminator tuned to a constant frequency f_0. The narrowband filter, whose frequency band Δf_{NBF} is approximately equal to the bandwidth of the difference signal Δf_d is also tuned to the frequency f_0.

$$\Delta f_{NBF} \approx \Delta f_d \qquad (5)$$

The frequency discriminator shapes a voltage proportional to the deviation of the difference frequency f_d from the tuned frequency f_0. This voltage is integrated in the frequency-modulated signal control circuit and is used to control the modulation frequency F_M in the modulator circuit. The frequency f_M is adjusted in the direction that reduces the deviation $\Delta f = f_d - f_0$. For preliminary coarse matching of the frequencies f_d and f_0 a search circuit (SSC) is required. Using this circuit, the frequency f_M is continuously adjusted until the spectrum of the difference signal fits within the frequency band of the, and the mode switching circuit (MSC) switches the radio altimeter into the mode for tracking the difference signal. The frequency f_0. is usually set to a value of 20 to 30 kHz. The modulation period is evaluated in the circuit from the output of the controlled generator (CG). The modulation period meter (MPM) shapes a signal H, proportional to the flight altitude.

The check mode is activated several times per second using the synchronizer (Synch). The check circuit includes the devices of the basic circuit, as well as a reference delay line (DL), connected to the circuit via antenna switches (AS-1 and AS-2), and a frequency discriminator (FD-2). This part of the circuit operates in the same way as the basic circuit. The voltage from the frequency discriminator is used to monitor the signal level by the check circuit (CHC)**.** In the check mode, the stability of the radio altimeter constant is verified. The modulation frequency from the control generator (whose value is determined by the delay line DL and must remain constant in the check mode) is fed to the mixer (MX). At the same time, a signal from the reference generator (RG) is also fed into the mixer. The error signal generated by the mixer carries information about the magnitude and direction of the deviation of the control generator frequency from the value set by DL and is used in the control circuit (CC-2) to adjust the amplitude of the modulation signal, which in turn changes the deviation of the difference signal frequency. The modulation signal amplitude control is carried out in the modulator (M). In the presence of a difference signal and with the radio altimeter constant stable (within acceptable tolerance), the check circuit (CHC) generates the correct operation signal of the radio altimeter (H_{norm}). The comparison circuit (COMP) is used to generate the H_{DA} signal when the altitude drops below the preset dangerous height.

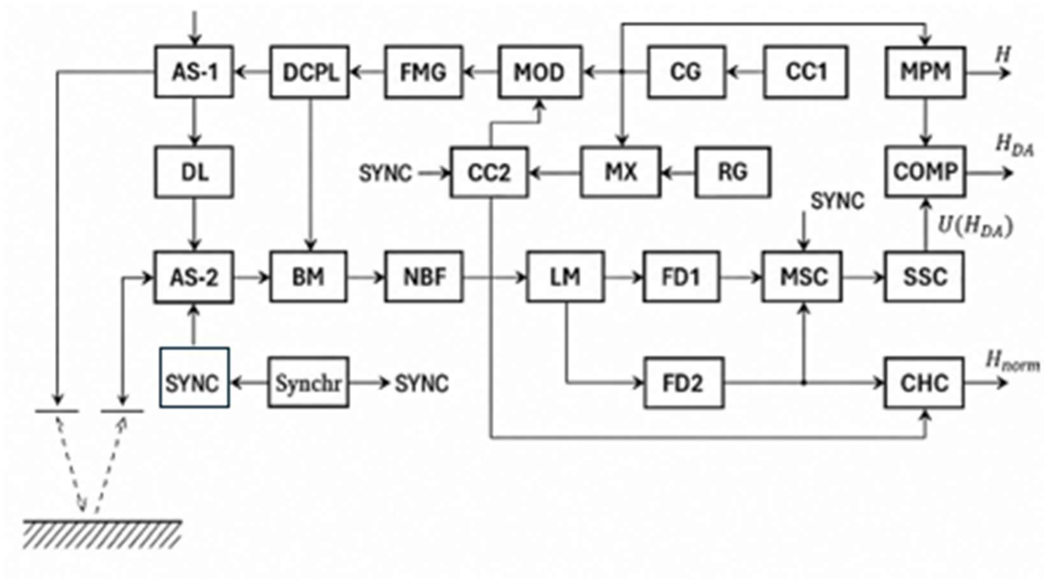

Fig. 8 Narrowband frequency-modulated radio altimeter

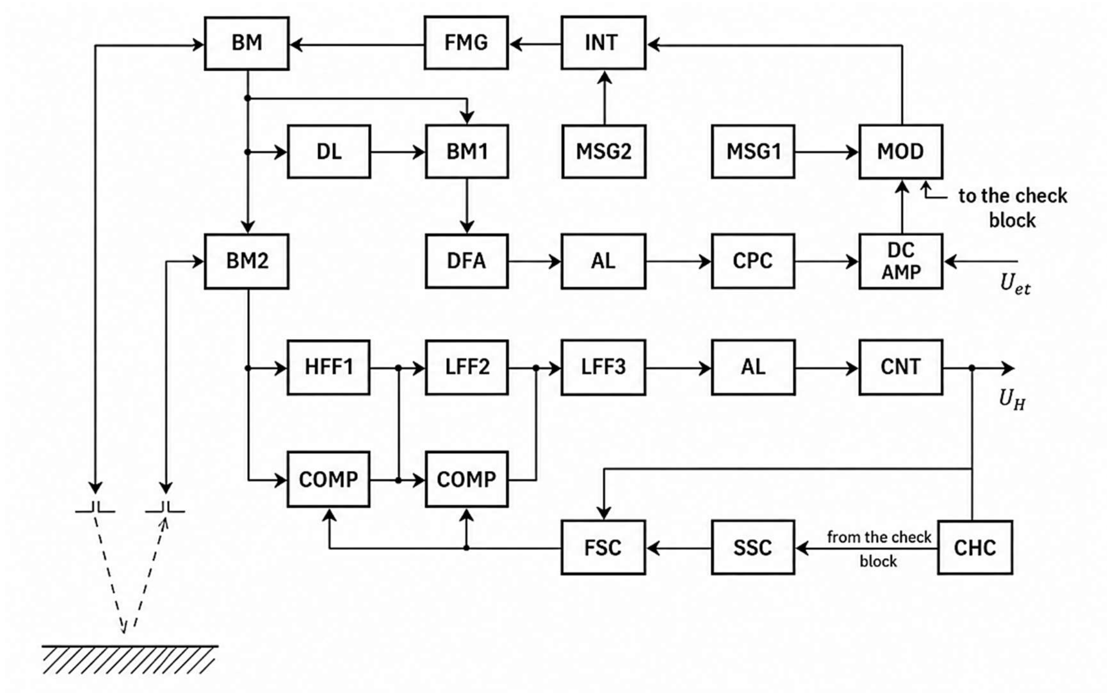

Fig. 9 Broadband frequency-modulated radio altimeter

3.2.2 Broadband frequency-modulated radio altimeters

The broadband radio altimeter has a band-pass amplifier (BPA) whose bandwidth Δf_{BPA} is:

$$\Delta f_{BPA} \gg \Delta f_d \tag{6}$$

The limit frequencies f_{dmin}. a f_{dmax} and the frequency band are determined by the range of measured altitude. In the amplitude limiter (AL), the difference signal is converted into a sequence of constant-amplitude pulses, which are fed to the pulse counter (CNT). The average value of the measured pulses is equal (in the absence of disturbances) to the root mean square value of the frequency of the measured signal. The pulse counter generates a voltage proportional to the number of input pulses, and the lag element (LA) shapes the average value of this voltage. Typically, the limiter generates pulses whenever the signal crosses zero voltage. Therefore, this counter is often called a zero-crossing pulse counter. The broadband radio altimeter with a filter system, integrated into the band-pass amplifier, has a passband whose width depends on the measured altitude. Limiting the frequency band width allows for a reduction in the radio altimeter's error. The operation of the radio altimeter in the altitude measurement mode and in the check mode is shown in Fig. 9. The measurement mode is implemented by a measurement circuit, which includes: a) modulation signal generator MSG-1, b) integrator INT, c) frequency modulated signal generator FMG, d) transmitting and receiving antenna, e) directional coupler DCPL, f) balanced mixer BM-2, g) filter bank FB, h) amplifier-limiter LA, i) pulse counter CNT. The modulation generator MG-1 produces rectangular pulses, the length of which is equal to half the modulation period (the modulation frequency is usually around 150Hz). These pulses are fed to the integrator via the modulator M, which is designed to control their amplitude. The voltage from the integrator (in the form of a symmetrical sawtooth) is used to control the frequency of the emitted signal. To reduce the influence of disturbances (noise), a filter system is used, consisting of a high-frequency filter HFF-1, which attenuates harmonic components less than 10 kHz, and two low-frequency filters LFF-2 and LFF-3 with cutoff frequencies of 30 kHz and 160 kHz. The selection of the frequency characteristic of the filter system is carried out by the switching circuit SW, when the signal is activated, the corresponding filter is bypassed. The width of the frequency band of the filter system changes depending on the flight altitude, using the filter switching circuit FSC. During the absence of a differential signal, the control block (BK) activates the search circuit (CHK), which switches the filters in such a way that the entire frequency spectrum band — in which the differential frequency may be located is scanned. Automatic gain control (AGC) is usually not used in these radio altimeters. This is due to the possible signal loss (up to 30 dB) caused by interference from single and multiple reflections (from the ground surface and the aircraft fuselage) within the antenna radiation pattern of the radio altimeter. Because the AGC time constant must be sufficiently large, signal loss may occur during the mentioned interference. In the radio altimeter, amplitude limiters are used — signals with high levels are limited in the first amplification stages, while signals with low levels are limited at the output of the amplifier.

The control mode is essential for maintaining the radio altimeter's constant, thereby increasing the accuracy of altitude measurement. A circuit is operated in this mode, which consists of a reference delay line (DL), a balanced mixer (BM-1), a difference frequency amplifier (DFA), an amplitude limiter (AL), a control pulse counter (CPC), a direct current amplifier (DC AMP), and a modulator (MOD).

In this circuit, the signal delay in the delay line is continuously measured. It is known that the output voltage of the control channel should remain constant and equal to the value U_{ref} when the radio altimeter coefficient is stable. If this equality is disturbed, a signal is taken from the direct current amplifier, which is then used to adjust the amplitude of the modulation signal going to the integrator. Consequently, the frequency deviation — which falls within the range of the radio altimeter coefficient also changes. The voltage U_{ref} supplied to the modulator is used to determine the mean value of the frequency deviation. The low-frequency generator MG-2 (with a frequency of 20 - 25 Hz) is used to reduce the adverse effects of discrete evaluation of the signal from the reference delay line on the accuracy of fine-tuning the radio altimeter constant. This is achieved through secondary amplitude modulation of the voltage used for the frequency modulation of the transmitted signal. By applying double frequency modulation, several low-frequency components appear in the spectrum of the differential signal, thereby reducing the likelihood of discrete reading of the control signal.

3.3 Requirements for altitude measurement accuracy of radio altimeters

Accurate altitude measurement is particularly important during the landing maneuver, specifically in the flare phase, when the aircraft transitions from the descent path and performs the final maneuver to touch down. In this stage, the aircraft is flying at a very small descent angle and at such a low altitude that the signal from the glide path beacon becomes practically unusable. Therefore, during this phase, a precision radio altimeter is essentially the only instrument capable of accurately determining the aircraft's height above the ground and, when processed appropriately, its rate of descent a crucial factor for ensuring a safe landing on the runway. The simple principle of altitude measurement has the disadvantage of relatively low accuracy. The efforts of radio altimeter manufacturers to improve measurement precision are reflected in the variety of methods used for processing and evaluating the difference frequency. This fact is also evidenced by the large number of different types of aircraft radio altimeters that exist.

Radio altimeters are used for altitude determination in various fields of application. Table 1 shows the permissible altitude measurement errors for several tactical tasks performed by different types and classes of flying devices.

Table 1

Range of measured height and permissible errors for some tactical tasks

Tactical task	**Height measurement range** [m]	**Measurement error** [±m]
Horizontal aircraft flight	300 ÷ 21 000	±7.5 ± 0,25%H
Aircraft descent for landing	150 ÷ 750	± 0.9 ± 5%H
Aircraft landing	0 ÷ 150	± 0.9 ± 3%H

Cartographic imaging from an aircraft	200 ÷ 15 000	± (1.5 ÷ 3)
Soft landing of space probes	3 ÷ 760	±1.5 ± 1,4%H
	More than 760	±4.5 ± 1,4%H
Launching a space rocket into orbit	4. 10^4 ÷ 5. 10^5	± (10 ÷ 20)
Orbital measurements	Up to 5 . 10^5	± (30 ÷ 150)
Geographical and oceanographic measurements	Up to 10^6	± (1 ÷ 5)

The resulting error of a frequency-modulated radio altimeter is influenced by various factors. From equation (3), it follows that the measured altitude is directly proportional to the difference frequency f_d. In reality, however, it is not that simple, because both the transmitted and received signals are frequency-modulated, and the modulation signal is a periodic function of time.

$$h = \frac{cf_d}{2k} \tag{7}$$

WhereT_M and c is the speed of light and k is the frequency modulation rate. However, the situation is more complex, because both the transmitted and received signals are frequency-modulated and the modulation signal is a periodic function of time. As stated, the spectrum of the difference signal is discrete and contains only frequency components that are multiples of the modulation frequency F_M. From this it follows that, by measuring the difference frequency, it is possible to detect only those altitude changes ΔH, that cause the appearance or disappearance of a spectral line in the spectrum of the difference signal. According to, the value of ΔH is given by the relation:

$$\Delta H = \frac{c}{8\Delta f} \tag{8}$$

This means that the altitude indicator readings do not change continuously with a gradual change in the measured altitude, but rather in discrete steps. The measured altitude can be read only with an accuracy of ΔH. This accuracy represents the methodological error of the frequency-modulated radio altimeter.

This fact means that the described operating principle allows only discrete altitude measurement. The value of ΔH differs for various types of radio altimeters. The assignment of the corresponding relation to individual types of radio altimeters is shown in Table 3 (row f). Typical values for frequency-modulated radio altimeters are presented in Table 2. An increase in the accuracy of measuring small altitudes with a frequency-modulated radio altimeter can be understood as a reduction of its methodological error, which significantly affects the overall altitude measurement accuracy. From relation (8), it follows that the methodological error of a frequency-modulated radio altimeter can be reduced only by increasing the frequency deviation Δf. This can be achieved in two ways:

1. *by decreasing the mean wavelength λ_0 while maintaining the same relative frequency deviation ξ,*
2. *by increasing the relative frequency deviation ξ, while maintaining the same mean wavelength λ_0*

The relative frequency deviation is given by the following relation:

$$\zeta = \frac{\Delta f}{f_0} \rightarrow \Delta \mathrm{f} = \zeta . f_0 = \frac{\zeta . c}{\lambda_0} \tag{9}$$

here:

ξ - relative frequency deviation,

Δf - frequency deviation,

f_0 - mean value of the carrier frequency,

λ_0 - mean value of the carrier wavelength.

Table 2

Some TTU (technical-tactical units) of frequency-modulated radio altimeters.

Type of RA	Make	Transmitter carrier frequency [MHz]	Freq. deviation [MHz]	Mod. frequency [Hz]	Range of measured altitudes [m]	Altitude measurement accuracy	
						to 10 m [m]	over 10 m [%]

RV-5	Russia	4 300	50	150	0÷750	0.6	6
RV-5M	Russia	4 300	90	variable	0÷750	0.6	6
AHV-5	France	4 300	80	variable	0÷750	0.3±3% H	4
KRA-405	USA	4 300	50	100	0÷600	1.52	7

Table 3

Signal waveforms illustrate the operation of frequency-modulated radio altimetersnd the magnitude of their methodological error.

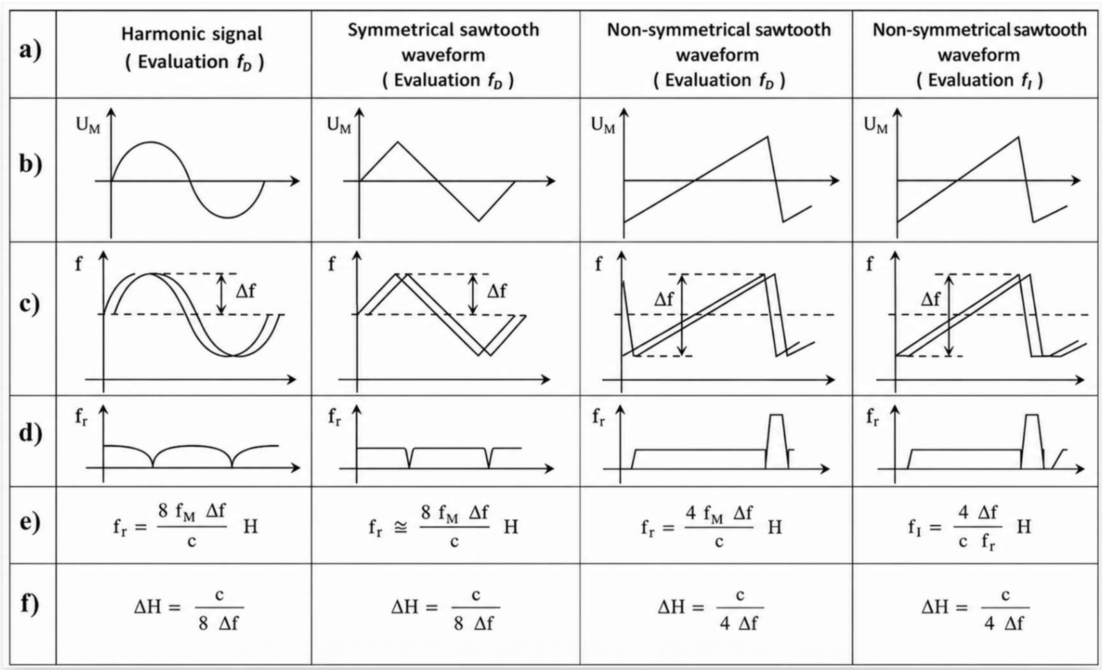

Legend to Table 3

Row,

a) description of the modulation signal,

b) shape of the modulation signal,

c) time courses of the RF signals,

d) time course of the difference frequency value,

e) relation for determining the evaluated parameter at altitude,

f) relation for determining methodological error.

4 MATHEMATICAL MODEL OF A RADIO ALTIMETER

4.1 Mathematical model of a frequency-modulated radio altimeter

A low-altitude radio altimeter operating with frequency modulation is a radio navigation device that utilizes the dependence of the difference frequency between the direct and reflected signals on altitude. A simplified block diagram of a frequency-modulated radio altimeter is shown in Fig. 3. The altimeter transmitter sends a frequency-modulated signal toward the ground via the transmitting antenna, which reflects off the ground and is received by the altimeter's receiving antenna. In the altimeter receiver, the instantaneous values of the transmitted and received signals are compared. The received signal is delayed relative to the transmitted signal by a time τ given by relation (1), due to reflection from the ground surface. The signal comparison is performed in a balanced mixer at the receiver input by summing the two signals. The result of this summation is the difference (beat) frequency, which represents the instantaneous frequency difference between the transmitted and received signals. From this signal, further circuits in the radio altimeter generate a voltage proportional to the altitude. The variation law of the frequency-modulated transmitted signal can generally be any periodic function of time. From a mathematical analysis perspective, the simplest is sinusoidal frequency modulation. Let us assume that the radio altimeter transmitter emits a high-frequency, frequency-modulated signal:

$$u_{fM}(t) = U_{FM} \sin\left(\varpi_0 t + \frac{\Delta\omega_0}{\Omega_M} sin\Omega_M t\right) \tag{10}$$

where: $\varpi_0 = 2\pi f_0$ - mean value of the transmitter carrier angular frequency,

$\Omega_M = 2\pi f_M$ - angular modulation frequency,

$\Delta\Omega\omega_0 = 2\pi f_0$ - deviation of the carrier angular frequency,

f_0 - mean value of the transmitted signal carrier frequency,

Δf_0 - transmitter frequency deviation,

f_M - modulation frequency.

For the sake of a simpler notation of relation (10), we introduce the following relation:

$$\varphi_v = \frac{\Delta\omega_0}{\Omega_M} \sin \Omega_M t \tag{11}$$

The high-frequency, frequency-modulated transmitter signal (10) will then have the form:

$$u_v(t) = U_v \sin(\ \omega_0 t + \ \varphi_v) \tag{12}$$

The signal reflected from the ground, which is received by the receiving antenna, has the same waveform as the transmitted signal but is delayed in time by "$\boldsymbol{\tau}$", and its amplitude is smaller than that of the transmitted signal due to scattering and absorption of electromagnetic energy during reflection.

For the signal received, we can write the following relation:

$$u_r(t) = U_r \sin\left(\varpi_0 t + \frac{\Delta\omega_0}{\Omega_M} sin\Omega_M(t-\tau)\right) \tag{13}$$

For the sake of a simpler notation of relation (13), we introduce the following designation:

$$\varphi_p = \frac{\Delta\omega_0}{\Omega_M} \sin \Omega_M(t-\tau) - \ \omega_0\, \tau \tag{14}$$

The high-frequency, frequency-modulated signal received by the receiving antenna will, after simplification, have the form:

$$u_p(t) = U_p \sin(\varpi_0 t + \varphi_r) \tag{15}$$

As mentioned above, both signals are fed to the input of a balanced mixer. The resulting signal, given by the sum of the transmitted (12) and received (15) signals, can be written as follows:

$$u(t) = \ u_v(t) + u_p(t)$$

$$u(t) = U_v\ [\omega_0 t + \varphi_v] + \ U_p sin\big[\omega_0 t + \varphi_p\big]$$

By introducing the simplified notation, we obtain:

$$u(t) = Usin\,[\omega_0 t + \varphi] \tag{16}$$

In relation (16), operations with sinusoidal quantities of the same frequency, were performed, where the amplitude is:

$$U = \sqrt{U_v^2 + U_p^2 + 2U_v U_p \cos(\varphi_p - \varphi_v} \tag{17}$$

and the phase is:

$$tg\varphi = \frac{U_v sin\varphi_v + U_p sin\varphi_p}{U_v cos\varphi_v + U_p cos\varphi_p} \tag{18}$$

The result is also a sinusoidal quantity with the same frequency. In the next section, we will focus separately on the analysis of the phase relationships and, separately, on the amplitude relationships of the resulting signal, which is formed as the sum of the transmitted and received signals in the balanced mixer [8].

4.2 Analysis of phase relationships

For simplicity, let us assume that the amplitudes of both signals are equal ($U_V = U_P$). This deliberately increases the influence of the reflected signal, but on the other hand simplifies the analysis of relation (3.9). In the analysis, we will use the well-known relations [8] for the sum of trigonometric functions. Under these assumptions, we can write:

$$tg\varphi = \frac{U_v sin\varphi_v + U_p sin\varphi_p}{U_v cos\varphi_v + U_p cos\varphi_p} = \frac{2sin\frac{\varphi_v + \varphi_p}{2}\cos\frac{\varphi_v - \varphi_p}{2}}{2cos\frac{\varphi_v + \varphi_p}{2}\cos\frac{\varphi_v - \varphi_p}{2}} = \frac{sin\frac{\varphi_v + \varphi_p}{2}}{cos\frac{\varphi_v + \varphi_p}{2}}$$
$$= tg\frac{\varphi_v + \varphi_p}{2}$$

The phase of the resulting signal will be:

$$\varphi\frac{\varphi_v + \varphi_p}{2} \tag{19}$$

If we substitute expression (11) for "φ_V" and expression (15) for "φ_P" we can, after a simple adjustment, write:

$$\varphi = \frac{1}{2}\left\{\frac{\Delta\varpi_0}{\Omega_M}[sin\Omega_M t + sin\Omega_M(t - \tau)] - \varpi_0\tau\right\} \tag{20}$$

In relation (20), there is a sum of trigonometric functions. After simplification, we obtain:

$$\varphi = \frac{1}{2}\left[\frac{\Delta\varpi_0}{\Omega_M} sin \frac{\Omega_M t + \Omega_M(t-\tau)}{2} cos \frac{\Omega_M t - \Omega_M(t-\tau)}{2} \varpi_0 \tau\right] \tag{21}$$

We modify the argument of the sine function:

$$\frac{\Omega_M t + \Omega_M(t-\tau)}{2} = \frac{\Omega_M t - \Omega_M(t-\tau)}{2} = \Omega_M\left(\frac{2t - \tau}{2}\right) = \Omega_M\left(t - \frac{\tau}{2}\right) \tag{22}$$

We modify the argument of the cosine function:

$$\frac{\Omega_M t - \Omega_M(t-\tau)}{2} = \frac{\Omega_M \tau}{2} \tag{23}$$

Then relation (21) will take the form:

$$\varphi = \frac{1}{2}\left(\frac{\Delta\varpi_0}{\Omega_M}\left(\Omega_M\left(t - \frac{\tau}{2}\right)\right) cos \frac{\Omega_M \tau}{2} - \varpi_0 \tau\right) \tag{24}$$

By substituting relation (24) into relation (25), we obtain:

$$\begin{aligned} u(t) &= Usin(\varpi_0 t + \varphi) \\ &= Usin\left[\varpi_0 t + \frac{\Delta\varpi_0}{2\Omega_M} \sin\left(\Omega_M\left(t - \frac{\tau}{2}\right)\right) cos \frac{\Omega_M \tau}{2} \varpi_0 \tau\right] \\ u(t) &= Usin\left[\varpi_0(t - \frac{\tau}{2}) + \frac{\Delta\varpi_0}{2\Omega_M} \sin\left(\Omega_M\left(t - \frac{\tau}{2}\right)\right) cos \frac{\Omega_M \tau}{2}\right] \end{aligned} \tag{25}$$

We introduce a further simplification:

$$t_1 = t - \frac{\tau}{2} \tag{26}$$

By applying this simplification, we obtain the instantaneous phase of the resulting signal after mixing:

$$u(t) = Usin\left[\varpi_0(t_1) + \frac{\Delta\varpi_0}{2\Omega_M} \sin(\Omega_M t_1) cos \frac{\Omega_M \tau}{2}\right] \tag{27}$$

Conclusion of the analysis of phase relationships between the transmitted and received signals.

By comparing and analyzing relation (27) with relation (11), we conclude that the phase of the resulting signal is approximately the same as the phase of the transmitted signal.

$$u(t) = Usin\left[\varpi_0 t + \frac{\Delta\varpi_0}{2\Omega_M}\sin(\Omega_M t)\right] \tag{28}$$

$$u(t) = Usin\left[\varpi_0(t_1) + \frac{\Delta\varpi_0}{2\Omega_M}\sin(\Omega_M t_1)\, cos\frac{\Omega_M \tau}{2}\right] \tag{29}$$

The resulting signal, after summing the transmitted and received signals, is therefore again a frequency-modulated signal, modulated according to the same law as the transmitted signal, but with a frequency deviation $\frac{\Delta\varpi}{\Omega_M}$ is smaller cos $\frac{\Omega_M \tau}{2}$ times. For a typical low-altitude radio altimeter (e.g., RV-5), which has a frequency modulation of f_M = 150 Hz and H_{max} = 750 m, the value of the expression $cos\frac{\Omega_M \tau}{2}$ changes only slightly with altitude, approximately in the range 1 to 0.99.

Therefore, it can be assumed that for $U_v = U$ expression (29) for the resulting high-frequency signal practically does not differ from expression (10) for the transmitted signal. This conclusion becomes even more accurate when the amplitude of the received signal is smaller than that of the transmitted signal, which corresponds to reality.

From the above, it follows that the frequency of the resulting summed signal does not differ from the frequency of the transmitted signal and, therefore, measuring the frequency of the resulting summed signal cannot be used for altitude measurement.

4.3 Analysis of amplitude relationships

The amplitude relationships of the resulting signal are expressed by relation (17). We will assume that the amplitude of the received signal is much smaller than the amplitude of the transmitted signal, $Uv >> Up$. Therefore, in relation (17), we can neglect the term U_p^2 and we then obtain:

$$U = \sqrt{U_v^2 + 2U_v U_p \cos(\varphi_p - \varphi_v)} \tag{30}$$

If we denote

$$x = 2U_v U_p \cos((\varphi_p - \varphi_v) \tag{31}$$

it is then possible to take the square root of the entire expression using the approximate relation if

$$U >> x:$$

$$U = \sqrt{U_v^2 + x} = U_v \left(1 + \frac{x}{U_v^2}\right)^{\frac{1}{2}} = U_v + \frac{x}{2U_v} \tag{32}$$

By substituting the values from relation (32) into the approximate relation (33):

$$U = U_v + \frac{2U_v U_p \cos(\varphi_p - \varphi_v}{2U_v} \tag{33}$$

and after simplification, we obtain:

$$U = U_v + U_p \cos(\varphi_p - \varphi_{v)} \tag{34}$$

This simplification causes an error of about 0.1% $for\ U_p = 0{,}05\ U_v$. However, the amplitude of the received signal is actually even smaller. Therefore, in the following, we will no longer refer to this as an approximate expression.

If we now substitute expression (11) for "φ_v" and expression (15) for "φ_p" into relation (14), we can write:

$$U = U_v + U_p cos\left[\frac{\Delta\omega_0}{\Omega_M} sin\Omega_M(t - \tau) - \varpi_0 t - \frac{\Delta\varpi_0}{\Omega_M} sin\Omega_M t\right]$$

After a minor adjustment, we can write:

$$U = U_v + U_p cos\left[\frac{\Delta\omega_0}{\Omega_M} sin\Omega_M(t - \tau) - sin\Omega_M t\right]\varpi_0 \tau \tag{35}$$

Next, we will use the relation for the difference of trigonometric functions:

$$sin\alpha - sin\beta = 2cos\frac{\alpha + \beta}{2} sin\frac{\alpha - \beta}{2} \tag{36}$$

And we will get:

$$U = U_v + U_p cos\left[2\frac{\Delta\omega_0}{\Omega_M} cos\frac{\Omega_M(t-\tau)+\Omega_M t}{2} - sin\frac{\Omega_M(t-\tau)+\Omega_M t}{2} - \varpi_0\tau\right] \tag{37}$$

The values of the arguments can be adjusted similarly to relation (24):

$$\frac{\Omega_M(t-\tau)+\Omega_M t}{2} = \Omega_M\left(t-\frac{\tau}{2}\right) = \frac{\Omega_M(t-\tau)+\Omega_M t}{2} = \frac{\Omega_M\tau}{2} \tag{38}$$

After substituting, we obtain:

$$U = U_v + U_p cos\left[-2\frac{\Delta\omega_0}{\Omega_M}\cos\left(\Omega_M\left(t-\frac{\tau}{2}\right)\right) sin\frac{\Omega_M\tau}{2} - \varpi_0\tau\right] \tag{39}$$

By using the relations for the trigonometric functions of angles and the relation (26):

$$\sin(-\alpha) = -\sin\alpha, \quad \cos(-\alpha) = \cos\alpha, \tag{40}$$

we can write relation (39) in the form:

$$U = U_v + U_p cos\left(\varpi_0\tau + 2\frac{\Delta\varpi_0}{\Omega_M} sin\frac{\Omega_M\tau}{2} cos\Omega_M t_1\right) \tag{41}$$

Since the value of $\frac{\Omega_M\tau}{2}$ is small in real measurements with a radio altimeter, the following relation holds: $sin\frac{\Omega_M\tau}{2} = \frac{\Omega_M\tau}{2}$

Thus, expression (41) can be written in its final form:

$$U = U_v + U_p cos(\varpi_0\tau + \Delta\varpi_0\tau cos\Omega_M t_1) \tag{42}$$

For further mathematical considerations, we can simplify relation (42) by introducing:

$$\varphi_{0=}\varpi_0\tau \qquad \varphi_{M=}\Delta\varpi_0\tau. \tag{43}$$

In this way, we obtain:

$$U = U_v + U_p cos(\varphi_0 + \varphi_{M=} cos\Omega_M t_1) \tag{44}$$

where the term φ_0 is called the initial phase and φ_M the variable phase.

Conclusion of the analysis of amplitude relationships between the transmitted and received signals.

Expression (44) represents the amplitude of the resulting signal, which varies with time t_1, and thus we can write:

$$U(t_1) = U_v + U_p cos(\varphi_0 + \varphi_{M=} cos\Omega_M t_1) \tag{45}$$

We factor U_V out of the parentheses:

$$U = U_v \left[1 + \frac{U_p}{U_v} cos(\varphi_0 + \varphi_{M=} cos\Omega_M t_1)\right] \tag{46}$$

Next we denote:

$$\frac{U_p}{U_V} = m \tag{47}$$

$$\varphi_0 + \varphi_{M=} cos\Omega_M t_1 = f(t_1) \tag{48}$$

Then we obtain:

$$U(t_1) = U_v[1 + m \cos f(t_1)] \tag{49}$$

The amplitude of an amplitude-modulated signal is, as is generally known, given by the expression:

$$U(t_1) = U_v[1 + m \cos f(t_1)] \tag{50}$$

In which: $f(t) = \Omega . t$

By comparing relations (49) and (50), we conclude that the amplitude of the resulting signal varies with time, meaning that the resulting signal is amplitude-modulated, even though the modulation law is quite complex. The modulation period is equal to:

$$T_M = \frac{2\pi}{\Omega_M} \tag{51}$$

Since φ_0 and φ_M are functions of time, the amplitude of the resulting signal is also a function of time. see Fig. 10.

From the above, it follows that the altitude of the aircraft can be determined based on the shape of the modulation envelope.

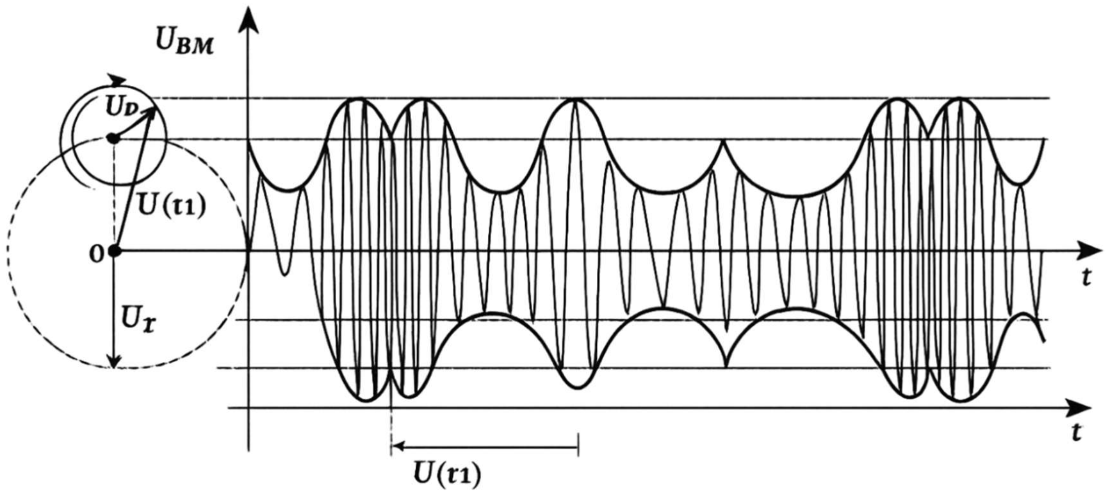

Fig. 10 Waveform of the balanced mixer signal

4.4 Analysis of the envelope shape of the difference-frequency signal

Through the mathematical analysis of the phase relationships of the resulting signal relation (27) and the analysis of its amplitude relationships relation (42) we conclude that the resulting signal is modulated both in frequency and amplitude. This is illustrated in Fig. 10. At the same time, the altitude information is encoded only in the amplitude of the resulting signal, which is formed by summing the transmitted and received signals in the balanced mixer. Its mathematical description, given by expression (42), represents a complex periodic process of the carrier frequency ω_0 amplitude, modulated at the rate of the modulation frequency Ω_M, which varies depending on the altitude.

Next, we will examine, both temporally and graphically, several special cases of the modulation envelope shape of the difference signal, which will allow us to form an understanding of the resulting difference signal. In doing so, we base our analysis on relation (42).

The shape of the difference signal envelope is determined by a) *initial phase* φ_0 and b) *variable phase* φ_M.

a) ***The initial phase*** φ_0, depends only on the altitude and can be expressed by the relation:

$$\varphi_0 = \varpi_0 \tau = 2\pi f_0 \frac{2H}{c} = \frac{4\pi}{\lambda_0} H \qquad (52)$$

b) ***The variable phase*** φ_M, depends on the altitude and changes with the modulation frequency (and thus with time); this phase can be expressed as:

$$\varphi_M = \Delta\varpi_0 \tau = 2\pi \Delta f_0 \frac{2H}{c} = \frac{4\pi \Delta f_0}{c} \cdot \frac{\Delta f_0}{f_0} H = \frac{4\pi\xi}{\lambda_0} H \qquad (53)$$

In which: ζ - relative change of the carrier frequency

$$\zeta = \frac{\Delta f_0}{f_0} \qquad (54)$$

The temporal variation of this phase is expressed by the relation:

$$\varphi_M(t) = \varphi_M cos\Omega_M t_1 \qquad (55)$$

where: T_M – modulation period

$$T_M = \frac{2\pi}{\Omega_M} \qquad (56)$$

In analyzing the phase relationships of the difference signal envelope, we vary the altitude H. The variable phase Ω_M reaches its maximum value when the expression cos φ_M,t_1 attains ± 1. The altitude change H is implemented in steps of $1/16\ l$, as shown in Table 4. Graphically, the behavior of the initial and variable phases is depicted only for the first twelve values. The resulting difference signal is illustrated only for certain initial values due to the large scale of the figures (Fig 10).

Table 4

Values of the initial and variable phases of the difference signal

S.n.	altitude	φ_0	φ_M	S.n.	altitude	φ_0	φ_M
1	1/16λ0	1/4π	1/4 ξ π	17	17/16λ0	17/4π	17/4 ξ π
2	1/8λ0	1/2π	1/2 ξ π	18	9/8	9/2 π	9/2 ξ π
3	3/16λ0	3/4π	3/4 ξ π	19	19/16λ0	19/4π	19/4 ξ π
4	1/4λ0	π	ξ π	20	5/4λ0	5π	5 ξ π

5	5/16λ_0	5/4π	5/4 ξ π	21	21/16 λ_0	21/4 π	21/4 ξ π
6	3/8λ_0	3/2π	3/2 ξ π	22	11/8λ_0	11/2π	11/2 ξ π
7	7/16λ_0	7/4π	7/4 ξ π	23	23/16 λ_0	23/4 π	23/4 ξ π
8	1/2λ_0	2π	2 ξ π	24	3/2λ_0	6π	6 ξ π
9	9/16λ_0	9/4π	9/4 ξ π	25	25/16λ_0	25/4π	25/4 ξ π
10	5/8λ_0	5/2π	5/2 ξ π	26	13/8	13/2 π	13/2 ξ π
11	11/16λ_0	11/4π	11/4 ξ π	27	27/16 λ_0	27/4 π	27/4 ξ π
12	3/4λ_0	3π	3 ξ π	28	7/4λ_0	7π	7 ξ π
13	13/16λ_0	13/4π	13/4 ξ π	29	29/16 λ_0	29/4 π	29/4 ξ π
14	7/8λ_0	7/2π	7/2 ξ π	30	15/8λ_0	15/2π	15/2 ξ π
15	15/16λ_0	15/4π	15/4 ξ π	31	31/16 λ_0	31/4 π	31/4 ξ π
16	λ_0	4π	4 ξ π	32	2λ_0	8π	8 ξ π

The values of the initial phase φ_0 and the variable phase φ_M dependent on the altitude H and listed in Table 4 under serial numbers (1 ÷ 12) are illustrated in polar coordinates in Fig. 11.

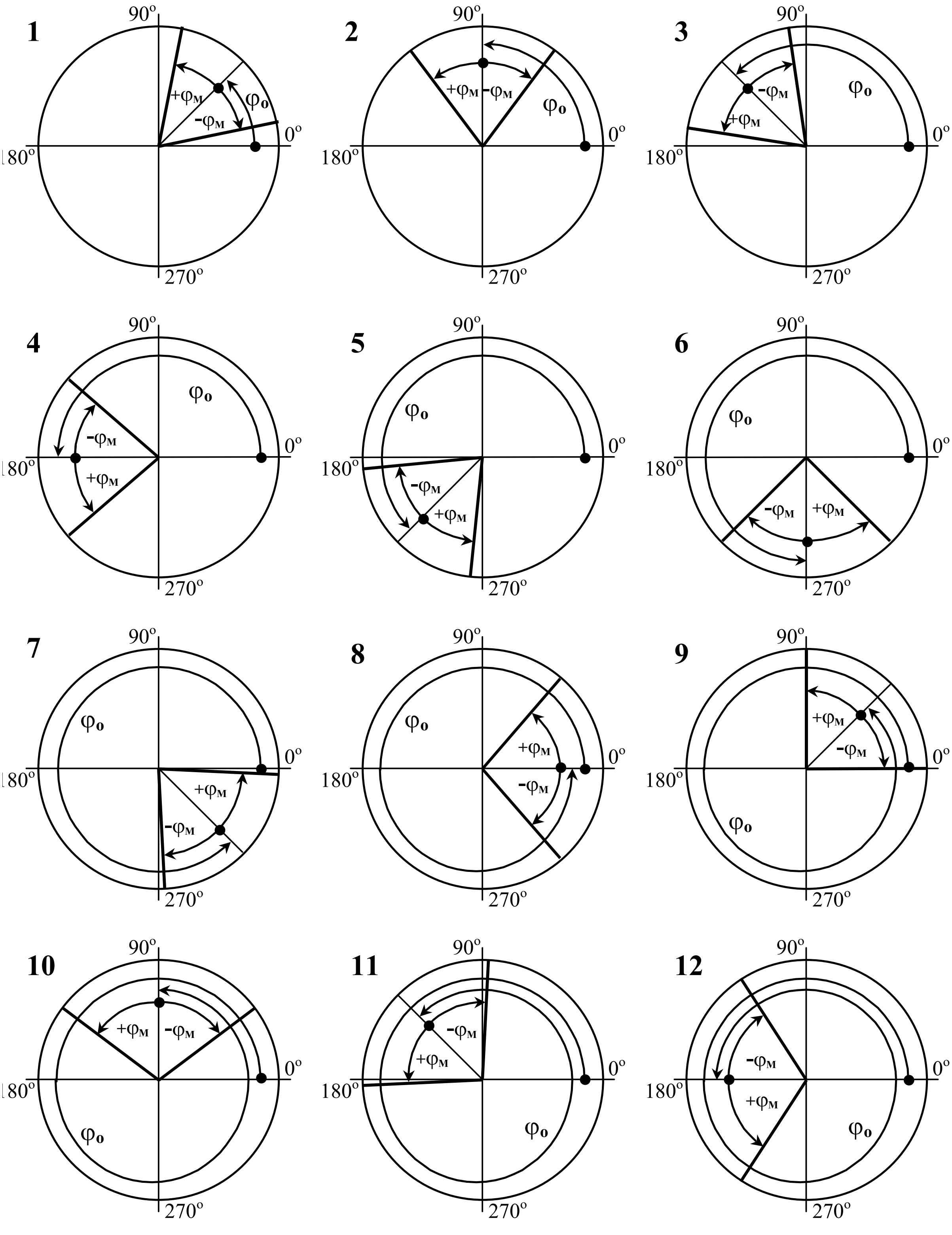

Fig. 11 Variation of the initial phase φ_0 and the variable phase φ_M as a function of altitude H with altitude values listed in Table 3.1 under the corresponding serial number

A) <u>Let us assume H = 0 .</u>

Then: $\tau = \frac{2}{c} H = 0,$ $\varphi_0 = \frac{4\pi}{\lambda_0} H = 0,$ $\varphi_M = \frac{4\pi\xi}{\lambda_0} H = 0$

This means that at zero altitude, the resulting signal is not amplitude-modulated, and the radio altimeter indicator will show zero altitude.

B) <u>Let us assume</u> $H = \frac{\lambda_0}{8}$

$$\varphi_0 = \frac{4\pi}{\lambda_0} \frac{\lambda_0}{8} = \frac{\pi}{2}, \qquad \varphi_M = \frac{4\pi\xi}{\lambda_0} \frac{\lambda_0}{8} = \xi \frac{\pi}{2} ,$$

The resulting signal amplitude varies with time:

1) For $t_1 = 0$ Þ t_0 the phase shift between U_v a U_p is equal to: $\varphi = \varphi_0 + \varphi_M$,.

2) For $t_1 = T_M / 4$ Þt_1 , the phase shift between U_v a U_p is equal to: $\varphi = \varphi_0$.

3) Pre $t_1 = T_M / 2$ Þ t_1, the phase shift between U_v a U_p is equal to: $\varphi = \varphi_0 - \varphi_M$,.

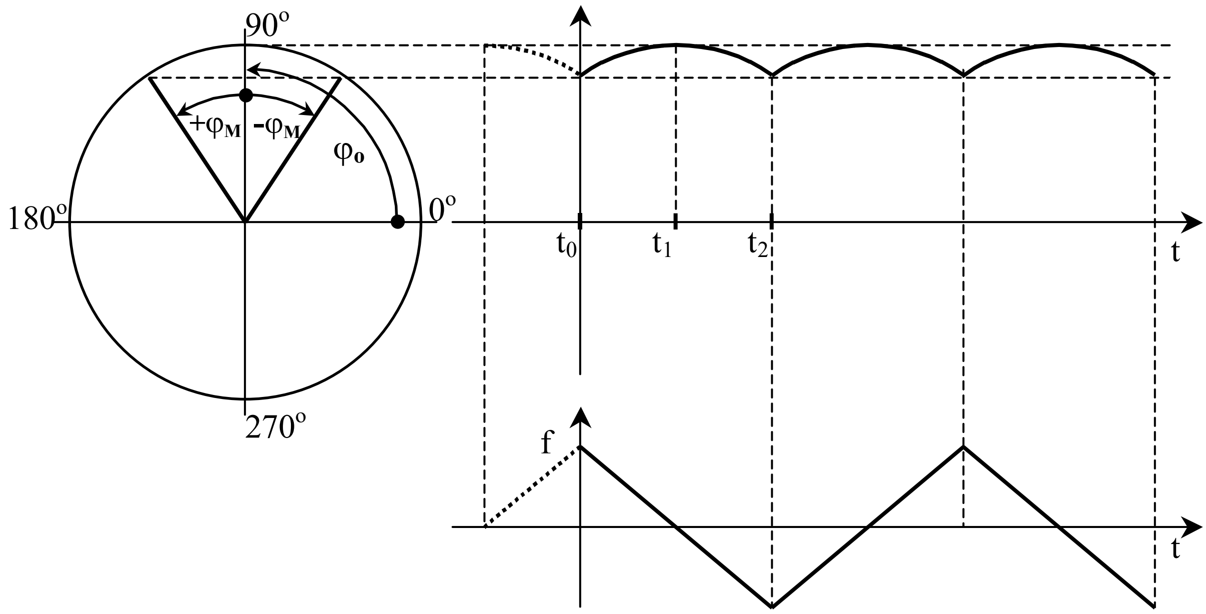

Fig. 12 Formation of the difference signal depending on the changes of the initial and variable phases at an altitude H = l0/8

From the above, it follows that the phase between U_v and U_p oscillates within the range $\varphi_0 + \varphi_M$,to at the frequency f_M. By projecting the sum of both vectors onto the direction of vector Uv and Up we obtain the time variation of the resulting signal amplitude, as illustrated in Fig. 12.

We can see that the amplitude of the modulation envelope reaches its maximum twice and its minimum twice during a modulation period. In this case, the second harmonic component of the resulting signal's frequency spectrum will be the most pronounced. However, the shape of the modulation envelope also indicates the presence of higher harmonic components.

C) <u>Let us assume the altitude</u> $\boldsymbol{H = \frac{3}{16}\lambda_0}$

$$\varphi_0 = \frac{4\pi}{\lambda_0}\frac{3}{16}\lambda_0 = \frac{3}{4}\pi, \qquad \varphi_M = \frac{4\pi\xi}{\lambda_0}\frac{3}{16}\lambda_0 = \frac{2}{3}\xi\pi$$

Graphically, this case is illustrated in Fig. 13. As can be seen from the figure, in this case the amplitude modulation has an asymmetric saw tooth character. During the modulation period T_M the amplitude of the resulting signal reaches one maximum and one minimum value.

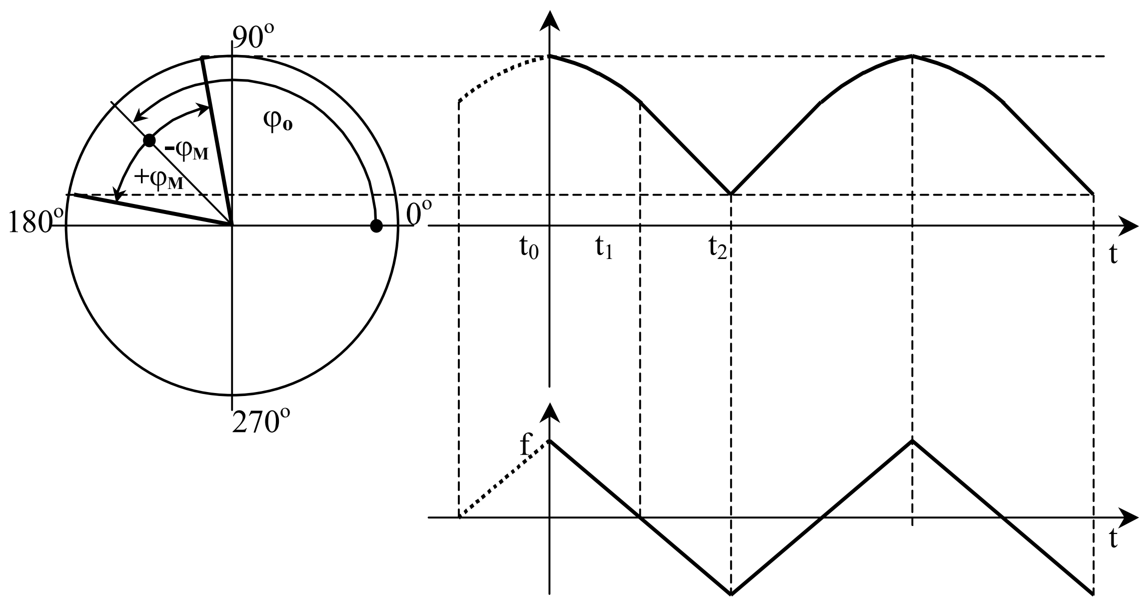

Fig. 13 Formation of the difference signal depending on the changes of the initial and variable phases at an altitude H = (3/16)l₀

D) <u>Let us assume the altitude</u> $H = \frac{\lambda_0}{4}$

$$\varphi_0 = \frac{4\pi}{\lambda_0}\frac{\lambda_0}{4} = \pi, \qquad \varphi_M = \frac{4\pi\xi}{\lambda_0}\frac{\lambda_0}{4} = \xi\pi$$

Graphically, this case is illustrated in Fig. 14.

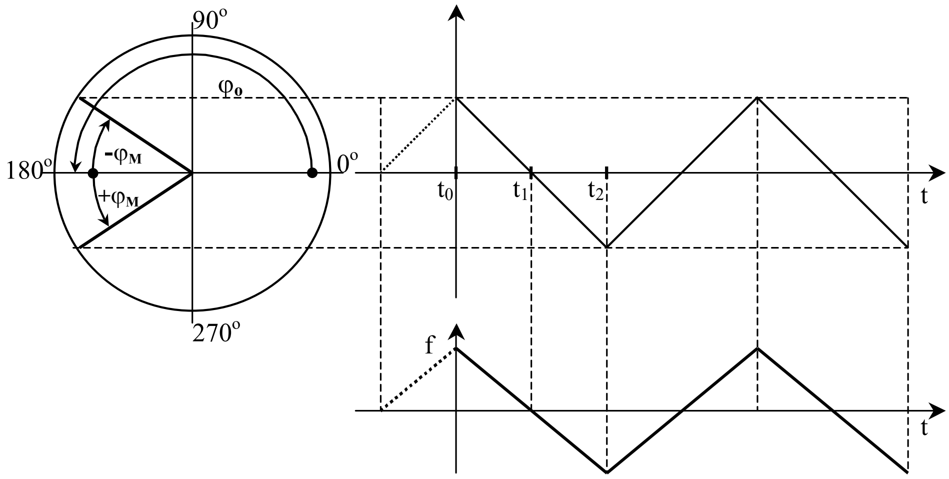

Fig. 14 Formation of the difference signal depending on the changes f the initial and variable phases at an altitude H = l0/4

As can be seen from the figure, in this case the amplitude modulation again has a symmetric sawtooth character. During the modulation period T_M the amplitude of the resulting signal also reaches one maximum and one minimum value.

E) <u>Let us assume the altitude</u> $H = \frac{3}{8}\lambda_0$

$$\varphi_0 = \frac{4\pi}{\lambda_0}\frac{3}{8}\lambda_0 = \frac{3}{2}\pi, \qquad \varphi_M = \frac{4\pi\xi}{\lambda_0}\frac{3}{8}\lambda_0 = \frac{3}{2}\xi\pi$$

Graphically, this case is illustrated on Fig. 15.

Cases b), c), d), and e) show that, with increasing altitude, the difference frequency does not increase as suggested by the simplified theory. Instead, when the altitude changes by $\lambda_0/16$ the character of the modulation envelope of the resulting signal changes abruptly.

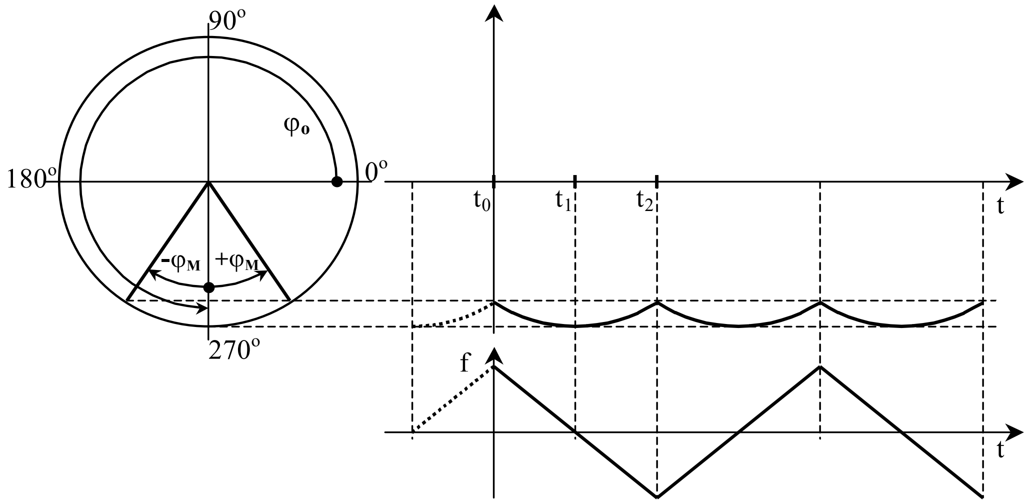

Fig. 15 Formation of the difference signal depending on the changes of the initial and variable phases at an altitude H = $(3/8\lambda_0)$

F) <u>Let us assume the altitude</u> $H = \frac{\lambda_0}{2}$

$$\varphi_0 = \frac{4\pi}{\lambda_9}\frac{\lambda_9}{2} = 2\pi \qquad \varphi_M = \frac{4\pi\xi}{\lambda_9}\frac{\lambda_9}{2} = 2\xi\pi$$

Graphically, this case is illustrated in Fig. 16.

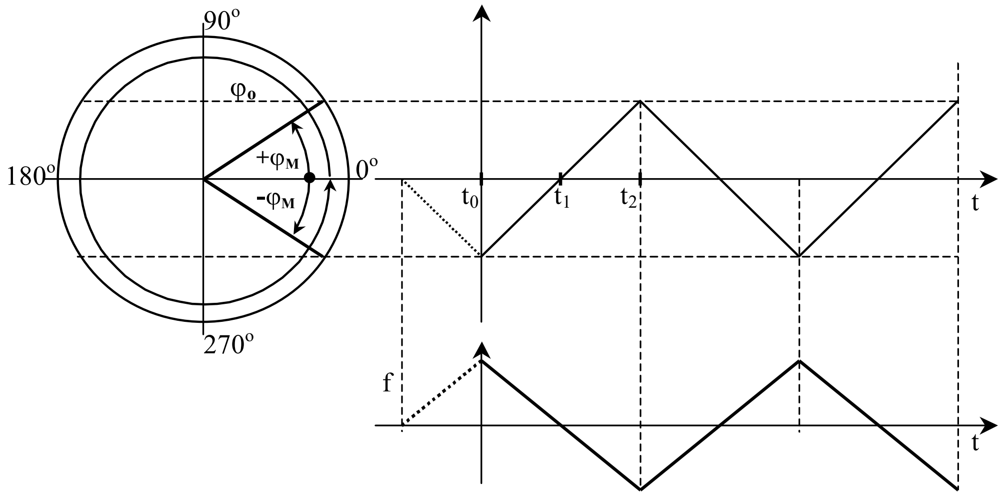

Fig. 16 Formation of the difference signal depending on the changes of the initial and variable phases at an altitude H =$\lambda_9/2$

G) <u>Let us assume the altitude</u> $H = \frac{275}{3}\lambda_0$

$$\varphi_0 = \frac{4\pi}{\lambda_0}\frac{275}{3}\lambda_0 = \frac{1100}{3}\pi, \qquad \varphi_M = \frac{4\pi\xi}{\lambda_0}\frac{275}{3}\lambda_0 = \frac{1100}{3}\,\xi\,\pi = \frac{25}{6}\pi$$

Graphically, this case is illustrated in Fig. 17.

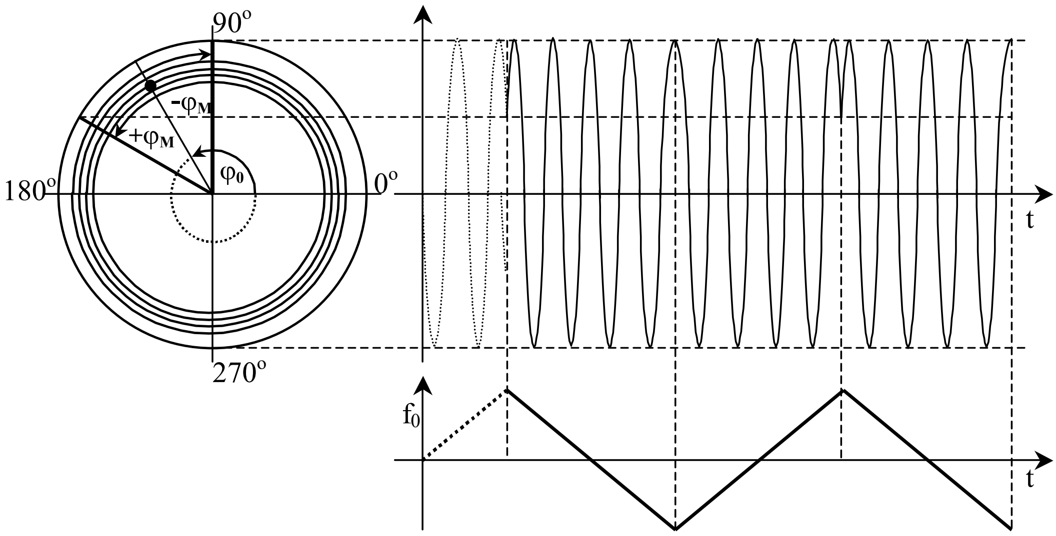

Fig. 17 Formation of the difference signal depending on the changes of the initial and variable phases at an altitude H = (275/3).λ_0

In Fig. 16 the situation is shown where the initial phase φ_0 corresponds to 366 times the value of $p\ +\ 120^0$ These results from measuring a greater altitude, corresponding to (275/3) l0, which for the RV-5 represents an altitude of 6.25 m. In terms of illustrating this phase in Fig. 16, it would require drawing a very large number of circles, i.e., 188 circles. For this reason, only the final position of the initial phase vector φ_0 i.e., 120°, is indicated in the figure. In this case, the value of the variable phase φ_M is equal to (25/6) p, i.e. 750°. The motion of this vector within the range ± φ_M tj. ± 750° is illustrated in the figure. The movement of the vector, which represents the instantaneous phase change φ_M generates the difference frequency f_d. At the moments of increase or decrease of the carrier frequency, the phase of the difference signal rotates by 180°. This phase rotation occurs twice within one modulation period. The position of the phase rotation point depends on the initial phase f_M which in turn depends on the aircraft's altitude H. This situation corresponds to the formation of the difference signal f_d when measuring within the range of real altitudes.

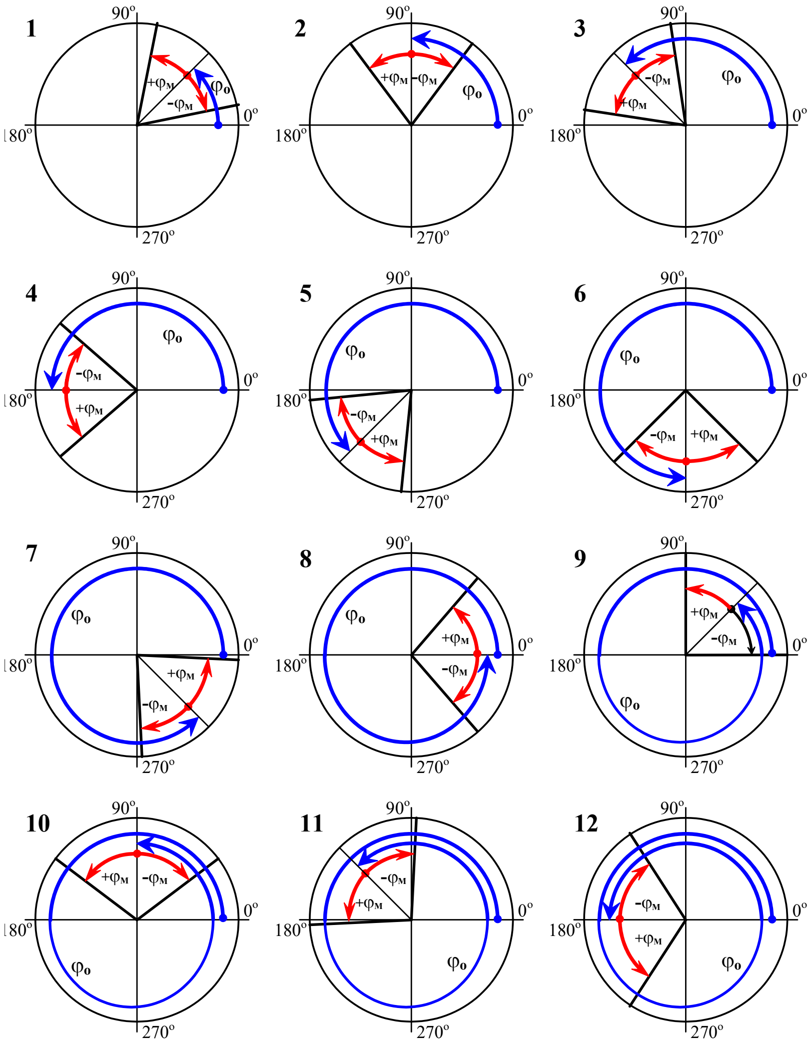

Fig. 18 Formation of the difference signal during real altitude measurement

4.5 Determination of the Frequency f_d of the Difference Signal

In a wideband frequency-modulated radio altimeter, altitude information is evaluated from the value of the frequency f_d of the difference signal. The difference frequency f_d depends on the measured altitude H. This relationship is expressed by the so-called fundamental equation of the radio altimeter:

$$f_d = \frac{8.\Delta f_M}{c}.H \tag{57}$$

The value of the difference signal frequency f_d can be determined mathematically from the following parameters characterizing the difference signal:

a) the time delay τ of the received signal,

b) the variable envelope phase φ_M of the difference signal,

c) the critical altitude ΔH the radio altimeter.

The derivation of the difference frequency f_d from the time delay $\boldsymbol{\tau}$ of the received signal is based on a graphical representation of the frequency variation of the high-frequency signals and, subsequently, on the fundamental rules of trigonometry. The derivation of the difference frequency f_d from the variable envelope phase φ_M of the difference signal is based on the fundamental rules of shaping the phase of the difference signal over one modulation period T_M. The derivation of the difference frequency F_r from the critical altitude ΔH of the radio altimeter is based on the principles governing the generation and disappearance of steady pulses within one modulation period T_M.

4.5.1 Determination of F_d from the Time Delay t of the Received Signal

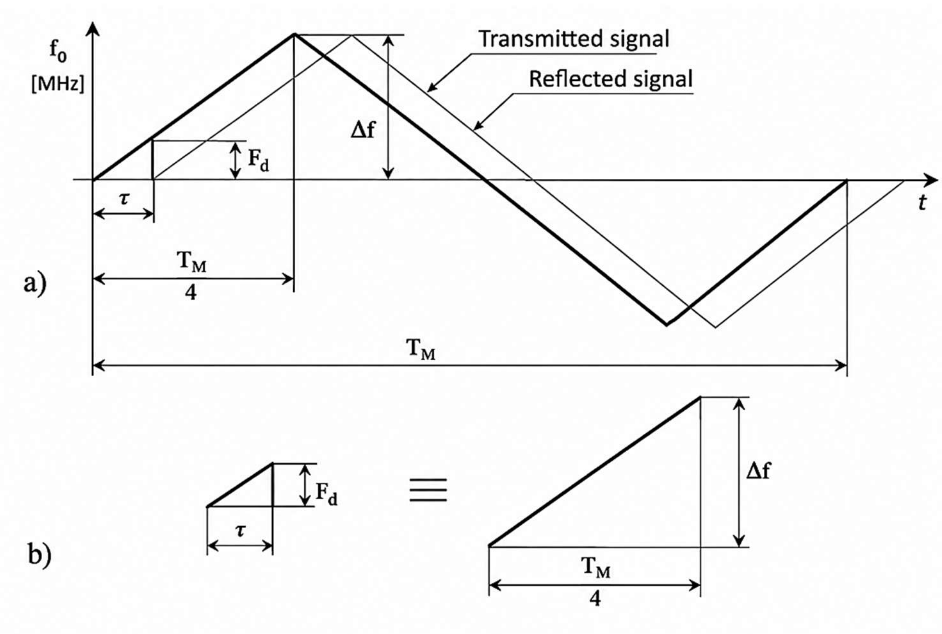

Fig. 19 Time waveforms of the transmitted and received signals of the radio altimeter

From the time waveform in Fig. 19a, it can be seen that the value of the difference frequency depends on the time delay τ of the reflected signal. Based on the similarity of triangles (Fig. 19b) derived from the time waveforms, for which the ratios of the corresponding sides are equal, we can write:

$$\frac{f_d}{\tau} = \frac{\Delta f}{\frac{T_M}{4}} \tag{58}$$

After substituting relation (1) and rearranging, we obtain:

$$\frac{f_d . c}{2H} = \frac{4\Delta f}{T_M} \tag{59}$$

By substituting the modulation frequency T_M for the modulation period F_M, the well-known relation for determining the difference signal frequency is obtained:

$$f_d = \frac{8 . \Delta f . f_M}{c} . H \tag{60}$$

4.5.2 Determination of f_d from the Variable Phase φ_M of the Difference Signal

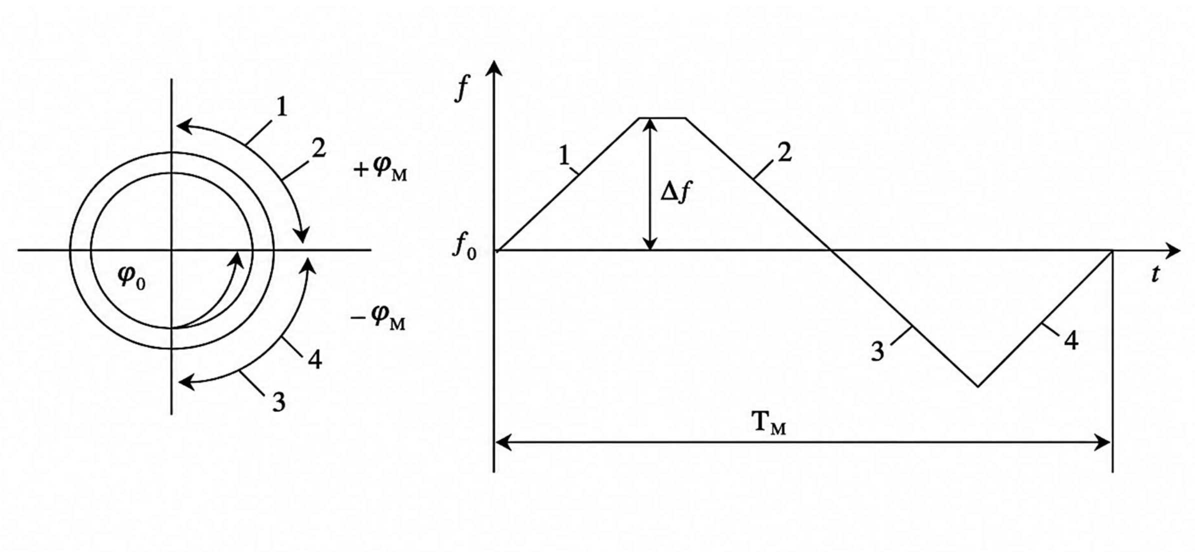

Fig. 20 Relationship between the variable phase φ_M and the time waveform of the RF signal

The variable phase Fig.20 of the modulation signal φ_M is given by the relation:

$$\varphi_M = \frac{4\pi\xi}{\lambda_0} H \tag{61}$$

This phase variation occurs over one quarter of the modulation signal period T_M, which is determined by the angular modulation frequency φ_M. Consequently, the total value of the variable phase φ_M over one modulation period T_M, is given by:

$$\varphi_{MC} = 4\,\varphi_M = \frac{16\pi\xi}{\lambda_0}\,H \tag{62}$$

The number of periods of the difference signal f_{dT} within one period of the modulation signal T_M can be expressed as:

$$f_{dT} = \frac{\varphi_{MC}}{2\pi} = \frac{8\xi}{\lambda_0}\,H \tag{63}$$

If the value f_{dT} is multiplied by the modulation frequency f_M, the difference frequency f_d, t at the given altitude H is obtained:

$$f_d = f_{dT} f_M = \frac{8\,.\zeta f_M}{\lambda_0}\,H \tag{64}$$

4.5.3 Determination of f_d from the Critical Altitude DH of the Radio Altimeter

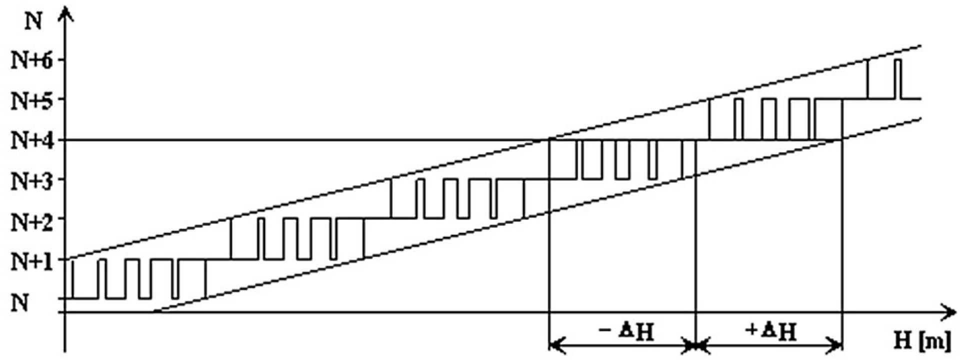

Fig. 21 Indication of the methodical error of the radio altimeter

A change in altitude H corresponds to the generation of X stable pulses per modulation period T_M, .An altitude change of DH corresponds to the generation of one new steady pulse per modulation period T_M (Fig. 21). This fact can be expressed by simple proportionality.

$$\frac{H \;\ldots\ldots\ldots\ldots\; \frac{x}{T_M}}{\Delta H \;\ldots\ldots\ldots\ldots\ldots\; \frac{1}{T_M}} \tag{65}$$

By replacing the modulation period T_M, with the modulation frequency f_M, the following relation can be written on the basis of the direct proportionality:

$$\frac{H}{\Delta H} = \frac{X\, f_M}{f_M} \qquad (66)$$

In relation (66), the numerator term X. f_M, represents the difference frequency f_d, which is directly proportional to the height H. After substituting this relation into the equation and applying a minor modification, the following expression can be written:

$$f_d = \frac{f_M}{\Delta H}\, .H \qquad (67)$$

By substituting expression (8) for the methodological error ΔH, the following relation can be obtained:

$$f_d = \frac{f_M}{\frac{c}{8\Delta f}}\, .H \qquad (68)$$

Then the difference frequency f_d is again given by the relation: $f_d = \frac{8.\Delta f.f_M}{c}\, .H$

5 ERRORS OF AIRCRAFT RADIO ALTIMETERS

Navigation tasks can only be accomplished through the measurement of navigation quantities, one of which is the measurement of an aircraft's flight altitude. This navigation quantity is continuously variable as a result of the aircraft's motion. When assessing the applicability of radio altimeters, two fundamental aspects must be taken into consideration:

a) quantitative - assessing the range of measured altitudes,

b) qualitative - assessing the accuracy of altitude measurement.

The accuracy of altitude measurement can be defined directly by the measurement accuracy parameter, or indirectly through the errors that affect the measurement result.

Absolute and Relative Errors of Altitude Measurement

Errors in altitude measurement can be expressed as:

a) absolute - in the units of the measured quantity,

b) relative - as a numerical ratio, most often expressed as a percentage (%).

Let the measured flight altitude be denoted by the symbol H, and the n-th measurement result byh_nThen the magnitude of the absolute error of altitude measurement Δh je is given by the value by which the result of the n-th measurement differs from the true value of the measured altitude h_0, i.e. from the constant value that should be measured at a given instant. Consequently, it holds that:

$$\boldsymbol{\Delta h = h_n - h_0} \tag{70}$$

The absolute error is most commonly used to define the accuracy of radio altimeters, because it allows different types of radio altimeters to be compared with one another. However, assessing accuracy solely on the basis of this error may lead to a distorted view of the quality of a radio altimeter, since the value $\boldsymbol{\Delta h}$ is determined without regard to the second, quantitative aspect the range of the measured quantity. Therefore, in addition to the absolute error, the so-called relative error (most often expressed as a percentage) is also defined. The relative error is defined as the ratio:

$$\varsigma = \frac{Abslotute\ altitude\ error}{Altitude\ Measurement\ Range}\ .100\% \qquad (71)$$

evaluating radio altimeters solely on the basis of the relative error z may, in some cases, be misleading. Therefore, both the relative error and the absolute error are specified for radio altimeters.

Systematic and Random Nature of Radio Altimeter Errors

Errors of a radio altimeter may be systematic or random in nature.

Systematic errors (v) are usually caused by one or several permanently acting factors, such as incorrect adjustment of the zero altitude on the altitude indicator, replacement of a faulty radio-altimeter component with one having different characteristics, improper antenna installation, etc.

The common characteristics of this type of error are that it occurs in every measurement with the same magnitude and the same sign. Therefore, a systematic error can be identified in practice and eliminated by appropriate means before the measurement process begins.

Random errors (r) are errors that arise as a result of the simultaneous action of a large number of random phenomena. Typical partial phenomena include, for example, instability of the modulation frequency, aircraft flight dynamics, variations in the parameters of the Earth's surface beneath the aircraft, instability of the supply voltage, etc.

Even if it were possible, through more detailed analysis, to evaluate quantitatively and qualitatively the effect of each partial random phenomenon on the value of the resulting altitude-measurement error, in practice the time, cost, and effort required for such an evaluation would in most cases exceed acceptable limits. Therefore, when assessing altitude-measurement results, all such partial errors ρ_{φ} can be regarded as collective random phenomena whose combined effect results in the overall random error ρ. Accurate measurement of the aircraft's true altitude is particularly critical during the flare phase of landing, when the aircraft transitions from descent along the glide path to a small pitch angle relative to the ground in preparation for touchdown. Glide-path radio beacons of meter-wavelength landing systems do not provide, on board the aircraft, the signal required for flight control during this phase. Consequently, in such landing systems, a precision radio altimeter is practically the only means of determining the aircraft's vertical position. At the same time, it is used to calculate the rate of descent, which is essential for controlling the aircraft's longitudinal motion during the flare maneuver.

The accuracy of altitude measurement is characterized by twice the standard deviation, 2δ, which corresponds to a probability of 0.95. This means that the true altitude H lies within the interval [(H - 2δ), (H + 2δ)] with a probability of 0.95. For radio altimeters used in automatic aircraft landing systems, the error magnitude 2δ must not exceed ± 0,2m. In addition, the dependence of the output voltage (or current) on the instantaneous altitude within the range 0 to 30 m must be linear.

The time constant of the radio altimeter must not exceed 0.1 s. Errors in altitude measurement arise due to the action of various and highly diverse causes and under the influence of many different factors. This is because a radio altimeter is a relatively complex radio-electronic device that operates under varying conditions over different types of terrain, at different flight speeds, and dependent on the external power supply.

The main list of radio altimeter errors includes:

1. Methodical Error
2. Doppler Effect Error
3. Shift Error
4. Fluctuation Error
5. Dynamic Error
6. Parasitic Modulation Error
7. Instrument Error
8. Error Caused by External Conditions
9. Errors due to Instability of FM Parameters

5.1 Methodical Error

Methodical error is a fundamental drawback of frequency-modulated radio altimeters with a constant modulation period. It manifests itself as a discrete change of output information during a continuous change of the true altitude._The dependence of the measured altitude H_m (output information) on the true altitude H_{AGL} je is illustrated in Fig. 22.

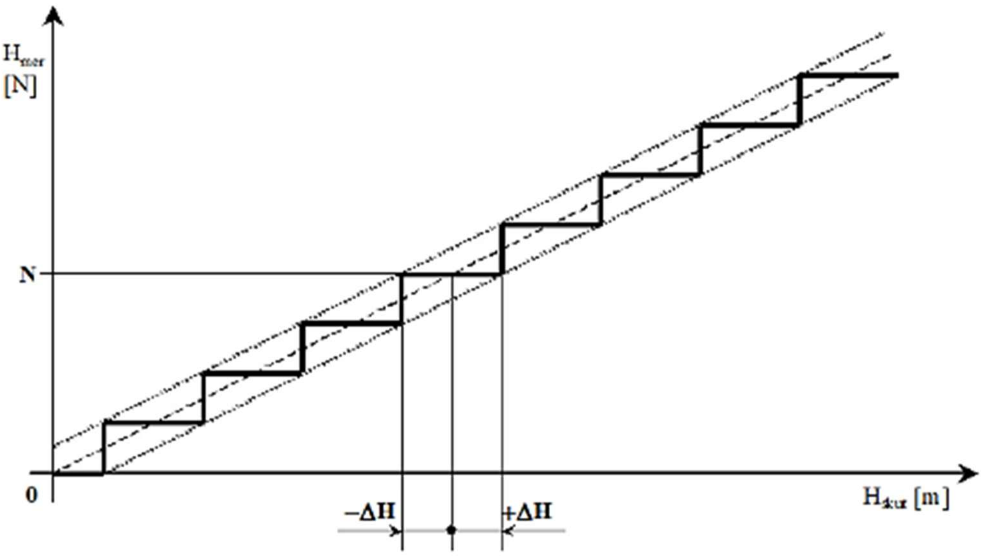

Fig. 22 Dependence of the measured altitude H_m on the true altitude H_{sk}

The cause of the methodological error in continuous-wave, frequency-modulated radio altimeters lies in the inherently periodic nature of the frequency-modulation law. The amplitude spectrum of the difference signal is discrete and contains only frequencies that are integer multiples of the modulation frequency F_M, moreover, as altitude increases, the spectrum of this signal becomes progressively more complex. This fact degrades the determination of the frequency that is proportional to the aircraft's flight altitude.

Therefore, in the processing circuits, pulses are formed from the difference signal, the number of which per modulation period is proportional to the aircraft's flight altitude. Since the frequency meter (counter) determines the number of pulses per second, its output is discrete, with the discreteness of the change in the pulse count being equal to the modulation frequency f_M. These pulses are subsequently fed to a smoothing filter, which ensures their accumulation; as a result, certain additional DC voltage components appear, distorting the output information of the radio altimeter. The methodical error also determines the minimum measurable altitude. The minimum altitude H_{min} is given by the relation:

$$H_{min} = \frac{c}{8\,\Delta f}\,\Delta H \tag{72}$$

In which: Df - frequency deviation, c - propagation velocity of radio waves.

This relation also defines the minimum measurable altitude difference ΔH. Consequently, as the flight altitude increases, the indicated altitude changes in integer multiples of this minimum height increment.

From relation (72) it is evident that, to reduce the error ΔH, it is desirable to use the maximum possible frequency deviation Df. A partial reduction of this error can also be achieved by introducing an auxiliary frequency modulation with a frequency several times lower than the fundamental modulation frequency. Further reduction of the error ΔH can be achieved by employing a number of specialized circuits, which, however, increase the complexity of the radio altimeter. The above-mentioned methodological error applies to radio altimeters employing the direct method of difference-frequency measurement. In recent years, radio altimeters using frequency locking to the evaluated frequency, or radio altimeters with a controlled modulation-frequency period employing a frequency discriminator, have been increasingly used worldwide. This approach is known as the resonant method. When the resonant method is used for measuring the difference frequency, implemented by means of a frequency discriminator with two narrowband tuned circuits, the methodological error in the form of a discrete error does not occur. Nevertheless, a methodical error is still present, caused by the use of narrowband resonant (tuned) circuits in the receiver chain of the radio altimeter. This error also arises because of the periodic nature of frequency modulation, more specifically due to the existence of phase-change zones of the difference signal resulting from step changes in its instantaneous frequency. Such frequency changes induce transient phenomena in the resonant circuits and ultimately lead to the generation of spurious pulses (ringing) in the output voltage of the frequency discriminator. With stable frequency-modulation parameters, this methodical error does not depend on changes in altitude H and is therefore referred to as a static error of the radio altimeter. This error poses the greatest hazard in radio altimeters with a controlled modulation period, such as the RV-5M, during low-altitude flight. At low altitudes, the modulation period T_M of this radio altimeter undergoes only minimal variations, which are comparable to the changes caused by transient phenomena in the receiver. Under these conditions, the accumulation effect of spurious pulses in the altitude-tracking system of the radio altimeter becomes most pronounced. To reduce the methodological error, it is necessary to ensure that the minimum value of the measured modulation-frequency period T_i, is longer than the duration of the transient phenomena in the narrowband receiver of the radio altimeter. In addition, intentional decoupling of the connection between the frequency discriminator and the smoothing filter during the action of transient phenomena makes it possible to increase measurement accuracy at low altitudes. The methodological error of radio altimeters has the greatest impact on the accuracy of altitude measurement; therefore, a separate section 4, entitled "Pulse Shaping in Radio Altimeters," is devoted to this error.

5.2 Doppler Effect Error

Errors of frequency-modulated radio altimeters also include the error caused by the Doppler effect during aircraft climb or descent. To explain the frequency shift of the radio altimeter transmitter signal upon reception due to the Doppler effect, let us assume that the aircraft is descending with a vertical velocity v_v. The electromagnetic wave of the radio altimeter transmitter signal is radiated at a instantaneous transmitted frequency f_v(t) and reaches the Earth's surface with a frequency shift f_{v1}(t) which is given by the relation:

$$f_{v1}(t) = f_v(t)\frac{c}{c - v_v} \tag{73}$$

Let us assume that the aircraft, and thus the signal source, is moving towards the ground, while the observer on the ground remains stationary. The signal is radiated normal to the Earth's surface, and the vertical component of the aircraft's velocity during descent corresponds to the radial component of the propagating signal. This assumption is justified by the very small aircraft velocity compared to the propagation velocity of electromagnetic waves. This condition is influenced by the antenna arrangement on the aircraft fuselage and by the aircraft flight altitude.

Upon reflection of the signal from the Earth's surface, the ground becomes a secondary signal source, and the receiving antenna represents the observer. When the aircraft is descending, this corresponds to the case in which the observer approaches the source, and the frequency of the received signal f_p(t) is given by the relation:

$$f_p(t) = f_{v1}(t)\frac{c + v_v}{c} \tag{74}$$

After modification, we obtain:

$$f_p(t) = f_{v1}(t)\frac{c}{c - v_v} \cdot \frac{c + v_v}{c} = f_v(t)\frac{c + v_v}{c - v_v} \tag{75}$$

This expression represents the Doppler effect. Assuming that v_v << c, we can write in simplified form:

$$f_p(t) = f_v(t)\left(1 + \frac{2v_v}{c}\right) \tag{76}$$

The difference between the frequency of the received signal and that of the transmitted signal is the Doppler frequency f_D :

$$f_D = f_p(t) - f_v(t) = f_v(t)\frac{2v_v}{c} \tag{78}$$

This value of the Doppler frequency represents:

a) an increase in frequency added to the transmitted signal when the aircraft is descending,

b) a decrease in the transmitter frequency when the aircraft is climbing.

For the sake of simplification, let us assume:

$$f_v(t) = f_0 \tag{79}$$

In which: f_0 - mean value of the carrier frequency.

During a dynamic change in the aircraft's flight altitude, the difference frequency, including the Doppler frequency, is expressed by the relation:

$$f_{dD} = f_d \pm f_D = \frac{8\,\Delta f\, f_M}{c}H \pm f_0\frac{2v_v}{c} \tag{80}$$

Figure 23a illustrates the frequency shift of the received signal relative to the transmitted signal caused by *time delay (a)* and *the Doppler frequency during aircraft descent (b).* In Figs. 23b and 23c, it can be observed that when the frequency modulation has the form of a symmetric sawtooth, the difference frequency increases due to the Doppler frequency during one half-period of the modulation frequency and decreases during the other half-period. From the figures, it can be concluded that with symmetric sawtooth modulation, the negative effect of the Doppler frequency does not manifest itself. This is because the frequency increase during the first half-period and the frequency decrease by the same amount during the second half-period do not result in a change of the difference frequency over the entire modulation period. If asymmetric sawtooth modulation is used for frequency modulation, this error has the greatest impact at low altitudes and higher vertical velocities. In this case, the effect of the Doppler frequency is not canceled, and the error is introduced into the difference-frequency evaluation circuit.

This may occur, for example, in the radio altimeter, which is currently in widespread use. Fig. 23. Formation of the difference frequency of the radio altimeter without the Doppler effect.

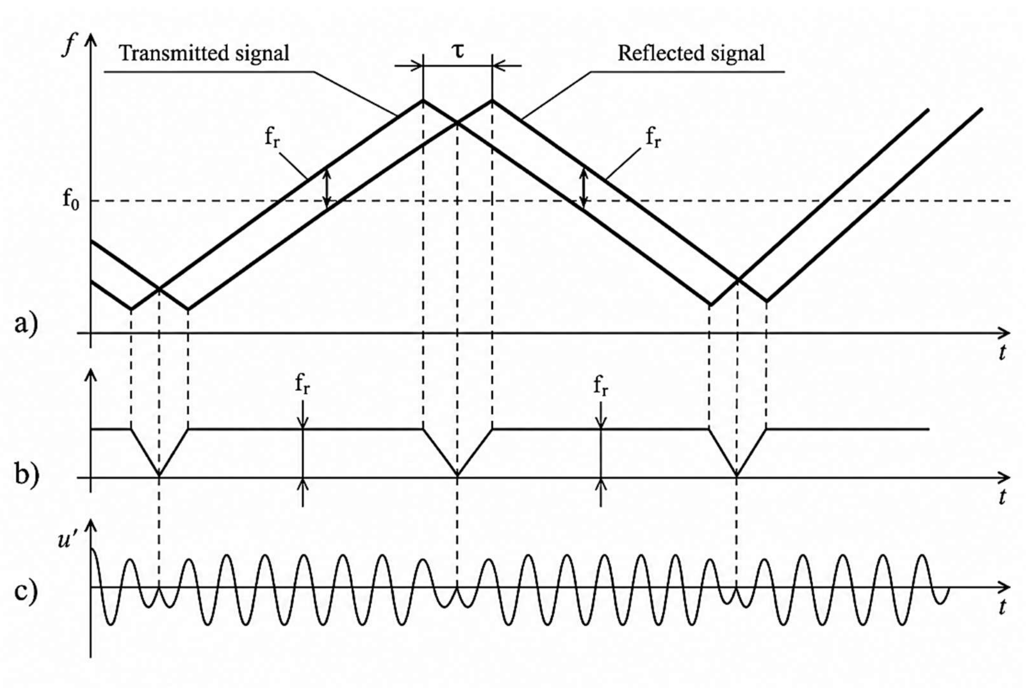

Fig. 23 Effect of the Doppler effect on the formation of the radio altimeter difference frequency

From the above, it follows that a large Doppler frequency increase can significantly influence the measurement result, and for this reason it must be considered primarily during descent. For the calculation of Doppler frequency increases, the vertical velocities of aircraft of the Armed Forces of the Slovak Republic during approach to the flare point were taken as the basis; these values are listed in Table 5.

Table 5

Aircraft Type	L - 39	MiG - 21	MiG - 29	SU - 22	L - 410
Vertical speed to the flare point [km.h^{-1}]	230	355	330	335	180
Calculated vertical speed "v_v" [m.s^{-1}]	5	9	8	6	4
Type of radio altimeter used	RV-5	RV-UM	RV-5M	RV-15	KRA 405
Radio altimeter carrier frequency "f_0" [MHz]	4300	440	4300	4300	4300
Calculated frequency "f_D " [Hz]	143	27	229	172	115

5.3 Shift Error

This is an error caused by a shift of the energy spectrum of the difference signal. The cause of the shift error is:

a) asymmetry of the energy spectrum of the difference signal,

b) a shift of the maximum value of the spectrum to the right along the frequency axis, proportional to the frequency corresponding to a greater height.

It is generally known that the difference-frequency counter evaluates the root-mean-square frequency of the signal spectrum, whereas the frequency discriminator evaluates the mean (centroid) frequency of the signal spectrum. In both cases, however, these evaluated frequencies, as is well known, do not correspond to the frequency associated with the actual measured altitude.

The shift error depends on:

a) the shape of the spectrum of the additive mixture of the difference signal,

b) internal noise propagating to the input of the frequency evaluator,

c) the signal-to-noise ratio at the input of this evaluator,

d) the width of the antenna radiation pattern,

e) the aircraft flight altitude,

f) the aircraft attitude (tilt or pitch angle).

This error has a random character, because the shape of the spectrum of the difference signal is determined by the characteristics of the illuminated surface, which in practice cannot be predicted.

To reduce the shift error, it is necessary to ensure:

a) a high signal-to-noise ratio at the input of the frequency evaluation circuit,

b) a receiver bandwidth that corresponds to the bandwidth of the difference signal.

It is also possible to use special circuits that ensure the separation and measurement of the left-hand edge frequency, which is a component of the signal spectrum and is located close to the evaluated frequency.

Explanation of the frequency shift error

The radiation patterns of transmitting and receiving antennas are generally identical and symmetrical about their axis. If we assume horizontal flight of the aircraft over a homogeneous and isotropic ground surface, the reflection pattern of the ground surface will also be directional and symmetric about its axis. All elementary reflectors on the ground surface can be arranged into rings $\Delta S_0, \Delta S_1, \Delta S_2, \Delta S_3, \ldots \Delta S_n$, which correspond to different slant ranges R_0, $R_1 R_2 R_3 R_n$ associated with illumination angles Θ_0, $\Theta_1 \Theta_2 \Theta_3 \Theta_n$ (Fig. 24). The true flight altitude H corresponds to the difference frequency F_{r0} obtained from the area ΔS_0, which represents a small surface located exactly around the foot of the perpendicular dropped from the aircraft to the ground surface and corresponding to the first Fresnel zone. The energy spectrum G_0(t) of this signal is concentrated around the frequency F_{r0}, the value of which corresponds to the flight altitude of the aircraft, R_0 H. The energy spectrum G_0(t) of the signal u_{Fr0}(t) is shown in Figure 24. The difference signal $u_{fd1}(t)$ obtainded from the first ring ΔS_1 has an amplitude energy spectrum G_1(f) concentrated around the difference frequency F_{r1}, the value of which corresponds to the slant range of the aircraft R_1

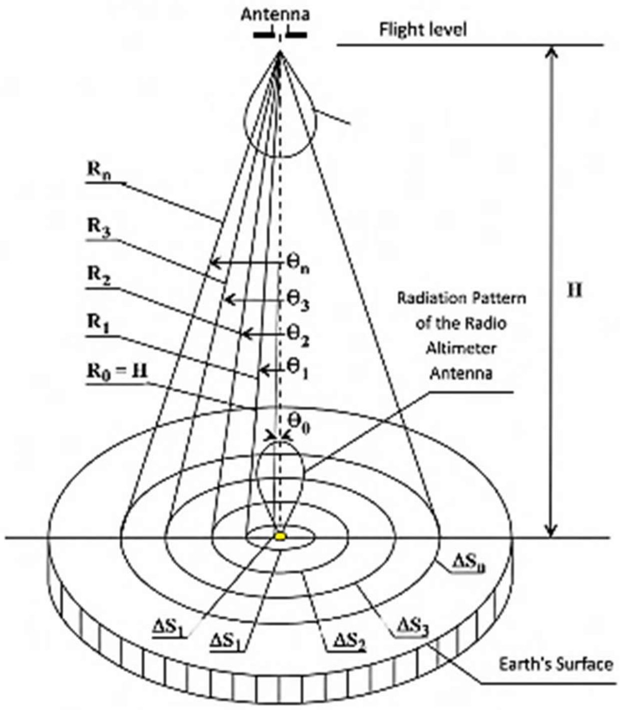

Fig. 24 Relationship between the radius of illumination of the Earth's surface and the slant range

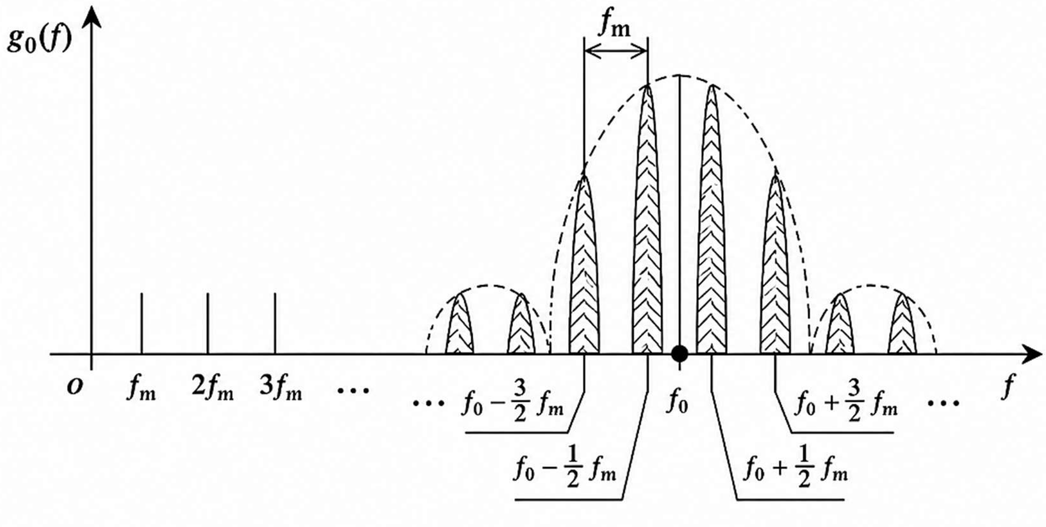

Fig. 25 Energy spectrum of the signal $u_{fd0}(t)$ of the difference frequency f_{d0}

In general, we can state that the difference signal $u_{fdn}(t)$ obtained from the n-th ring ΔS_n is random, and its energy spectrum G_n(t) is concentrated around the frequency f_{dn}. The measured value of the difference frequency then corresponds to the slant range R_n to the aircraft. This situation is illustrated in Fig. 26. The energy spectrum G_s(f) of the composite (summed) signal u_{fd}(t) is the superposition of the individual energy spectra. Its envelope has a maximum frequency $F_{r\,max}$, which in the general sense does not have to coincide with any of the individual frequencies f_{dn}. It is therefore evident that the maximum of the envelope of the total energy spectrum G_s(f) corresponds to a signal obtained from elementary scatterers located on intermediate rings of slant ranges, and that it does not originate from the ring ΔS_0 under any circumstances. Consequently, the evaluated frequency f_d, which corresponds to the frequency f_{dmax}, is higher - i.e. shifted in the frequency spectrum - than the frequency f_{d0}, which corresponds to the true flight altitude of the aircraft above the ground surface. With increasing altitude, the dimensions of the illuminated surface increase, which in turn increases the magnitude of the frequency shift and thus the altitude-measurement error.

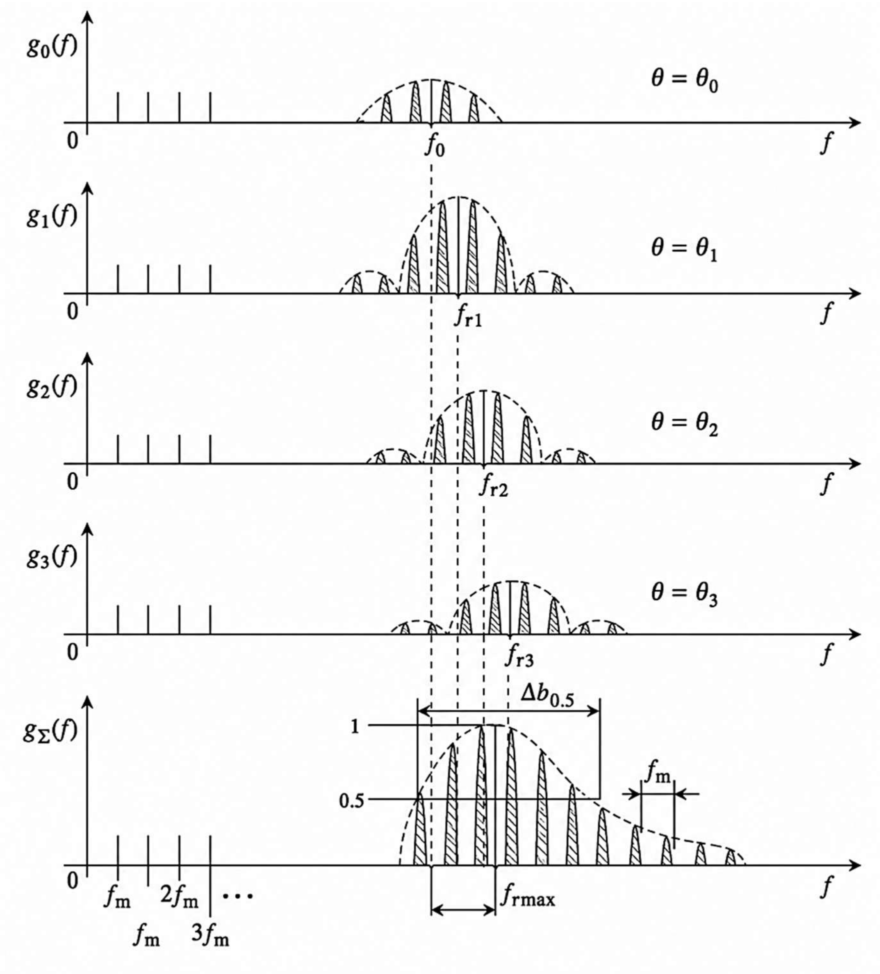

Fig. 26 Shaping of the Energy Spectrum of the Difference Frequency f_d

For practical applications, the spectrum bandwidth (measured at the half-power level) may be considered sufficient when it reaches the value:

$$B_{0,5} \leq (0.03 \div 0.05) f_{d0} \tag{81}$$

The shape of the envelope of the received signal spectrum depends predominantly on the radiation pattern of the transmitting antenna and on the reflective properties of the ground surface.

5.4 Fluctuation Error

The fluctuation error in altitude measurement is caused by the random nature of the reflected signal and by the influence of the receiver's internal noise. The altitude measurement error caused by fluctuation has a normal (Gaussian) distribution; therefore, a sufficient characteristic of this error is the variance δ^2. At low flight speeds and with low inertia of the radio altimeter, a different error distribution may occur. In such cases, in addition to the dispersion characteristic, it is necessary to introduce another characteristic - namely, the probability that the error does not exceed a specified value.

It is known that the level of fluctuation errors for any radio altimeter is determined by:

a) the parameters of the modulation signal,

b) the signal-to-noise ratio,

c) the parameters of the radio altimeter,

d) the bandwidth of the fluctuation spectrum of the input signal.

When the signal is reflected from the Earth's surface, the bandwidth of the fluctuation spectrum depends on:

a) the properties of the Earth's surface,

b) the directional characteristics (radiation patterns) of the antennas,

c) the aircraft's flight speed,

d) the parameters of the modulation signal.

Fluctuation errors depend on all of the above-mentioned factors, and their distribution law is non-stationary, with a varying variance depending on the aircraft's flight path.

To reduce fluctuation error, it is necessary to ensure a higher signal-to-noise ratio at the input of the frequency evaluation unit and to select the largest possible time constant of the smoothing filter that determines the time constant of the entire radio altimeter.

5.5 Dynamic Error

The dynamic error of a radio altimeter can be divided into two groups:

a) dynamic error caused by the inertia of the radio altimeter,

b) error caused by the flight dynamics of the aircraft.

a) Dynamic error caused by the inertia of the radio altimeter during altitude measurement results from the inertial properties of the electronic circuits and the mechanical moving parts of the radio altimeter. This error causes the indicated altitude to continuously lag behind the true instantaneous altitude of the aircraft above the terrain. To reduce the dynamic error, it would be desirable to select the smallest possible value of the radio altimeter time constant. However, this requirement conflicts with the requirement on the time constant imposed by errors caused by signal fluctuations. In practice, the time constant of the radio altimeter is therefore chosen as a compromise, such that the sum of the mean square fluctuation error and the dynamic error is minimized. It is generally stated that the time constant of a radio altimeter should not exceed 0.1s.

b) Error caused by the flight dynamics of the aircraft arises as a result of the use of directional antennas installed on board the aircraft.

During aircraft roll and pitch maneuvers, due to the use of directional antennas, the true flight altitude H is not measured. Instead, the slant range H_n is measured (Fig. 27). In this case, the true flight altitude is given by:

$$H = H_n \cos\gamma \tag{82}$$

In which: γ - aircraft attitude angle (roll/pitch angle).

Thus, the altitude measurement error caused by the use of directional antennas is:

$$\Delta H_S = H_n - H \frac{1 - \cos\gamma}{\cos\gamma} \tag{83}$$

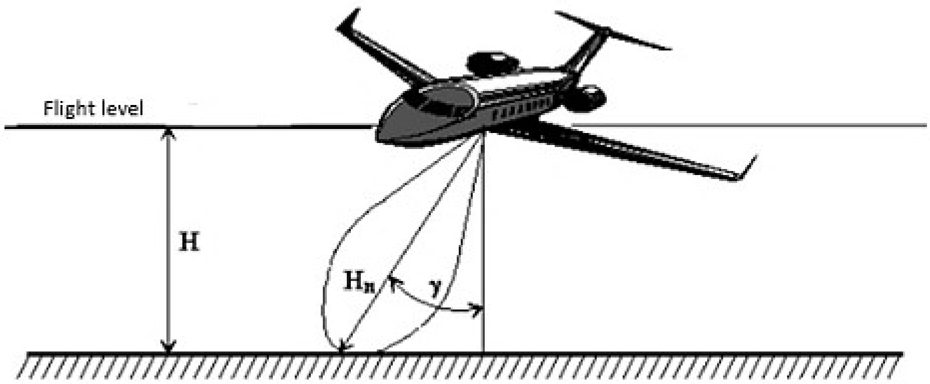

Fig. 27 Effect of the bank (pitch) angle on the measured altitude

From relation (82) it follows that the resulting altitude-measurement error is proportional to the magnitude of the bank (pitch) angle and can be reduced by widening the antenna radiation patterns. However, widening the directional characteristics degrades the radio altimeter's immunity to interference. For this reason, when the bank (pitch) angle exceeds the permissible limit (with respect to the width of the radiation patterns), the radio altimeter readings should be considered invalid. Radio altimeters use antennas with a beamwidth of approximately 45° to 50°, which means that the radio altimeter readings are considered valid for bank (pitch) angles up to about 22.5° to 25°. In this case, the true flight altitude is:

$$H = (\ 0{,}92\ till\ 0{,}9)H_n \tag{84}$$

The error in measuring the true altitude of an aircraft above the terrain caused by the use of directional antennas is:

$$\Delta H_s = (\ 8\ till\ 10)H \tag{85}$$

5.6 Parasitic Modulation Error

This is an error caused by an unwanted (parasitic) change in the amplitude of the received radio altimeter signal.

Parasitic modulation arises:

a) due to parasitic amplitude modulation,

b) due to a parasitic (interfering) signal.

Both causes have approximately the same effect on the error and on the operation of the radio altimeter. The presence of parasitic amplitude modulation and various parasitic signals penetrating the receiver input creates a parasitic signal spectrum within the received-signal band. These components propagate to the input of the frequency-evaluation circuit and thereby distort the measurement result. These adverse effects also degrade the sensitivity of the radio altimeter in the mode of acquiring the useful signal.

a) Parasitic modulation caused by unwanted amplitude modulation

In most types of radio altimeters, the balanced mixer is designed so that, in addition to generating the difference frequency, it simultaneously suppresses parasitic amplitude modulation.

Amplitude modulation of the radio frequency (RF) carrier is undesirable for the operation of a radio altimeter and is therefore suppressed. Amplitude modulation itself arises from the following causes:

1. Antennas and other RF circuits tuned to the center of the high-frequency band exhibit lower gain at the band edges. As a result, the transmitted and received RF signal energy is lower at the edge frequencies. This leads to parasitic modulation of the carrier. In this case, the parasitic modulation frequency is equal to the transmitter's modulation frequency.

2. Non-uniform reflection coefficients of the ground surface, from which the RF energy of the radio altimeter transmitter is reflected back towards the aircraft.

Method of AM modulation suppression

A circuit that provides more than tenfold suppression of AM modulation is shown in Fig. 28. It should be emphasized that the suppression of AM modulation in the balanced mixer takes place directly at the receiver input, before the actual processing of the signal carrying information about the measured altitude. Resistors R1 and R2 limit the effect of aging of diodes D1 and D2, resistor R3 serves as a load and, by means of its slider, allows adjustment of the balance of the mixer circuits between points 3 and 4. Since only the circular waveguide section between points 4-2-3 participates in both the generation of the difference frequency and the suppression of amplitude modulation in the mixer, this section from Fig. 28 is redrawn as an electrical equivalent circuit, shown in Fig. 29.

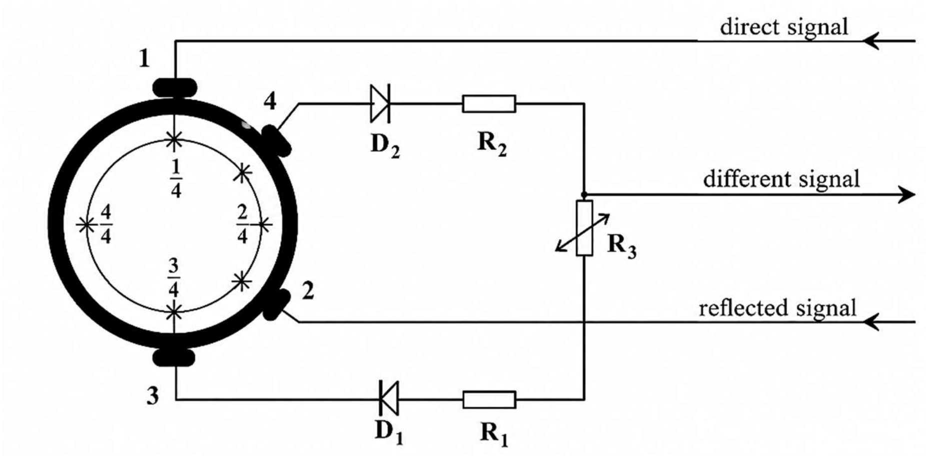

Fig. 28 Simplified circuit of a balanced mixer

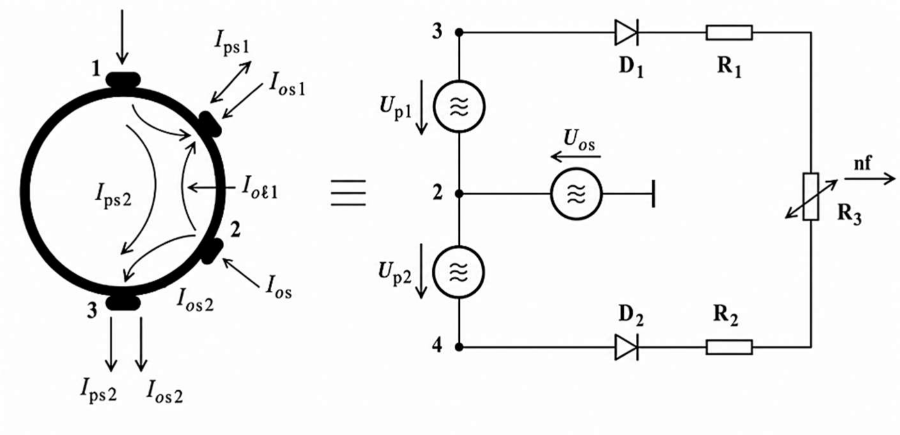

Fig. 29 Equivalent electrical circuit of the balanced mixer

The electromotive force that enables the transfer of RF energy of the direct signal from input 1 to output 3 is, in Fig. 28, redrawn for section 3-2 as the voltage source U_{p1} and for section 2-4 as the voltage source U_{p2}. By analogy, the corresponding current is denoted as I_{PS} with components I_{PS1} and I_{PS2} and the current of the reflected signal as I_{OS} with components I_{OS1} and I_{OS} . The source of the reflected signal is denoted as U_{OS}. From what has been stated so far, the unwanted amplitude modulation appearing at the receiver input is imposed only on the signal reflected from the ground, U_{OS}. The direct signal does not contain this parasitic modulation. Therefore, for the purpose of explaining the method of suppressing this modulation, the equivalent circuit in Fig. 28 can be further simplified by omitting the sources of the direct signal U_{p1}. and U_{p2} The diodes D1 and D2, which are driven by the voltage of the direct signal, are replaced by their dynamic resistances R_{D1} and R_{D}. The circuit redrawn in this manner is shown in Fig. 30.

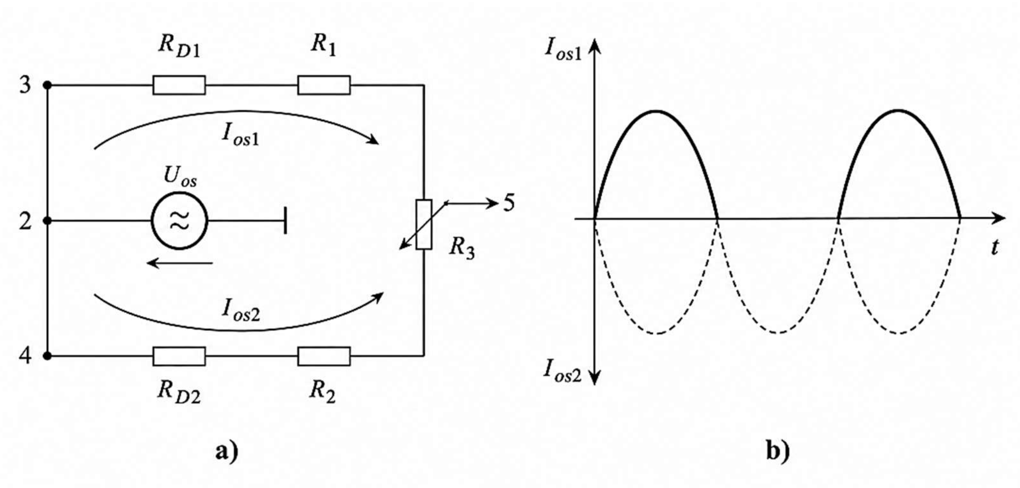

Fig. 30 Ratios in the balanced mixer for the case of amplitude modulation suppression

As is evident from Figures 29 and 30a, the reflected signal - represented in Fig. 30a by the source U_{OS} and fed into the waveguide at point 2 - arrives at outputs 3 and 4 in the same phase due to the equal distance l/4. The currents I_{OS1} a I_{OS2} flow through resistor R3 in opposite directions, so the resulting current is zero:

$$I_{\Sigma} = I_{OS1} + (-I_{OS2}) = 0 \tag{86}$$

This situation is shown graphically in Fig. 30b. We can see that with properly adjusted symmetry of the balanced mixer's arms, the output voltage taken from potentiometer R3 will be zero for the reflected signal. This means that the unwanted amplitude modulation has been suppressed. The operating mode of diodes D1 and D2 is set by controlling the amplitude of the direct signal, while the balancing potentiometer R3 ensures the suppression of amplitude modulation.

From the output of the balanced mixer, the difference-frequency signal is fed into the input of the difference-frequency amplifier.

b) Parasitic modulation caused by parasitic (interfering) signals

Parasitic modulation can also arise due to parasitic signals at the input of the receiver section of the radio altimeter.

Parasitic signals include:

a) the radio altimeter's own modulation signal,

b) signals received through the side lobes of the radio altimeter's antenna,

c) signals reflected from various structural elements of the aircraft,

d) signals that, especially at low altitudes, reach the input after multiple reflections between the ground and the aircraft,

e) modulation and reflected signals from a second radio altimeter if two are operating simultaneously on board.

To reduce the influence of parasitic amplitude modulation, the central value of the radiated frequency of the radio altimeter in the centimeter-wave range is deliberately selected. This ensures that, for the required frequency deviation, the level of parasitic amplitude modulation does not exceed the permissible limit.

5.7 Instrument Error

This is an error caused by the radio altimeter as a measuring instrument. Instrumental errors of a frequency modulated radio altimeter include:

a) Error in evaluating the difference frequency - counter error.

b) Error in altitude indication.

a) The error in evaluating the difference frequency has a significant impact on the accuracy of altitude measurement. The error in a difference-frequency evaluation circuit of the zero-counter type can essentially be caused by:

1) instability of the signal amplitude-limiting level,

2) instability of the counted pulse duration,

3) drift of the DC amplifier zero.

The error in a difference-frequency evaluation circuit of the frequency discriminator type can essentially be caused by instability of the tuned frequency.

To stabilize this parameter, it is possible to use:

1) an automatic tuning circuit for the evaluated frequency,

2) the use of highly stable components in the discriminator circuit.

b) The altitude indication error is determined by the accuracy class of the altimeter indicator used in the radio altimeter. For analog indicators, this error can range from tenths to a few percent of the measured altitude. The indication error can be reduced by using indicators with digital altitude readout. Table 6 shows the error introduced into the altitude measurement results by the altimeter indicator itself.

Table 6

No.	Measurement error		RV-5	RV-5M	KRA405
1	Altitude measurement range: 0 to 10 m	Voltage, analog output	±0,6m	±0,6m	±0,9m
		Altitude indicator	±0,8m	±0,8m	±1,2m
2	Altitude measurement range: over 10 m	Voltage, analog output	±6%	±6%	±5%
		Altitude indicator	±8%	±8%	±7%

5.8 Error Caused by External Conditions

This is an error caused by the conditions under which the radio altimeter operates. This error can be caused by changes in the properties of the environment surrounding the radio altimeter, for example:

a) pressure, temperature, humidity,

b) shocks, impacts, vibrations, acceleration,

c) acoustic noise,

d) precipitation, weather conditions,

e) electrical discharges, radioactivity,

f) other external conditions, such as improper placement, unsuitable orientation, proximity of nearby objects, etc.

For radio altimeters, this is indicated in tactical-technical data as external influences, under which the radio altimeter still operates reliably while maintaining the specified measurement accuracy. Table 7 lists the external influences for some types of radio altimeters.

Table 7

No.	External Influence	RV-5	RV-5M
1	Acoustic noise – intensity: in the range from 50 Hz to 10 kHz	to 125 dB	X
2	Acoustic noise in the real noise spectrum – intensity:	to 135 dB	to 130 dB
3	Acceleration: with frequency:	5g 10 to 300Hz	5g 5Hz to 2kHz
4	Shock overload: – number of shocks / min: – allowable overload:	40 to 80 6g	40 to 80 8g
5	Minimum temperature:	-50 ° C	-55 ° C
6	Maximum temperature:	+50 ° C	+55 ° C
7	Maximum temperature for short-term exposure up to 15 min:	X - manufacturer does not specify.	+ 70 ° C
8	Permissible drop in atmospheric pressure: – at ambient temperature:	26,664kPa -40 ° C	5,46 kPa +25 ° C
9	Relative humidity: – at temperature:	85 to 89 % +(25to35) ° C	98% 35 ° C

5.9 Errors due to Instability of FM Parameters

It is an error caused by the instability of the modulation signal parameters. This group primarily includes errors caused by:

a) instability of the frequency deviation Δf,

b) instability of the modulation frequency f_M,

c) nonlinearity of the frequency modulation,

A significant reduction of this error can be achieved by using circuits that stabilize the parameters Δf, f_M and the slope of the f_M modulation law, or by using the automatic tuning mode of the radio altimeter. At the same time, instability of the mean value of the transmitted frequency f_0 does not cause an error in altitude measurement. This error also includes nonlinearity of the frequency swing itself. Correction of this deficiency is usually carried out by incorporating circuits into the automatic calibration system that influence the linearity of the frequency deviation. The stabilization of f_M parameters receives the greatest attention in the design of radio altimeters. Instability of f_M parameters negatively affects the stability of the radio altimeter constant, which ultimately results in a nonlinear relationship between the true altitude and the measured result. For this reason, this error is treated in a separate chapter titled "Stabilization of the Radio Altimeter Constant".

5.10 Evaluation of Radio Altimeter Errors

Low-altitude radio altimeters currently used in aviation measure the true flight altitude based on the evaluation of the difference frequency. An analysis of the errors of these altimeters shows that various factors influence the overall measurement accuracy. Based on the analysis conducted analysis of low-altitude radio altimeter errors, it is possible to determine the percentage contribution of each type of error to the total altitude measurement inaccuracy for frequency-modulated altimeters operating in the 4.4 GHz band. The percentage distribution can be presented under the following assumptions:

1) the aircraft is flying in horizontal flight over a flat terrain,

2) external conditions are within allowable tolerances, *3) the altitude reading is in the form of a direct-current voltage (not a visual reading from an altitude indicator).*

Based on the stated conditions, the total error of the radio altimeter (100%) is distributed as follows:

- *Methodical error …………………………......……………...... 70%,*
- *Error due to instability of FM parameters…………………. 20 %,*
- *Error due to aircraft flight dynamics……………………… 6%,*
- *Remaining errors…………………………………………. 4 %.*

From this analysis, it follows that for frequency-modulated radio altimeters measuring low altitudes, their measurement accuracy is primarily limited by methodical error. This error causes the resulting altitude reading to have a discrete character.

6 STABILIZATION OF THE RADIO ALTIMETER CONSTANT

6.1 Radio Altimeter Constant

A simplified functional diagram of a frequency-modulated radio altimeter is shown in Fig. 31.

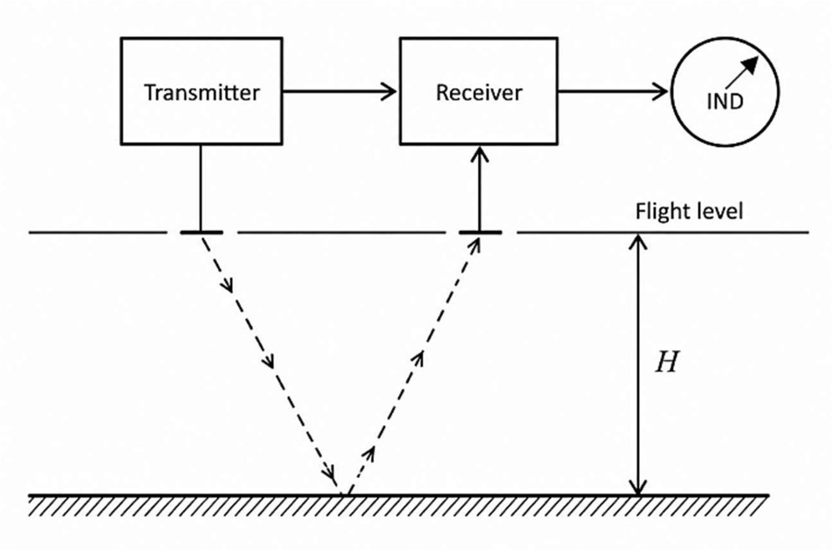

Fig. 31 Simplified operational diagram of the radio altimeter

As shown in this figure, the transmitting antenna radiates a high-frequency, frequency-modulated signal towards the ground. For simplicity, let us assume it is a linear frequency modulation with a modulation period T_M and a frequency deviation Δf_0 . A portion of the reflected signal is received by the receiving antenna after a certain time and is fed into the receiver. Simultaneously, a portion of the transmitter's signal, called the direct signal, also enters the receiver. The received signal in the frequency domain is an exact copy of the transmitted signal, only delayed in time by τ. This situation is illustrated in Fig. 31. By evaluating the instantaneous frequency difference between the direct and reflected signals in the balanced mixer, a so-called difference frequency f_D is generated, which is defined by the relation:

$$f_d = \frac{4\Delta f f_M}{c} H \tag{87}$$

In radio altimeter theory, the term in the fraction given in relation (88) is called the radio altimeter constant, which serves to determine the difference frequency of the measured signal.

$$\frac{4\Delta f f_M}{c} = K \tag{88}$$

For the proper operation of the radio altimeter, it is necessary to ensure that the frequency deviationΔf and the modulation frequency f_M remain sufficiently stable. Otherwise, an altitude measurement error occurs due to the instability of the frequency modulation parameters.

Changes in the values of the components Δf and f_M can occur due to:

- changes in aircraft operating conditions:
- *variation in onboard electrical load,*
- *shocks and vibrations during flight,*

changes in flight dynamics:

- *aircraft attitude,*
- *sudden changes in altitude, pitch, and bank angle during flight,*

changes in physical properties of the surrounding atmosphere:

- *changes in temperature, pressure, humidity,*

changes in antenna load during flight over varied terrain:

- *arable land, forests, cities, water, etc.,*

instabilities of the radio altimeter itself:

- *slow and rapid changes in altimeter parameters due to aging, heating, and other stresses on components.*

In the early stages of development, evaluating the radio altimeter constant was not given much importance, because the instability of this constant caused a very small percentage error compared to the methodological error of these radio altimeters. It was only later when radio altimeters began to be used in the 4300 MHz frequency band - significantly reducing their methodological error (e.g., RV-5) that the error caused by the instability of the radio altimeter constant became comparable to this methodological error. In these newer radio altimeters, circuits have already been implemented that evaluate the instantaneous value of the altimeter constant and ensure its correction.

6.2 Evaluation of the Instantaneous Value of the Radio Altimeter Constant

In evaluating the instantaneous value of the radio altimeter constant, an indirect measurement of the time τ_{et} is used. This time represents the passage of a sample of the transmitted signal through a reference delay line, which introduces a delay proportional to a reference altitude H_{et}.

Passing the signal through the reference delay line simulates the reference altitude H_{et}. In practice, the reference altitude is typically 15 m. The reference delay line is a thin coaxial cable, physically integrated into the radio altimeter. The actual length of this coaxial cable l_{et} corresponds to twice the reference altitude, multiplied by the shortening factor "ζ" of the coaxial cable:

$$l_{et} = 2.H_{et}\ .\xi \qquad (89)$$

The time delay τ_{et} for the passage of a signal sample through the delay line is given by the relation:

$$\tau_{et=}\frac{l_{et}}{c} \qquad (90)$$

The operating principle can be traced from the following figure.

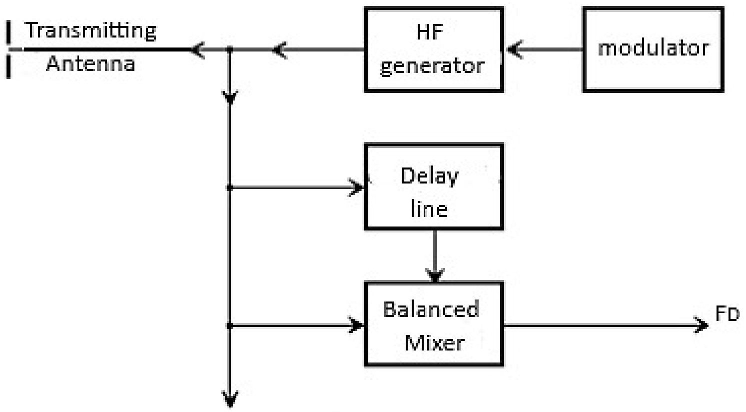

Fig. 32 Principle of Evaluating the Instantaneous Value of the Radio Altimeter Constant

A portion of the signal generated by the high-frequency transmitter of the radio altimeter is fed both into a delay line and into a balanced mixer. Simultaneously, the signal that has passed through the delay line with a delay time proportional to the selected reference height H_{et} (15m) is also fed into the balanced mixer. The resulting low-frequency difference signal f_d, created by mixing the direct and delayed signals at the mixer output, is proportional to the equivalent height H_{et} Assuming that all components of the radio altimeter constant remain unchanged during flight, the frequency of the output low-frequency difference signal f_d also remains constant. If any component of the radio altimeter constant changes - due to one of the causes mentioned earlier - the value of the difference frequency f_d changes even though the delay time τ_{et} remains constant. The effect of a change in the respective component on the difference frequency can be observed in Figures 33 and 34.

In Fig. 33, the influence of a change in the modulation frequency f_M (illustrated by the change in the modulation period T_M) on the value of the difference frequency f_{dk} is shown, assuming that the frequency deviation Δf remains constant. If we assume that the situation in Fig. 33b occurs without the negative influence of the modulation frequency, then the value f_{d2} in this figure corresponds to the reference height H_{et}. If, however, the value of the modulation frequency f_M increases, which is manifested by a decrease in the modulation period T_M the difference frequency f_d also increases (see Fig. 33a). This condition represents a change in the value of the radio altimeter constant. In the case of a decrease in the modulation frequency f_M, which results in an increase in the modulation period T_M the difference frequency f_d decreases, as shown in Fig. 33c. In this way, any unfavorable change of the constant caused by a change in the modulation frequency of the radio altimeter is manifested.

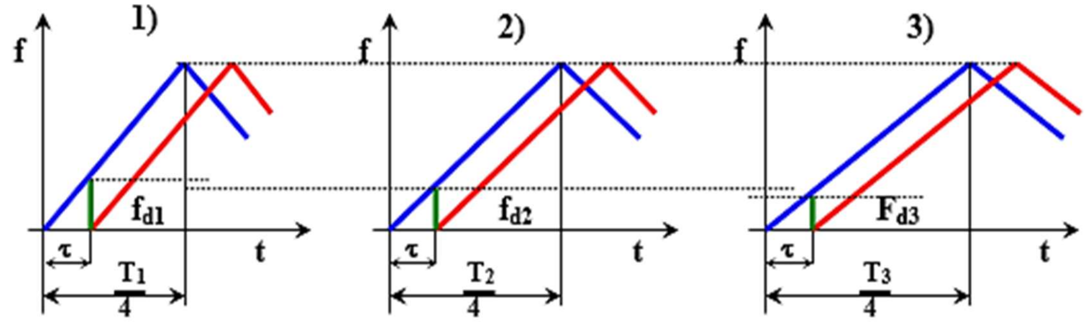

Fig. 33 Effect of a Change in the Modulation Frequency Period T_M on the Value of f_d

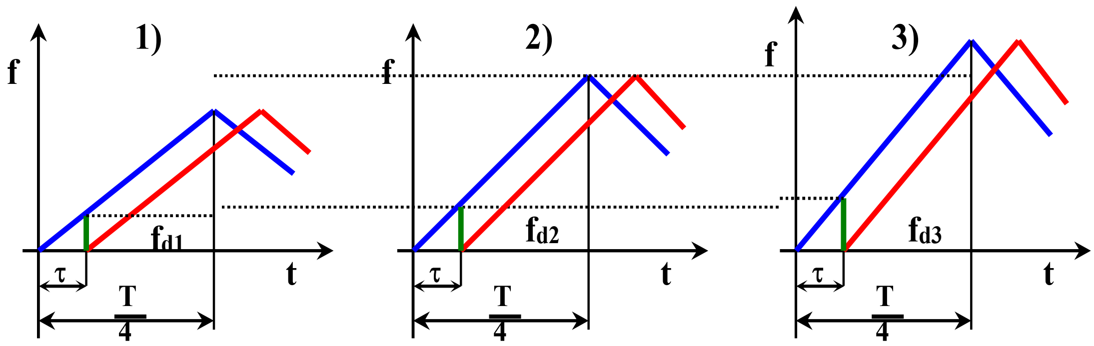

Fig. 34 Effect of a Change in Frequency Deviation Δf on the Value of f_d

Similarly an unfavorable change in the frequency deviation Δf, either to a higher value (Fig. 34a) or to a lower value (Fig. 34c), leads to a change in the value of the difference frequency compared with the standard value illustrated in Fig. 34b. In this manner, the balanced mixer circuit together with the delay line (configuration according to Fig. 32) is able to evaluate the instantaneous deviation of the radio altimeter constant. This deviation is manifested by a change in the value of the difference frequency f_{dk} at the output of the balanced mixer. Further use of the signal carrying information about the instantaneous change of the radio altimeter constant is applied for its automatic correction in two ways:

1. by controlling the radio altimeter constant on the transmitter side.

2. by correcting the measurement result on the receiver side.

In the first case, the signal of the instantaneous deviation of the radio altimeter constant is used to control the transmitter so that the radio altimeter constant remains stable over time and throughout the entire altitude measurement range. This principle is illustrated in Fig. 35.

In the second case, the signal of the instantaneous deviation of the radio altimeter constant is used to correct the already measured altitude value in the receiver section of the radio altimeter. This principle is illustrated in Fig. 36. Both of these methods ultimately have a positive effect by compensating for the influence of changes in the radio altimeter constant on the accuracy of altitude measurement.

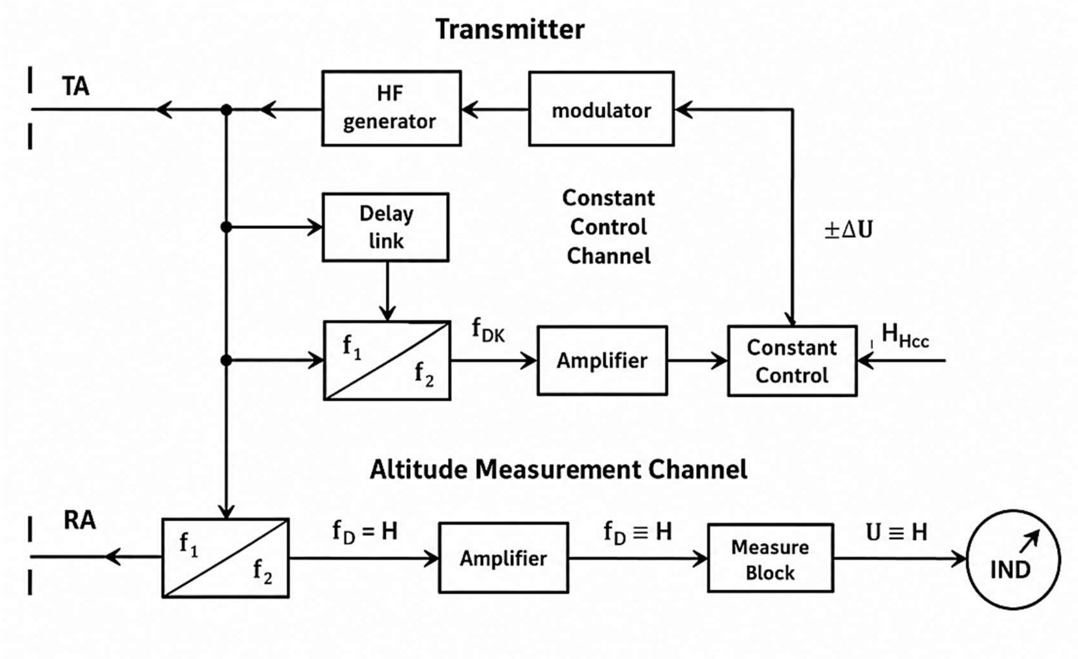

Fig. 35 Controlling the radio altimeter constant on the transmitter side

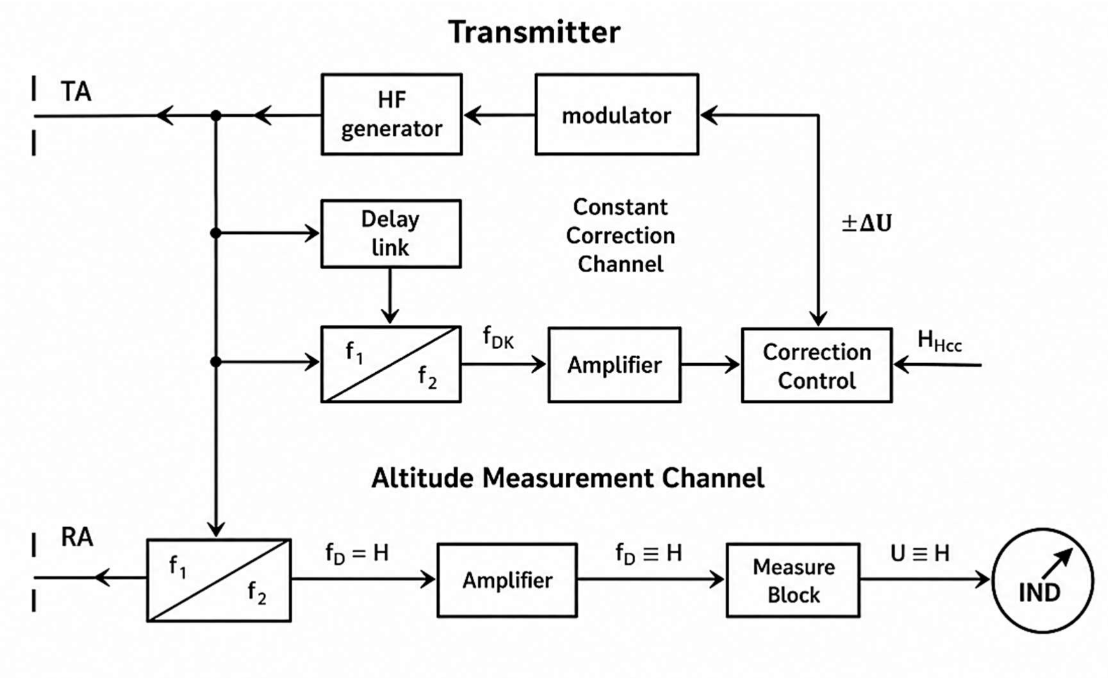

Fig. 36 Correction of the measurement result by the radio altimeter constant

6.3 Control of the Radio Altimeter Constant on the Transmitter Side

In radio altimeters, control of the constant is implemented by an Automatic Tuning Circuit of the Radio Altimeter Constant (see Fig. 35).

This circuit forms a control loop that includes:

- *evaluation of the instantaneous value of the radio altimeter constant (delay line and mixer f_{dk}),*
- *an error-voltage generation circuit – comparator DU,*
- *a modulation-signal generation circuit - modulator,*
- *a radio-frequency generator – transmitter.*

During control of the radio altimeter constant, two voltages are continuously compared in the comparator:

1) the voltage of the reference signal U_{ref}, whose fixed value is set according to the selected equivalent altitude,

2) the voltage of the delayed signal U_d, whose constant delay time corresponds to the selected equivalent altitude.

By comparing these two voltages, an error signal DU is obtained, which is then processed by subsequent circuits to adjust the radio altimeter constant in the transmitter to its correct value. The voltage of the delayed signal U_d is obtained by first amplifying, limiting, differentiating, and detecting the difference-frequency signal F_{rk}. In the counter, the positive pulses are then converted into a DC voltage U_d proportional to the value of the difference frequency. If, as a result of a change in any of the parameters (f_M or Df), the value of the difference frequency f_{dk}, changes, the DC voltage of the delayed signal U_d changes proportionally. This DC voltage is compared in the comparator circuit with the reference voltage U_{nek}, whose value is constant and corresponds to the selected equivalent altitude. The result of comparing these two voltages is the error signal DU. The amplitude of this error signal represents the magnitude of the change in the constant, while the sign of the signal indicates the direction of deviation of the constant. The error signal is processed in subsequent circuits so that the radio altimeter constant is returned to its correct value. In principle, the radio altimeter constant can be controlled:

- *changing the period of the modulation frequency,*
- *changing the amplitude of the modulation frequency.*

In practice, control by changing the amplitude of the modulation frequency is more commonly used, which results in a change of the frequency deviation Df (e.g., in the RV-5). The principle of such a configuration is shown in Figure 37.

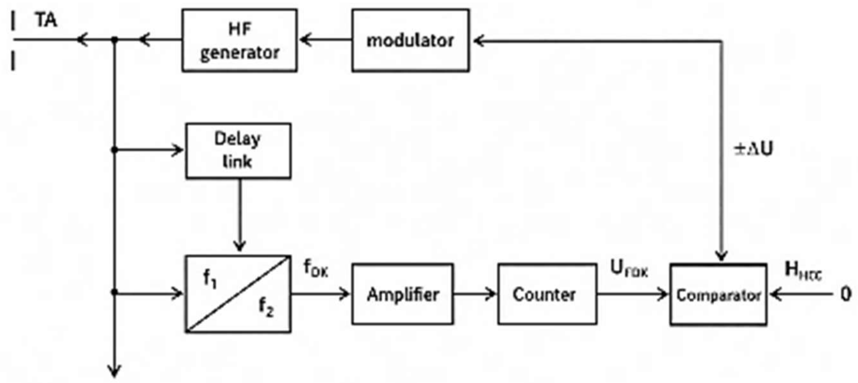

Fig. 37 Principle of operation of radio altimeter constant control

6.4 Correction of the Measurement Result on the Receiver Side

Correction of the measurement result on the receiver side is implemented in the radio altimeter by the *"Automatic Measurement Result Correction Circuit"* (see Fig. 36). This circuit comprises of:

- *evaluation of the instantaneous value of the radio altimeter constant (delay line and f_{dk} mixer),*
- *correction signal generation circuit (F_{rk} amplifier and constant correction),*
- *measurement result correction circuit (measurement block).*

The principle of measurement result correction on the receiver side is based on converting the ratio of two frequencies:

a) the difference frequency f_{dk} generated by the altitude measurement channel,

b) the difference frequency f_{dk} generated by the radio altimeter constant evaluation circuit into a voltage proportional to altitude.

Measuring the ratio of the difference frequencies, i.e., of the altitude measurement channel and the radio altimeter constant evaluation circuit, makes it possible to eliminate the dependence of the radio altimeter output voltage on variations of the frequency deviation Df and the modulation frequency f_M in the receiver section of the radio altimeter. Correction of the measurement result on the receiver side is performed as follows. The radio altimeter contains an altitude measurement channel in which the obtained difference frequency f_d is proportional to the measured altitude and is given by the relation:

$$f_d = \frac{4\Delta f . f_M}{c} H \tag{91}$$

This signal, after amplification and amplitude limiting, is fed into the circuit for measuring the ratio of the difference frequencies f_d/f_{dk}. At the same time, a signal from the circuit for evaluating the instantaneous value of the radio altimeter constant is applied to the second input of this circuit, the frequency of which is given by the relation:

$$f_{dk} = \frac{4\Delta f . f_M}{c} H_{et} \tag{92}$$

After amplification, this signal is converted into pulses of constant width τ (for example, in the RV-5, τ = 70ms), as shown in Fig. 38.

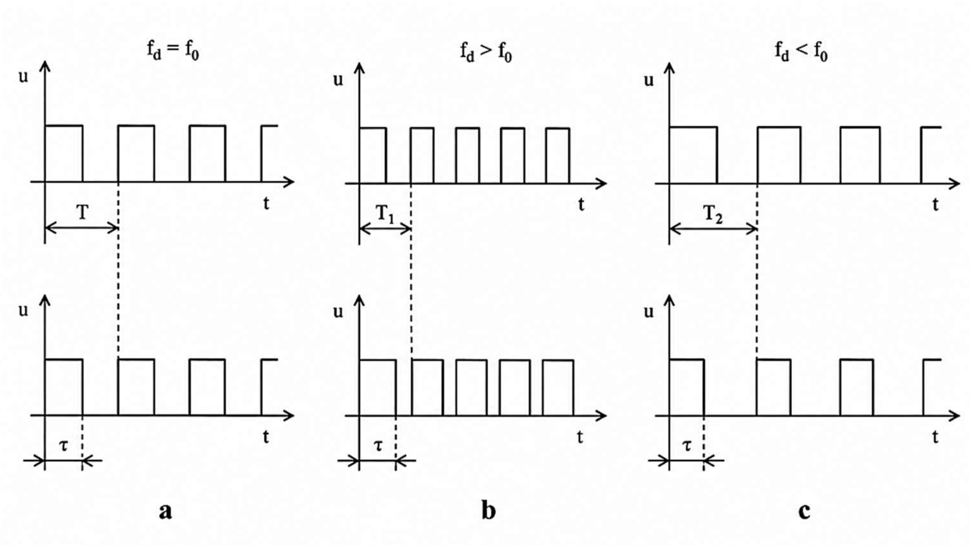

Fig. 38 Shaping of constant-width pulses

In this way, a change in the difference frequency f_{dk} manifests itself as a change in the number of constant-width pulses, by means of which the correction of the measurement result on the receiving side is performed in the circuit that measures the ratio of difference frequencies. The correction is achieved by changing the value of the feedback current in the amplifier of the measuring circuit. The circuit for measuring the ratio of difference frequencies is shown in Fig. 39.

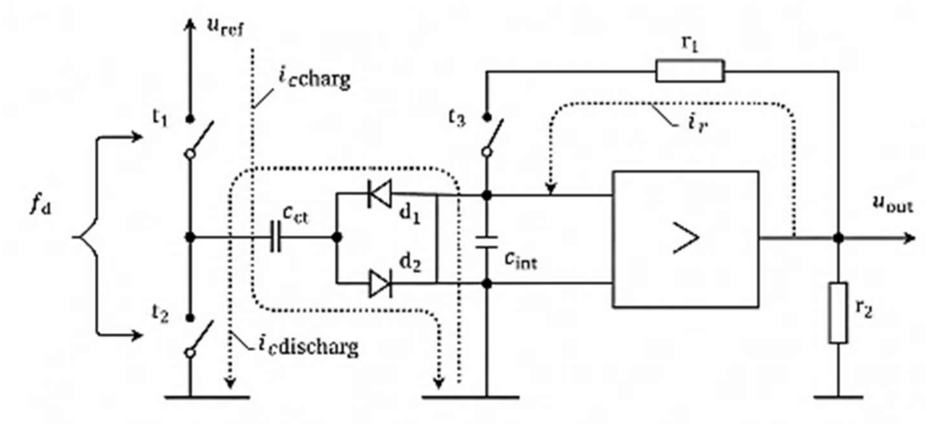

Fig. 39 Circuit for measuring the ratio of the difference frequencies

The circuit evaluates the ratio of the difference frequency f_d, which is proportional to the aircraft flight altitude H, to the difference frequency f_{dk}, which is proportional to the equivalent altitude H_{ek}.

This ratio can be expressed by the relation:

$$\frac{f_d}{f_{dk}} - \frac{H}{H_{ek}} \tag{93}$$

From this relation, it is possible to express the value of the difference frequency f_{dk} as being proportional to the instantaneous value of the radio altimeter constant.

$$f_{dk} = \frac{H_{ek}}{H} f_d \tag{94}$$

The input counter of the measuring circuit is driven by the difference frequency f_d. During one half-period of the difference frequency f_d the capacitor C_{cit} is charged from the voltage source U_{ref} through the conducting transistor T_1 and diode D_1. During the second half-period of f_d it is discharged through the conducting transistor T_2 and diode D_2. During one period of f_d the integrating capacitance (capacitor C_{int}) receives a charge proportional to the voltage U_{ref} and to the value of the capacitance C_{cit}. At the same time, the charge on the upper plate of this capacitor has negative potential. The mean value of the current i_c flowing through the capacitor C_{int} is equal to:

$$i_c = U_{ref} . C_{cit} . f_d \tag{95}$$

The amplifier connected after the counter maintains zero voltage across the capacitor C_{int} by means of the feedback current i_{fb} drawn from the positive supply voltage U_{out} . Since this current flows only during the duration of the time interval t, which is repeated with the frequency f_{dk}, the value of this current is given by the relation:

$$i_{fb} = \frac{U_{out}}{R_{fb}} \tau f_d \tag{96}$$

Zero voltage across the capacitor C_{int} is maintained provided that the counter currenti_c is equal to the feedback current i_{fb}

$$i_{fb} = i_c \tag{97}$$

After substituting for the individual currents from relations (97) and (96), we obtain:

$$\frac{U_{out}}{R_{fb}} \tau f_d = U_{ref} . C_{cit} . f_d \tag{98}$$

From this, the value of the output voltage U_{out}after substituting expression (98) is given by:

$$U_{out} = \frac{U_{ref} C_{cit} f_{dk} R_{fb}}{\tau f_{dk}} = \frac{U_{ref} C_{cit} f_d R_{fb}}{\tau \frac{H_{ek}}{H} f_d} \tag{99}$$

After modification we obtain:

$$U_{out} = \frac{U_{ref} C_{cit} f_{dk} R_{fb}}{\tau H_{et}} H \tag{100}$$

From expression (100) it is evident that:

- *the output voltage U_{out}, is a linear function of the measured altitude H,*
- *the remaining parameters (U_{ref}, C_{cit} , R_{fc} , τ , H_{et}) are constant.*

By using the circuit solution for evaluating height from the difference frequency according to expression (100), correction of the radio altimeter constant is achieved.

7 EXPERIMENTAL VERIFICATION OF ADVANCED RADIO ALTIMETER FUNCTIONS IN THE CONTEXT OF FLIGHT SAFETY

From the point of view of mathematical-physical applications carried out during long-term research in the field of radar technology of the FMCW type, it is clear that modeling allows for the analysis and subsequent use of all technical situations that the on-board radio altimeter provides as a separate technical system. Its functionality and the need for a solution are strongly intertwined with the issue of ensuring flight safety. Although the airborne radio altimeter is not in principle exceptional compared to other airborne systems, its position in the natural flight dynamics of the aircraft represents a specific approach to air traffic safety issues. The airborne radio altimeter, as is apparent from the previous chapters, exhibits certain technical limitations and dynamic characteristics that interact with automatic flight control systems (autopilot). The presentation of its functionality within the overall aircraft system is based on symmetrical theoretical models that allow for reliable determination of the terrain relief under the aircraft and the provision of output representing the real actual flight altitude. The results obtained by identifying its positive properties, as well as limits and measurement errors, were verified by conducting a technical experiment. This experimental approach clearly shifted the evaluation of the system from the level of theoretical estimates to the level of accurate practical measurements in real flight conditions.

Deepening the theoretical foundations of the on-board radio altimeter can be understood as the first level of knowledge, based on a detailed understanding of the technical and physical principles of its operation. This stage includes the analysis of differential frequency generation, the influence of the Doppler effect, methodological and dynamic errors, as well as the method of signal processing in the on-board environment.

The second level is to verify the dynamic stability of the system under real or simulated operating conditions. Experimental implementation in this phase serves to confirm, refine or possibly correct theoretical assumptions about the practical usability of the system, especially in terms of its behavior during changes in altitude, vertical speed and during transitions between flight modes.

The technically oriented experimental approach thus naturally passes to the level of mathematical-physical modeling, the aim of which is to support and increase the level of flight safety. In this phase, partial (parity) models of individual phenomena – altitude measurements, flight dynamics, pilot response are created, which are then integrated into a unified system model. Such an understanding requires that the radio altimeter be perceived not as an isolated measuring element, but as an integral part of a specific aircraft system. Understanding the interrelationships between the individual subsystems (measuring, control, warning and decision-making) and their integration into the functional unit of the aircraft complex is crucial.

Only in this context can its contribution to ensuring flight stability and safety be objectively assessed. The chosen system approach made it possible to achieve measurable and repeatable results that are usable for the experimenter in the effective application of knowledge in the field of radio and radio engineering technology. An essential feature of an objective examination of the aviation system is a comprehensive and systematic approach to the interpretation of partial results. These then create a comprehensive framework of thought enabling a correct evaluation of technical solutions in the context of aeronautical research. The theoretical basis, which reflects the technical specifics of complex aircraft systems and is based on the general principles of aeronautical sciences, is a necessary prerequisite for a qualified solution of safety issues. The issue of aviation sciences is interdisciplinary and also extends into the field of legislation that sets technical and operational standards ensuring a minimum level of air traffic safety.

The legislative framework creates a boundary between the recommended technical solution and the mandatory safety system implemented in a specific type of aircraft. In the context of the radio altimeter as one of the key elements of the safety chain, it turns out that the technological maturity of the system alone is not sufficient unless it is supported by normative anchoring and practical implementation in operation. Without a systematic link between research, experimentally verified results and legislative requirements, situations may arise where the available technology is not fully used to eliminate risks.

It is therefore essential to see airborne radio systems not as isolated technical devices, but as part of a wider aviation safety ecosystem, the functionality of which depends on the integration of technology, the human factor and the regulatory environment.

Currently, there are hundreds of manufacturers of small aircraft operating in the world, who are looking for the application of their products, especially in the field of operation in deteriorated meteorological conditions. Increasing air traffic density is a potential source of collision situations, especially in aerodrome approach modes, where aircraft of different categories may collide. Aircraft crews process a large amount of information in such areas – from air traffic control to on-board warning and assistance systems. In time-critical situations, the pilot must make a series of precise decisions and control interventions. For this reason, it is the task of scientific and research institutions, as well as manufacturers of avionics systems, to look for solutions that will increase the level of flight safety in conditions of increasing complexity of air operations.

Air accident statistics point to the fact that many small aircraft were not equipped with adequate collision prevention systems, leading to serious accidents. At the same time, the operators did not violate the legislation, as the obligation to implement these systems was not normatively determined. Crews were thus reliant on their own decision making without sufficient technical support in critical situations.

The current trend of avionics systems manufacturers is to equip aircraft with integrated assistance information systems that will be optimally interconnected with automatic flight control systems. Such integration represents an important step towards increasing the level of situational awareness of the crew and reducing the risk of collision or terrain events. In recent years, the development of aviation technology has reached such a level that major aircraft manufacturers are also involved in the development and integration of unmanned aerial systems (UAS/UAVs), which are considered a promising part of future air transport. This is related to the question of their safe integration into controlled airspace, in which manned aircraft operate at the same time. To enable such mixed operation, it is necessary to comply with the technical requirements for avionics and automatic UAV control systems and the applicable aviation legislation. The aim is to ensure that both manned and unmanned aerial vehicles have a comparable level of capability to detect and avert potential collision situations (so-called 'detect and avoid' / 'sense and avoid' systems). In the case of UAVs, the ability to deal with collision situations during flight must be multiple redundant, as there is no direct human intervention by the pilot on board. For this reason, the theoretical and experimental part of the monograph focuses on anti-collision systems and their assistance function in solving collision conditions during flight. To address the issue of collision avoidance systems in today's airspace, it is necessary to take into account the increasing traffic density and the coexistence of three main categories of aircraft: transport, general aviation (GA) and unmanned systems. Future solutions must allow for the safe integration of these categories without unduly restricting their operation.

The original references to JAA and FAE are no longer up-to-date.

1. *JAA (Joint Aviation Authorities) bolo replaced by agency EASA (European Union Aviation Safety Agency).*
2. *The FAE designation is not used in this context; in the USA, the relevant body is the FAA (Federal Aviation Administration).*
3. *Part 139 is a U.S. FAA (14 CFR Part 139) regulation regarding the certification of airports, not directly the integration of airborne collision control systems.*

In the European area, the following are currently relevant:

1. *Regulation (EU) 2018/1139 (EASA Basic Regulation);*
2. *Commission Implementing Regulation (EU) 2019/947 (operation UAS),*
3. *Commission Delegated Regulation (EU) 2019/945 (technical requirements for UAS);*
4. *Requirements for equipping aircraft with ACAS/TCAS systems according to ICAO standards (Annex 10 and Annex 6).*

In the area of airports in the EU, Regulation (EU) No 139/2014 applies, which regulates the requirements for airports, but not directly for airborne collision avoidance systems.

It follows that the implementation of collision avoidance systems is not limited only by the class of airport, but primarily by the aircraft category, type of operation and regulatory requirements set by EASA or FAA. Modern aircraft assistance systems also include anti-collision systems (e.g. ACAS/TCAS, TAWS/EGPWS, ADS-B In/Out). Their integration into the flight control system is an important element in increasing the situational awareness of the crew and reducing the risk of collisions in the air and impact with the terrain. The integration of these systems into the flight control architecture (Fig. 40) should be seen as part of a complex safety chain that includes technology, human factors and the regulatory environment.

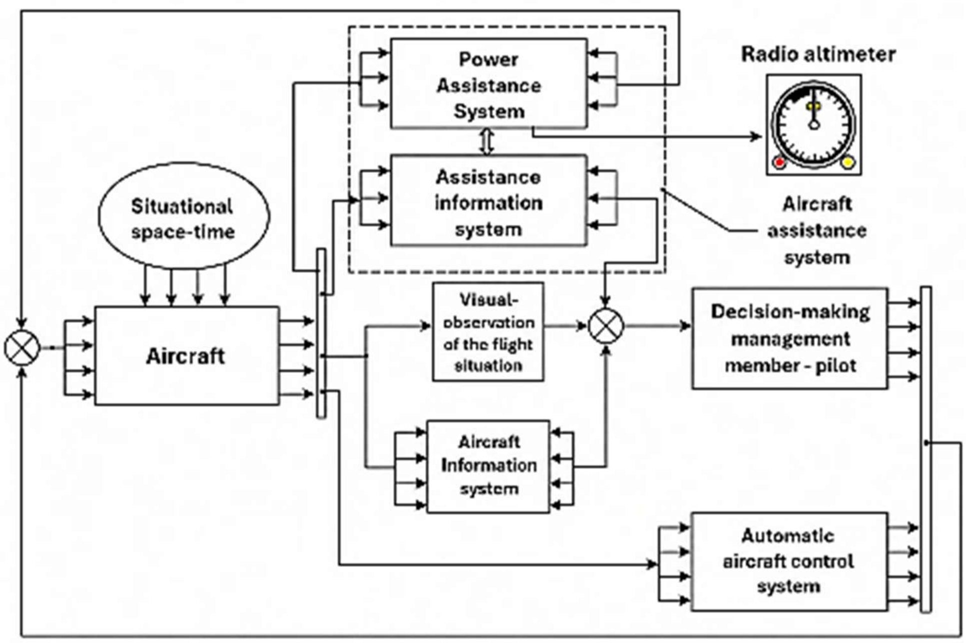

Fig. 40 Structural diagram of a flying object control with radio altimeter observation

An aircraft assistance system may include:

1. *critical flight mode warning systems.*
2. *control and signaling systems;*
3. *aircraft stability and steerability systems.*
4. *Other (especially for military aircraft systems).*

The assistance system instrumentally ensures the safety of the operating performance of the control system and prevents the execution of incorrect decisions by pilots. The importance of the presented knowledge lies in its applications in the creation of models and simulations.

In the next description of collision assistance systems, the term assistance will be omitted for assistive radio altimeters in the function of a collision indicator.

By using high-quality anti-collision systems and indicators, aviation events referred to as:

1. *Potential aircraft convergence*
2. *Dangerous approach of aircraft*
3. *Collision of two planes*
4. *controlled flight of aircraft into terrain – (CFIT)*

The development of aviation technology has made it possible for today's small aircraft and unmanned aerial vehicles (UAVs/UAS) to be able to achieve performance that is not fundamentally different from the altitudes and speeds of large airliners. These vehicles can fly in altitude and speed bands that have traditionally been occupied only by general or transport air traffic. Such a scenario presents new challenges for the integration of various flying vehicles in the airspace that is common to both piloted and autonomous systems. The integration of UAVs/UAs into controlled airspace requires not only legislative compliance, but also equivalent collision prevention capabilities between manned aircraft and autonomous systems. Legislative standards alone are not sufficient if avionics and autonomous systems do not have adequate technical means for detecting conflicts and safely averting them (so-called detect and avoid or sense and avoid technologies). For unmanned aerial vehicles, it is critical to ensure that the handling of in-flight collision situations is reproducibly robust, even in the absence of direct human response from pilots on board. This is one of the reasons why the research in this monograph focuses on anti-crash and anti-collision systems and their assistance in preventing dangerous situations during flight. When addressing the issue of collision avoidance systems, it is necessary to take into account the fact that the take-off, landing and circulation modes of aircraft will be complicated for both the systems on board the aircraft and the system elements of the airport surroundings as the traffic density increases. This means that control and assistance systems will have to process a significantly higher number of coordination and information commands to avoid unwanted conflicts between aircraft that could result in collisions or loss of life, whether in the air or in contact with the terrain.

The reason and principle for the use of modern anti-collision systems are shown in Figure 41, where the situation is shown as follows:

1. *Red: the conflict is resolved using TCAS/ACAS (Traffic/Airborne Collision b Avoidance System) systems, which are installed as standard in airliners.*
2. *Blue: the conflict is solved by prediction systems typical of small aircraft and UAVs (so-called detect and avoid capabilities).*
3. *Yellow: the situation is solved using Ground Proximity Warning System / Enhanced Ground Proximity Warning System (GPWS/EGPWS), especially for large airliners.*

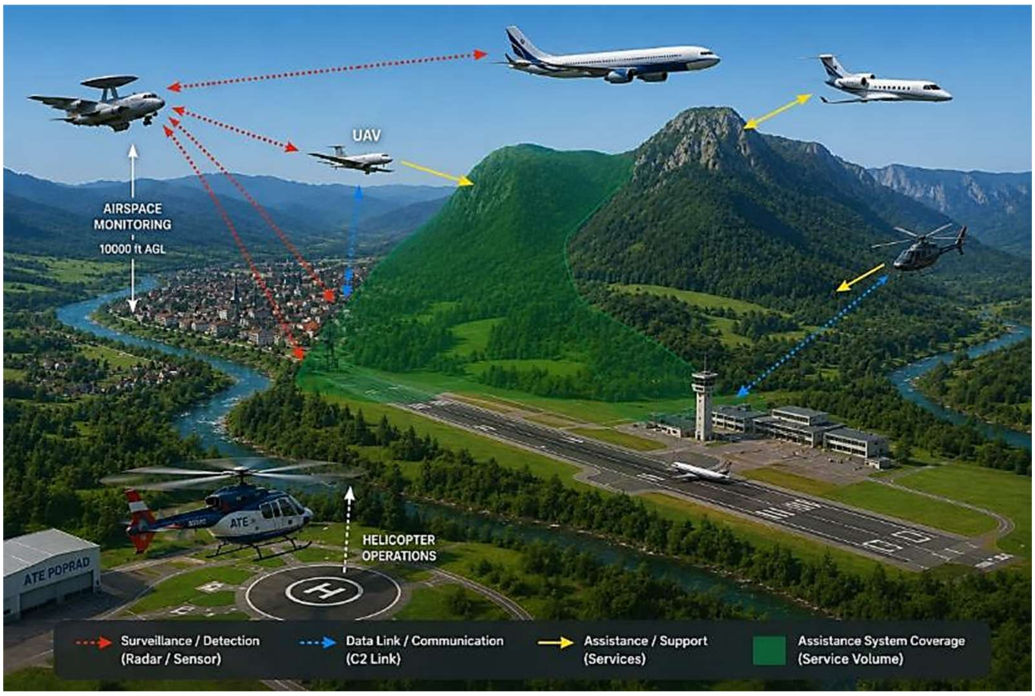

Fig. 41 Operation of flying vehicles in the vicinity of the airport's CTR with collision threats

Another issue of collision is the actual impact of the aircraft into the terrain, called Controlled Flight Into Terrain (CIFT). Such an impact is characterized by the fact that the pilot guides the aircraft into the terrain or other ground obstacle in a controlled (but unintentional) manner. This collision is currently sharply criticized, as technical progress in the field of avionics assumed that this matter already belongs to the less dangerous types of air accidents. Practice shows that CIFT has an important place in the field of air accidents. Prevention of such events is to the maximum extent possible with the full use of avionics, which, after their introduction, are carried out not only by aircraft with higher weight categories, but also by aircraft belonging to groups under 5000 kg. Today, these small planes and flying vehicles can carry up to 9-15 people and, as their number in the airspace increases, they are a threat to the crews of potential aircraft in a collision situation and passengers. In addition, by their nature, flying vehicles perform special tasks in the military field, where the difficulty of tasks is often on the verge of changes in weather conditions. The consequences of bad weather conditions and the difficulty of performing flight tasks that pilots have to overcome distract their real ability to perceive the aircraft's surroundings (although today airlines try to create an artificial reality of the environment in front of the aircraft in the cabin), which often results in a critical approach of the flying vehicle to the terrain.

Simple CFIT avoidance systems are a limiting measure for some aircraft in terms of disruptive messages. In the landing phases, pilots may receive erroneous reports and may lose control in the landing process. With the use of common avionics such as radio altimeters, or currently available map indicators of the terrain coupled with GPS, these errors are partially eliminated.

In reality, however, these systems do not fully replace high-quality GPWS/EGPWS systems. Aircraft without these systems expose the crew and passengers to the risk of a possible disaster.

We see a solution to conflicting realities in the future in a fully automated system, where the automated control system of a flying vehicle (fast flight in hilly terrain at ground altitudes) will depend on accurate input information about the terrain with subsequent automatic control according to these data only with the participation of the pilot control of random errors brought to the information system of the aircraft (flying vehicle).

7.1 Pilot decision-making process after receiving information about a hazardous situation

In conditions of reduced visibility and limited visibility, it is clear that the pilot needs accurate and timely information about air traffic in front of the aircraft, as well as potential dangerous approaches to terrain or obstacles, especially when performing tasks at ground and low flight altitudes.

Today, modern on-board collision protection systems are able to identify and predict the risk of hitting an obstacle or terrain and thus significantly contribute to the prevention of collision events. These systems include, in particular, ACAS/TCAS (Airborne Collision Warning), TAWS/EGPWS (Field Warning) and, in the case of unmanned systems, Detect and Avoid technologies.

Today's airlines do not only perform transport tasks, but also carry out specialized aerial work (e.g. aerial photography, infrastructure monitoring, agricultural work, rescue operations, etc.) that require the deployment of aircraft and unmanned aerial vehicles at low altitudes and in difficult operating conditions. The originally mentioned JAR-L2 regulation is no longer valid. The JAR (Joint Aviation Requirements) system has been replaced by EASA legislation. Currently, the issue of commercial air transport and specialized operations is mainly governed by:

1. *Regulation (EU) No 965/2012 (Air Operations Regulation) – vrátane časti SPO (Specialised Operations),*
2. *Regulation (EU) 2018/1139 – EASA Basic Regulation, for UAS, Regulations (EU) 2019/947 (UAS operations) and 2019/945 (UAS technical requirements).*

In the international context, the basic rules for the conduct of flights are also governed by ICAO Annex 2 – Rules of the Air, which regulates the general rules of flight, including operation in low visibility conditions. (construction of structures in high-altitude places and their transport, transport of materials, forestry work, firefighting and firefighter landing in inaccessible terrains, etc.). Fulfilling all these tasks is challenging. Flight weather becomes one of the factors that it multiplies and acts to fulfill the planned tasks. One of the ways to contribute to overcoming these problems is also

A suitable choice of an anti-crash system that will allow you to partially save money in a given environment and meet the required activity with regard to safety. From a legislative point of view, it is generally not the obligation of the operator to equip every flying vehicle with an anti-crash system. The obligation to install specific systems (e.g. TAWS/EGPWS or ACAS/TCAS) currently applies mainly to aircraft of a certain weight category or to aircraft engaged in commercial air transport, according to the applicable EASA regulations (in particular Regulation (EU) No 965/2012 – Air Operations). However, in the category of small aircraft and in specialised operations, such an obligation is often not provided. The installation of a crash protection system is therefore highly desirable from a safety point of view, but operators may be discouraged by an increase in acquisition and operating costs. The economic assessment of the implementation of the anti-crash system can be analyzed from two basic points of view:

1. *In terms of the risk of destruction of the flying vehicle due to impact with an obstacle or terrain.*
2. *In this context, the price of the crash protection system is negligible compared to the loss of the aircraft, possible human casualties and the consequent legal and reputational consequences.*
3. *In terms of comparing the price of the air activity performed with the cost of installing the anti-collision protection system.*

Especially for small aircraft or aerial work, investment in additional safety equipment can be perceived as a significant item in terms of operating economy. Information about the current flight altitude, or the predicted risk of impact with the terrain, is crucial for the pilot in the decision-making process. This information is generated by the aircraft information system (ASL) in encrypted form and only acquires meaning when it is correctly interpreted in the context of the current situational dynamics of the flight. The processing of information system outputs by the pilot is part of the decision-making chain in which the technical information is transformed into a control intervention. This process of interaction between the on-board system and the pilot when controlling a flying vehicle is schematically illustrated in Fig. 42.

In the pilot's activity, operations can be separated from each other:

1. *receiving information (detecting the signal, recognizing and determining its meaning),*
2. *estimation of the situation by comparison with ISL data and pilot experience, the output of which is the adoption of the control algorithm,*
3. *practical implementation – solving the flight situation,*
4. *control of the results of the control effect.*
5.

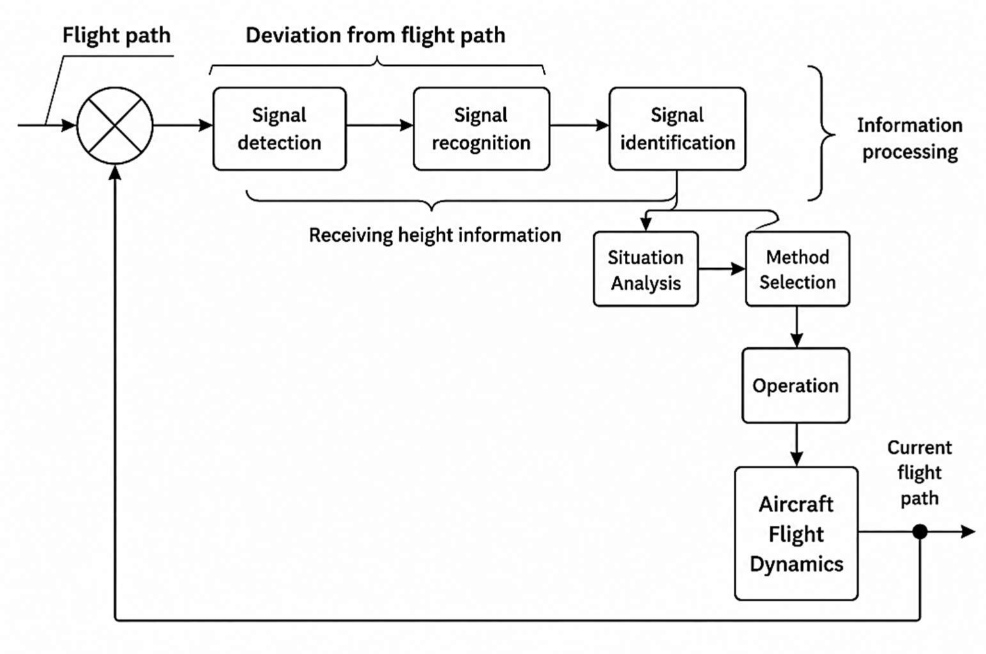

Fig. 42 Flight Information System, Flying Vehicle and Processing Process

The significance of decision-making lies in the possibility of time separation of the information processing process from the time required for effective control of the flying vehicle. The usefulness of the procedure is evident from the regularity of the links between the pilot's time response, the accuracy of his control performance and the determination of deviation (error). Pilot reaction time or (more precisely) the time required to perform one logical operation (LO) control t_{LO} can be expressed by the relationship:

$$t_{LO} = t_{Tt} + nt_{At} + t_{Dt} + t_{out} + t_M \quad (101)$$

Where: t_{Tt} - total time of detection of deviation (speed, height, position ...),

t_{At} - average time of receipt of information by the pilot,

n - number of ASL instruments checked (altimeter, horizon, airspeed indicator),

t_{Dt} - decision time in the control algorithm,

t_{out} - the time needed to check the outputs of operation activities,

t_M - time of motor activity (movement activity).

Operations, decisions, and strategies, control and forecasting of the flight situation are created according to logical laws. The results of the experiments showed (see video, altimeter - attachment) that the decision time of $t_{Dt}$is significantly dependent on the number of logical operations (Fig. 43) and information systems (e.g. anti-shock systems) and on the complexity of the logical process.

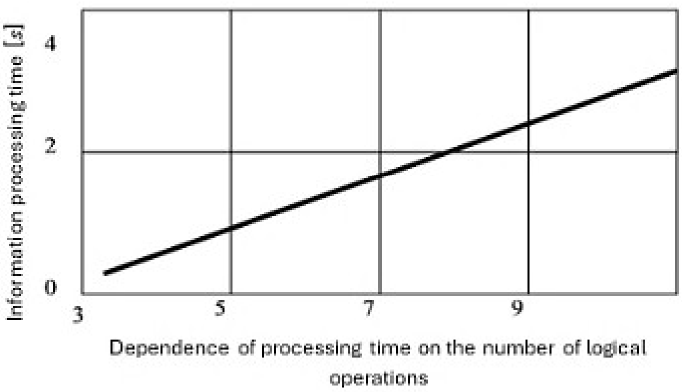

Fig. 43 Dependence of information processing time on the number of logical activities

It follows from the above that the greatest delay in the management process is caused by the need for decision-making. A quick and correct decision made in the shortest possible time is possible only if the structure and organization of the ISL is optimal and depends on the method of encoding the signals (light warnings, audible warnings from anti-collision and anti-collision systems).If we assume t hat the ISL includes an anti-crash system, then this must provide the pilot with a quick and error-free decision (thinking) and his reaction to the control activity in question. Warning signals (light, sound) have a significant effect on the control with a time deficit, which draw the pilot's attention from one working mode to another (collision danger signal) and significantly shorten the decision-making time. When designing an anti-impact system, a response time of 2 to 5 seconds can be expected. If we need less time, then it is desirable to fully automate the management process.

7.2 Factors acting on the flying vehicle to avoid terrain obstacles

The flight activity of flying vehicles performing specialized tasks (aerial work, search and rescue operations, monitoring, military missions, etc.) is often carried out at low and ground altitudes. In these modes, the flight altitude can range from approximately 50 to 150 ft AGL (15-45 m above the terrain), depending on the type of operation, the nature of the terrain, and legislative constraints. Flight speeds in these cases are typically in the range of 60-120 km/h for helicopters and higher for general aviation aircraft. Such a flight mode is usually limited to a well-defined workspace or operating area. After leaving it, the flying vehicle enters cross-country mode, where cruise speed is used, which is optimized terms of range and fuel consumption. For helicopters, this speed is usually in the range of 120-220 km/h, for small aircraft it is significantly higher.
The overflight altitude shall be adapted to the requirements for safe crossing of obstacles and to the minimum altitudes according to VFR/IFR rules, in practice, it is often above 1000 ft AGL (≈300 m) or according to the minimum safe altitudes set by legislation. When flying at ground altitudes, the risk of a Controlled Flight into Terrain event is significantly increased, especially in combination with:

1. *limited visibility.*
2. *rugged terrain.*
3. *high workload of the crew.*
4. *time pressure when performing tasks.*

In addition to navigational and situational factors, it is also necessary to consider technical risks, in particular the possibility of partial or complete loss of power of the power unit. At low altitudes, the time to react is significantly limited, which places high demands on the pilot's decision-making and on the reliability of the on-board systems.
When avoiding a terrain obstacle or a collision situation, the pilot shall take into account:

1. *Current altitude (AGL)*
2. *vertical speed,*

3. *engine power reserve,*
4. *aircraft configuration,*
5. *system and pilot response time,*
6. *the possibility of autorotation (for helicopters) or emergency landing.*

For this reason, the integration of crash and terrain warning systems (e.g. TAWS/EGPWS, radio altimeter with time-to-impact prediction) is a key element in increasing safety in low-altitude operations. Such systems provide the pilot with time to perform an evasive maneuver and at the same time reduce the likelihood of direct contact with the terrain.

In Fig. 44 a safety diagram (the so-called height–velocity diagram) is illustrated, which defines the areas of altitude and forward speed combinations in which it is not safe to remain in view of the possible failure of the engine and the subsequent need to transition to controlled descent or autorotation mode.

The diagram expresses the interdependence between the flight altitude above the ground and the forward speed required to safely transition to the descent and successfully perform autorotation.

A *- At speeds of 0-40 km/h, the flying vehicle can move at an altitude of up to approximately 35 ft AGL, with a high probability of a safe landing if the engine fails.*

B *- At higher speeds (from about 60 km/h) and at a low altitude of about 50 ft AGL, a limited area is created in which the flying vehicle has sufficient forward speed, but does not have sufficient time and space reserve space to safely cope with autorotation and avoid terrain or obstacles in a coordinated manner.*

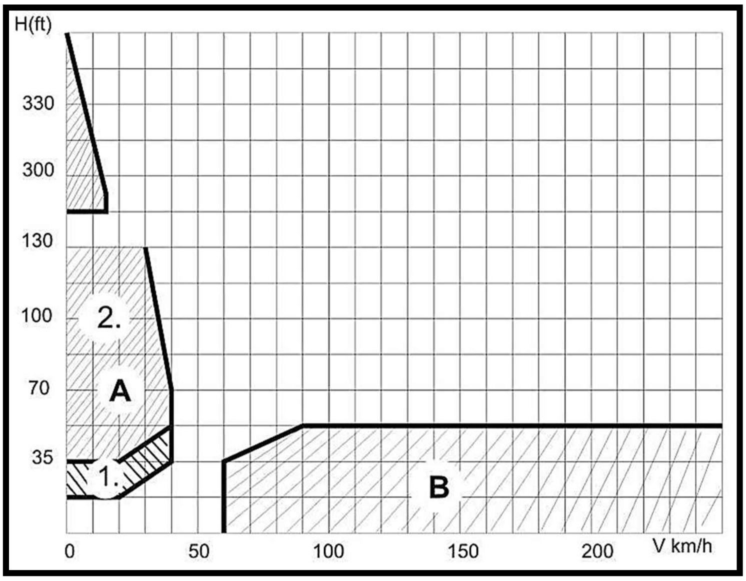

Fig. 44 Safety diagram: "Altitude-speed" danger zone for medium flying vehicle

The operational capabilities of a safe maneuver are further influenced by secondary factors such as the weight of the cargo, the amount of fuel, the direction and speed of the wind, the air temperature and the altitude (the so-called density altitude). These factors significantly limit the performance parameters of the flying vehicle, especially the rate of climb and the available power required to avoid an obstacle or to reach a safe height. Flights at low altitudes and speeds located in prohibited or restricted areas of the safety diagram are not recommended unless required by the nature of the activity e.g. HEMS operations or specialized aerial work. In these modes, the ability to land safely after an abrupt detonation of the power unit is not guaranteed. When flying under VFR rules in conditions of limited visibility, obstacle or terrain avoidance can be done by deviating from the track or making a turn. For flights at low altitudes (H_skut above 60 ft to approximately 300 ft AGL), the crew must pilot the flying vehicle in such a way that a 180° turn (the so-called escape turn) can be made at any time in rugged terrain. This maneuver is limited by a critical tilt, which depends on the current flight speed and available space. When flying at approximately 200 km/h in VFR conditions and with visibility reduced to approximately 1 500 m, the pilot shall be required to reduce the flight speed appropriately and decide in good time whether the obstacle can be safely overtaken (with sufficient power reserve) or whether it is necessary to perform an evasive manoeuvre by swerving or turning. In the case of an unintentional transition from VFR to IFR (non-standard situation), avoiding terrain obstacles by climbing or turning with a climb is significantly more difficult, as it is usually accompanied by an intense climb to a safe height. In such a manoeuvre, it is necessary to take into account the nature of the space, the current flight speed, the rate of climb and the permissible inclination of the flying vehicle (generally 15° to a maximum of 30° depending on the type and operating conditions) Fig.45.

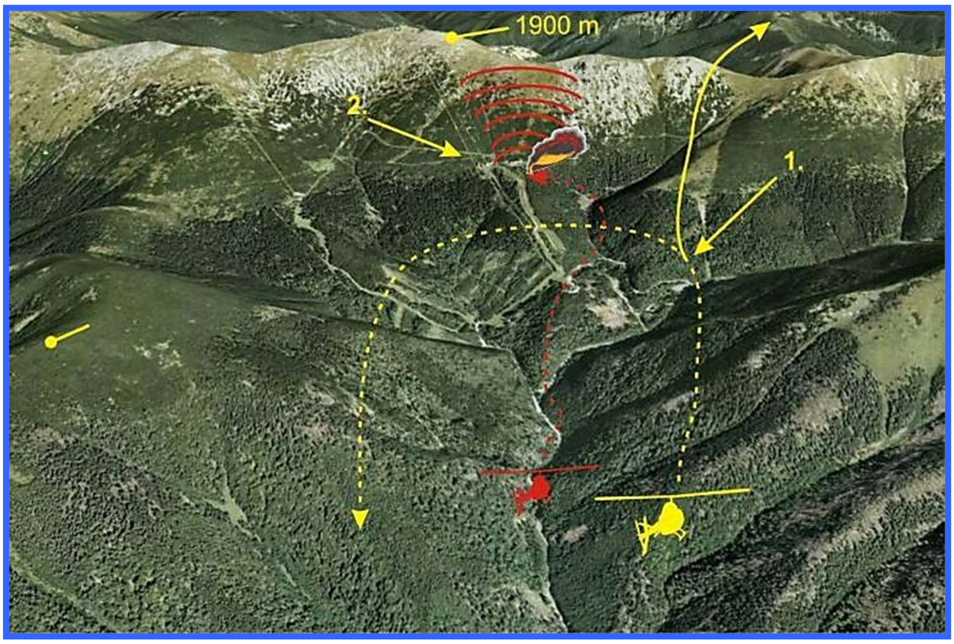

Fig. 45 Method of flight in hilly terrain

The image shows:

1. *Normal flight flying vehicle in VFR conditions adjacent to the terrain (yellow).*
2. *Incorrectly estimated flight directly uphill with insufficient power backup.*

Fig. 46 A real flight with a flying Mi – 17 in a given location. It can be seen that the crew can fly considering two options for flying over the hill.

7.3 Experimental verification of the influence of the Doppler effect in the operation of a radio altimeter

In the previous sections, the dependence of the differential frequency on the flight altitude in the ideal case of constant altitude was theoretically derived. However, in real operation, the aircraft moves at a non-zero vertical velocity, which causes the Doppler frequency shift of the received signal to occur. The aim of this subchapter is to experimentally prove the existence of the Doppler effect in the operation of a radio altimeter and to quantify its effect on the result of altitude measurement. A frequency-modulated radio altimeter creates a frequency addition to the differential frequency due to the dynamic altitude change and the Doppler effect. This change consists in the fact that when descending, the value of the differential frequency, which carries information about the height, is shifted by the value of the Doppler frequency. This will result in a frequency shift in the evaluated signal. In this situation, the instantaneous error of the measured altitude of some radio altimeters exceeds the value given in its parameters. The value of the Doppler frequency represents the increment the frequency of the received signal in relation to the transmitted signal if the aircraft is descending, and the frequency decrease if the aircraft is climbing. In this case, the differential frequency including the Doppler frequency is expressed by:

$$f_{dD} = f_d + f_D = \frac{8\,\Delta f\, f_M}{c}\, H \pm f_0 \frac{2\, v_v}{c} \tag{102}$$

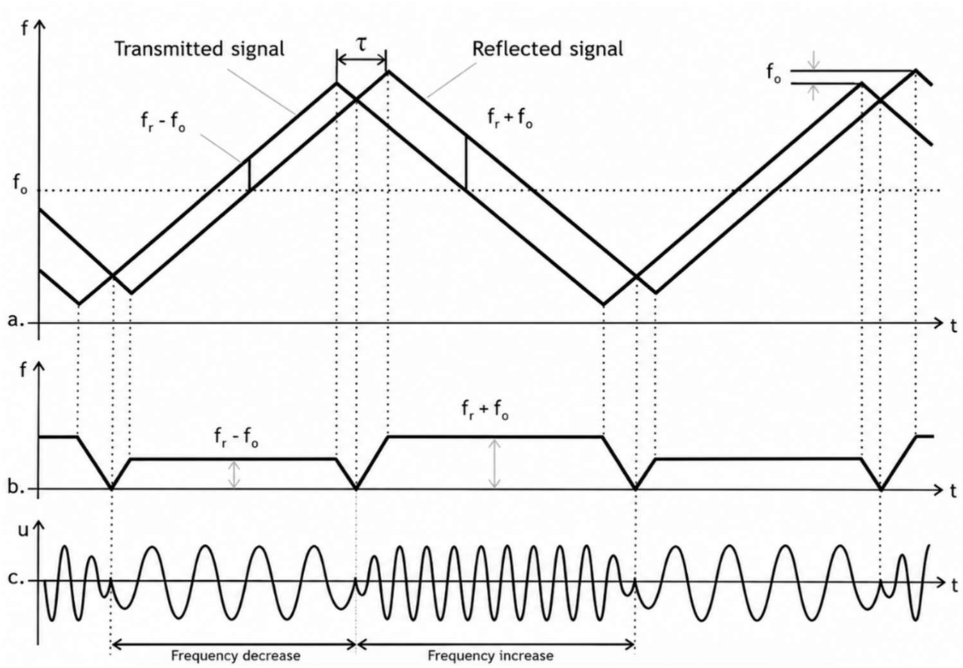

Fig. 47 Influence of the Doppler effect on the formation of the differential frequency RV

In Fig. 47 shows the dual frequency shift of the received signal compared to the transmitted one:

1. *shift along the timeline (to the right), due to a time delay of ,τ*
2. *shift along the frequency axis (upwards), due to the Doppler effect by the value of .F_D*

In the above figure, it can be observed that if the frequency modulation has the shape of a symmetrical saw, then in one half-period of the modulation frequency the differential frequency increases due to the Doppler frequency and decreases in the other half-period. From the figure, it can be concluded that when modulating with a symmetrical saw, the negative effect of the Doppler frequency in height measurement does not manifest itself, because the mean value of the differential frequency does not change for one modulation period. This does not occur, for example, with radio altimeters such as KRA - 405 (Honeywell / BendixKing) and similar types that use a symmetrical saw for modulation. However, if we use an unsymmetrical saw in frequency modulation, then the influence of the Doppler frequency is not canceled out and the error is entered into the differential frequency evaluation circuit, and thus into the data on the actual instantaneous height. A radio altimeter that uses an unbalanced saw for modulation and is now widely used. The formation of the differential frequency for this type of radio altimeter is shown in Fig. 48.

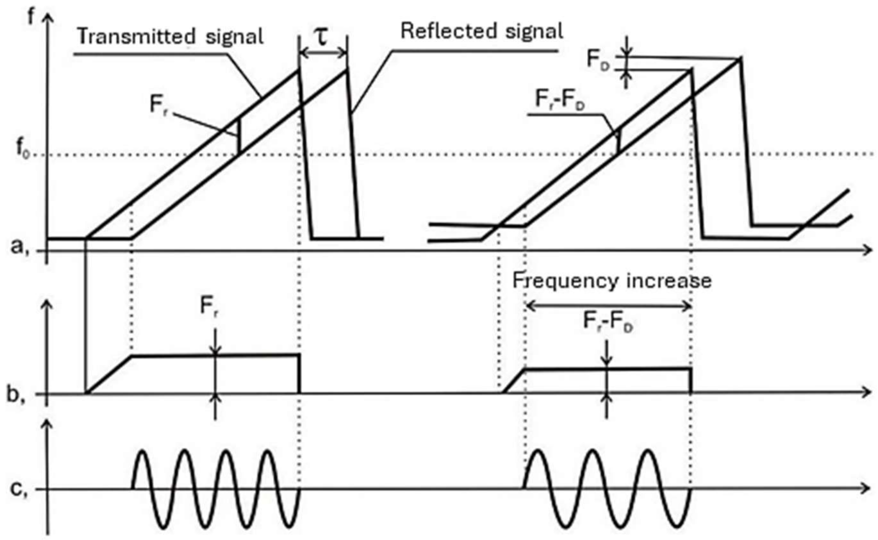

Fig. 48 Influence of the Doppler effect on the formation of the differential frequency of a radio altimeter with an unbalanced saw

It follows from the above that a large Doppler frequency increment can largely affect the measurement result and therefore it must be taken into account especially when descending. For the calculation of Doppler frequency increments, the vertical velocities of some aircraft when approaching for landing to the point of equalization were taken as a basis, which are given in (Table 4.) As the aircraft descends, the frequency of the received signal is increased by the Doppler increment and the value of the differential frequency to be evaluated decreases if the modulation period of the unbalanced saw according to Figure 54 is used. This is a concrete example of a radio altimeter.

Based on the above theoretical and experimental knowledge, it is possible to formulate the following expert conclusion about the influence of the Doppler effect on the result of altitude measurement during descent and in the leveling phase of the aircraft. When using a radio altimeter with symmetrical sawtooth modulation of the modulating signal, the Doppler frequency shift during one modulation period compensates for each other. In one half-period it causes an increase in the differential frequency and in the other it decreases by the same value. The mean value of the differential frequency, from which the flight altitude is evaluated, remains unchanged. Therefore, the Doppler effect is practically not reflected in the indicated altitude data during descent or when leveling the aircraft and does not cause a systematic measurement error. Conversely, when using a radio altimeter with unsymmetrical saw modulation, the Doppler frequency shift is not canceled out during the modulation period. A systematic component of the error shall be introduced into the evaluated differential frequency, which is directly proportional to the vertical speed of the aircraft. When descending, there is an increase in the received frequency, which leads to a change in the evaluated differential frequency and thus to an error in the indication of the instantaneous height. This phenomenon is especially evident in the approach and sub-alignment phase, when the vertical speed is non-zero and the accuracy of altitude measurement is critical from the point of view of flight safety. From the above, it follows that the design of the modulation course of the radio altimeter has a major impact on the elimination or, conversely, the manifestation of the dynamic error caused by the Doppler effect.

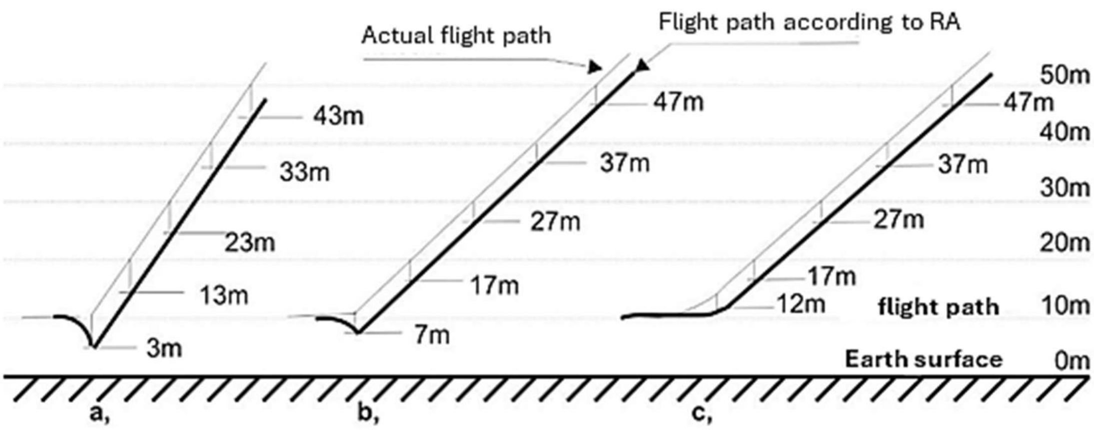

Fig. 49 Effect of the Doppler effect on the glide path of the aircraft monitored a radio altimeter with an unbalanced modulation signal saw

1. *When descending, the instantaneous value of the actual altitude is greater than the altimeter shows. The specific value is given by the descent speed of the aircraft.*
2. *When leveling, this measurement error is aligned with the error given in the parameters of the radio altimeter (for example, KRA - 405 = ± 0.6096 m).*

If the equalization occurs sharply (Fig. 49a), the radio altimeter will show a certain sway in altitude, the magnitude of which depends on the vertical component of the aircraft's speed. However, if the transition is gradual (Fig. 49c), so there will be no swaying. In Fig. 49. The course of the aircraft's descent path (thin line) and the descent path monitored by the radio altimeter (thick line) are shown. The course of the descent path is shown in the figure during a rapid descent (Fig. (49a) and on a slower descent (Fig. 49b), in both cases in the event of a sharp leveling. The above pictures show the course of the sway. In Fig. 49c is the course of the descent path in a gradual comparison. In this, when leveled, the actual flight altitude of the aircraft is aligned with the altitude of the radio altimeters without the indicated sway. The above facts do not endanger the safety of flying. The radio altimeter behaves in a similar way during the horizontal low flight of the aircraft, when the relief of the terrain changes under the aircraft.

7.4 Use of a radio altimeter to forecast an aircraft collision with the ground

Controlled flight of a flying vehicle in difficult meteorological conditions requires increased attention of the pilot, precise navigation and reliable operation of on-board systems in order to ensure flight safety and minimize the risk of collision with obstacles or terrain. In order to evaluate the experimental flight of a flying vehicle, it is necessary to initially determine the time until the collision of the aircraft with the terrain. Suppose that the aircraft is flying at a constant flight level at an altitude H above the terrain. Furthermore, let us assume that from a certain point A the terrain begins to approach the flying aircraft (Fig. 50).
The collision of the aircraft with the terrain occurs at point B for the time t when the aircraft crosses the runway *s*:

$$t = \frac{s}{v} = \frac{H.tg\alpha}{v} \quad ; \quad s = H.tg\,.\alpha \tag{103}$$

Where:

v = the speed of flight of the aircraft,

α = the angle of attack of the terrain.

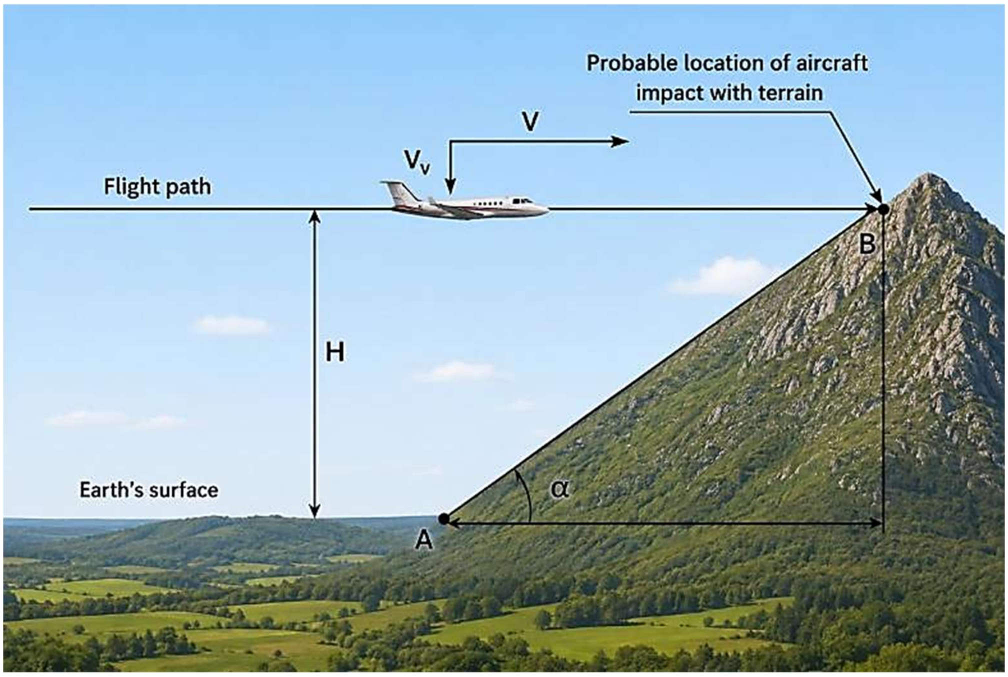

Fig. 50 Determining the time until the aircraft collides with the terrain

As the terrain approaches, the Doppler frequency f_d is formed, which is proportional to the vertical component of velocity v_v. According to Fig. 56, the vertical component of velocity is given by:

$$v_v = \frac{v}{tg\ \alpha} \tag{104}$$

$$t = \frac{H}{v_v} \tag{105}$$

The flight altitude of the aircraft H is evaluated classically, by a radio altimeter and is given by the value of the differential frequency f_d. A classic radio altimeter converts the measured value of the differential frequency f_d proportional to the height, into the voltage UH proportional to the height. The vertical component of velocity v_v corresponds to the value of the Doppler frequency f_d. To determine the dangerous time, it is necessary to convert the value of the Doppler frequency f_d in proportion to the vertical component of the velocity, to the voltage U_d proportional to the vertical component of the velocity. The state when these two voltages reach a certain ratio determines the dangerous time that remains until the aircraft hits the ground.

$$t = \frac{H}{V_v} = \frac{f_d}{f_D} = \frac{U_H}{U_D} \tag{106}$$

In the practical implementation of the perimeter solution of the anti-crash system, this means that when evaluating the time of collision of the aircraft with the terrain, it is sufficient to evaluate the ratio of the voltage U_H, proportional to the height H, to the voltage U_d proportional to the vertical component of velocity v_v. The values of the ranges of these voltages depend individually on the type of radio altimeter. By setting a certain ratio of the specified voltage values, we preset the time that remains until the aircraft hits the terrain.

7.5 Implementation of an additional safety circuit using the Doppler component of the signal

In the case of the circuit solution of the mentioned system, we must assume its connection to a classic broadband radio altimeter with frequency modulation, which works with a symmetrical saw, for example the radio altimeter shown in Fig. 51. Signal from a balanced mixer that also includes Doppler modulator is also supplied to this circuit F_M, which is used to evaluate the magnitude and sign of the Doppler frequency. The tracking circuit converts the Doppler frequency into voltage U_D. In the comparator, the voltage from the receiver block proportional to the height is compared U_H with the voltage from the Doppler frequency tracking circuit, proportional to the vertical component of the velocity U_D. When a certain set ratio of these two voltages is reached, the crash signaling circuit will warn in time about the collision of the aircraft with the terrain.

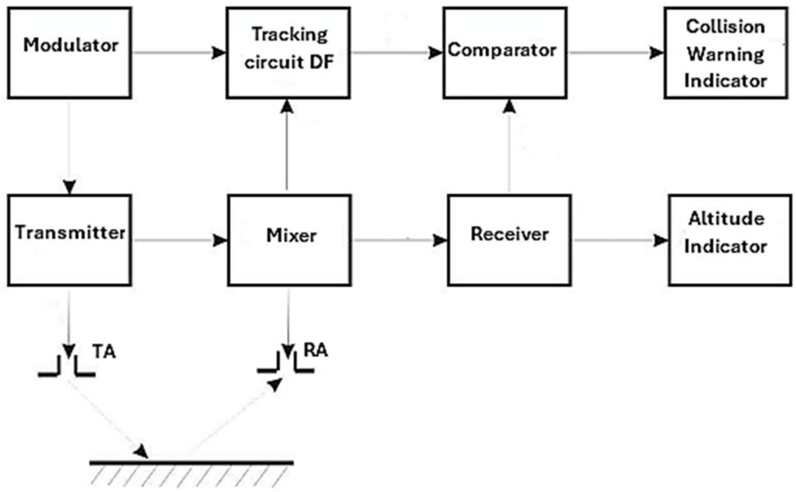

Fig. 51 Diagram of a radio altimeter with a built-in warning system of an aircraft collision with the terrain

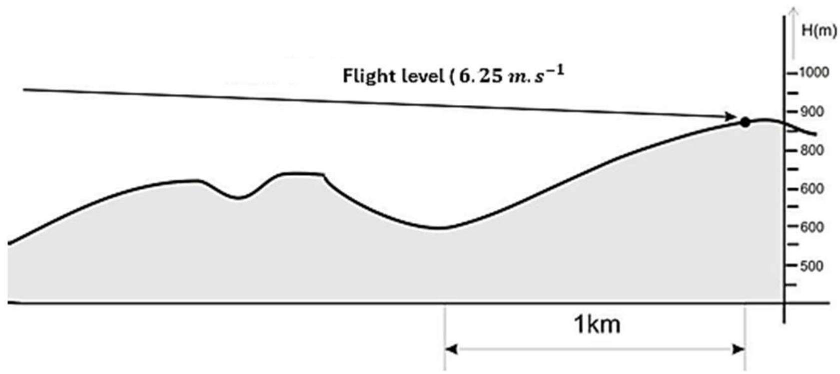

Fig. 52 Terrain relief in the direction of flight during an air disaster

In order for the intended theory to be credibly verified and subsequently applied to the flying vehicle after implementation, it is necessary to perform many basic theoretical and practical measurements. This measurement cannot be carried out in static mode, as the information necessary to obtain correctness would be very distorted and inauthentic. In order to confirm the theoretical assumptions of the operation of such a system, dynamic measurement in flight is required to confirm the existence of the Doppler frequency of the radio altimeter.

7.6 Experimental verification of measurements in flight conditions

The proposed measurement is focused on experimental verification of the presence of Doppler frequency in the differential signal of the radio altimeter and on the assessment of its influence on the result of altitude measurement. For this purpose, the RV-5 broadband radio altimeter, which is designed for medium and heavy helicopters, was chosen as the most suitable. In terms of the principle of operation, this type is also equivalent to other frequency-modulated radio altimeters used in practice (e.g. KRA-405, ALT-50/1000, etc.), which work on the same physical principle of differential frequency evaluation. The use of a different type of radio altimeter would be technically possible, but the implementation of measurements on another flying vehicle would require interventions in the on-board installation, modifications to the structure and recertification of the measurement configuration. These requirements would lead to a significant increase in both the financial and time costs of the experiment. For these reasons, the universally extended RV-5 type was chosen, which was laboratory modified and integrally adapted for experimental measurements on a helicopter. This configuration made it possible to carry out measurements in real flight conditions without interfering with the basic concept of the on-board system and while maintaining the representativeness of the results obtained.

1. *Technical implementation*
2. *Flight implementation*

The technical implementation from the design and installation point of view was divided into:

1. *Internal implementation – including modifications and wiring of measuring circuits, integration of the system into the on-board network, adaptation of signal outputs and provision of recording of measured quantities.*
2. *External implementation – including modifications related to the installation of the antenna system, routing of cable routes and ensuring electromagnetic compatibility in real operating conditions.*

The flight implementation represented a practical verification of the system's function in real operating conditions. It included:

1. *Pre-flight preparation and safety measures, including the establishment of flight profiles, restrictions and procedures in accordance with operational and safety rules;*

2. *Recording and processing of flight data, i.e. systematic recording of measured quantities during individual flights and their subsequent evaluation.*

Such a structured procedure made it possible to separate the technical preparation of the system from its experimental verification in flight conditions and ensured the methodological clarity of the measurements carried out. Recording and processing of flight data, i.e. systematic recording of measured quantities during individual flights and their subsequent evaluation. When implementing this issue of intervention in the electronic parts of the altimeter, it was necessary to analyze in detail one of the theoretically mentioned radio altimeters. Taking into account and within the technical and economic possibilities, it is most appropriate to use a radio privateer of the RV-5 type.

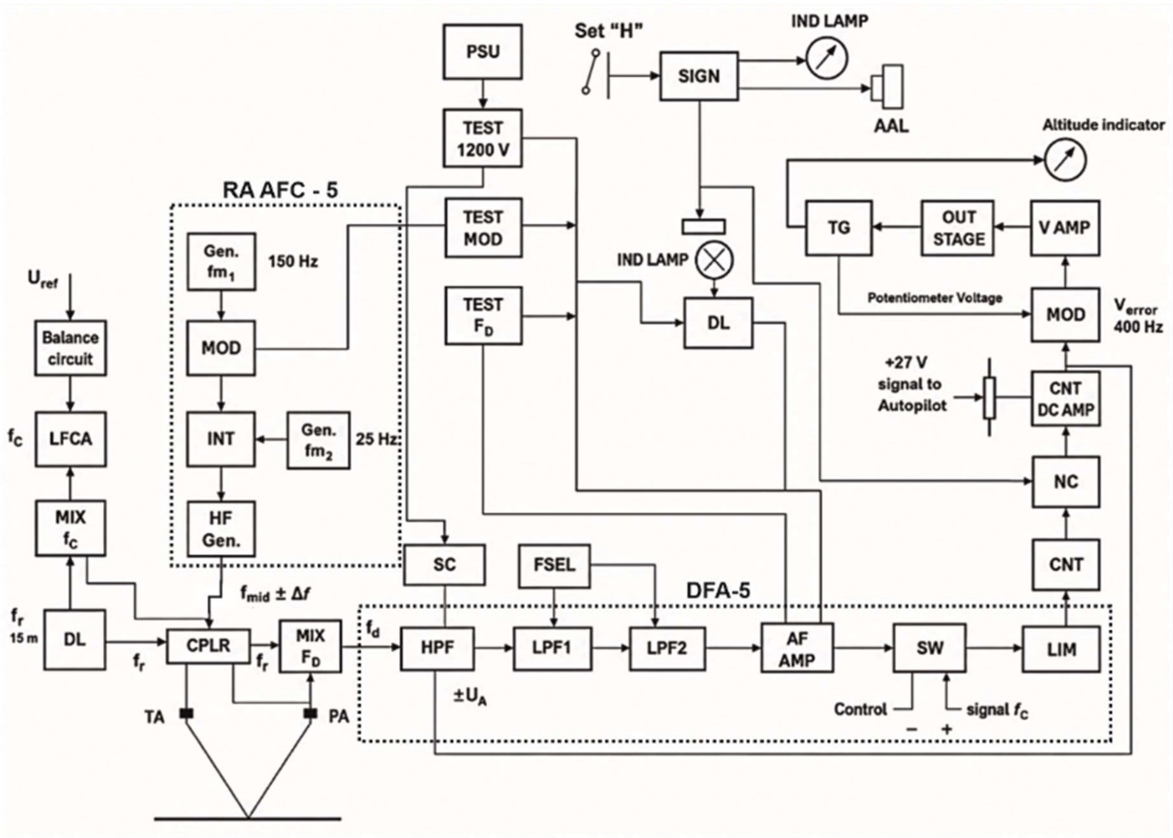

Fig. 53 Parts of the RV block diagram – 5

Legend: LFCA - Low-Frequency Command Amplifier , DL – Delay link, MOD – modulator, INT – integrator, CPLR - Directional Coupler, HPF - High-Frequency Filter, LPF1 (30 KHz) - Low-Pass Filter, LPF 2 (160kHz) - Low-Pass Filter, AF AMP – Low-frequency filter, SC – search circuit, SW - Switching Circuit, FSEL - Filter

Selector, LIM – limiter, CNT – counter, NC – noise circuit, DC AMP - Direct-Coupled Amplifier, V AMP - Voltage Amplifier, OUT STAGE - Output Stage, TG – tach generator, SIGN – Signalization, PSU – power supply, IND LAMP – Indicator lamp, AAL -Audio Alarm, U_A *– Voltage of altitude, DFA-5 - Difference Frequency Amplifier Block,* RA AFC – 5 *Radio Altimeter Automatic Frequency Control.*

The block diagram (Fig. 53) indicates which signals have been analyzed as signals determining the anti-impact character of the altimeter. Measurements have led to the fact that it is necessary to derive signals from blocks RA AFC – 5 (gen. f_{m1} = 150Hz) and block DFA – 5 - (F_r from the RF filter input). From altimeter only as an additional connection in the area of the high-frequency part of the radio altimeter.

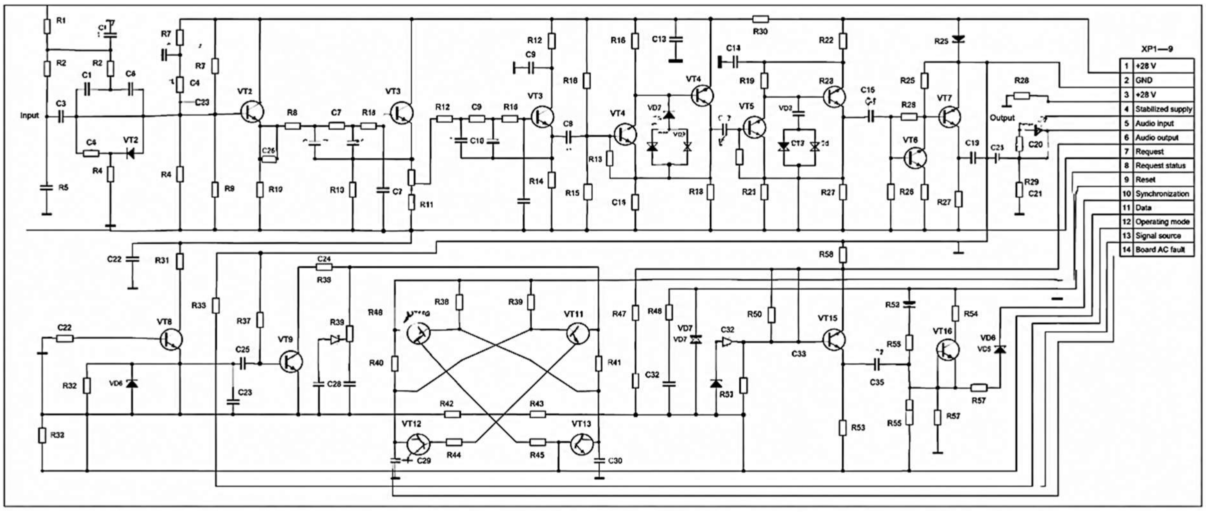

Fig. 54 Selected parts of the principle diagram of the DFA block – 5

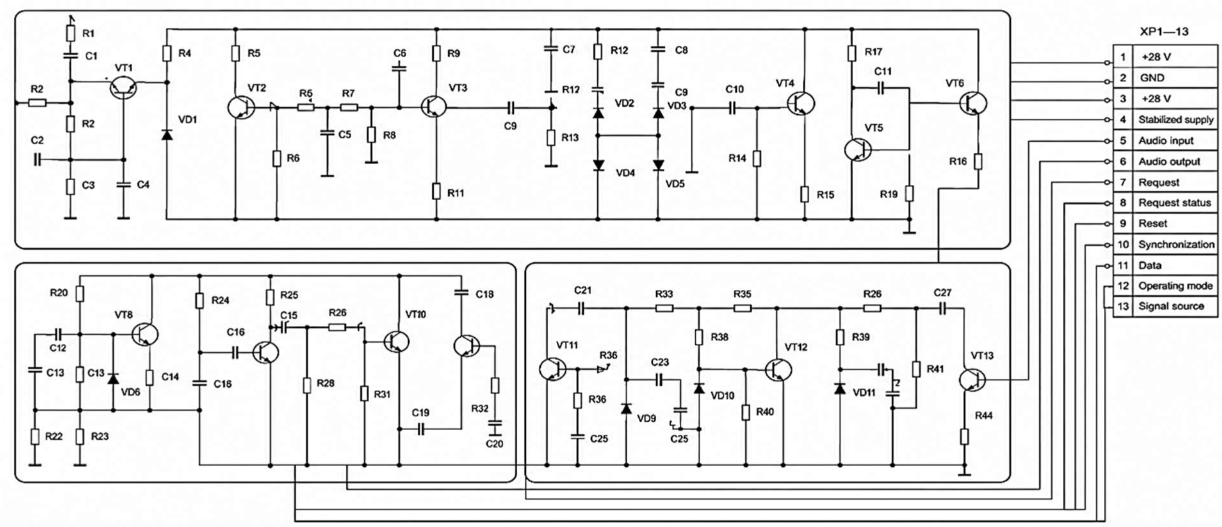

Fig. 55 Selected parts of the RA AFC - 5 schematic diagram

The connection of measuring nodes and cabling is illustrated by yellow arrows on specific parts of the radio altimeter of the RA AFC – 5 - (RA Automatic Tuning Block), DFA – 5 block in Fig. 56, 57.

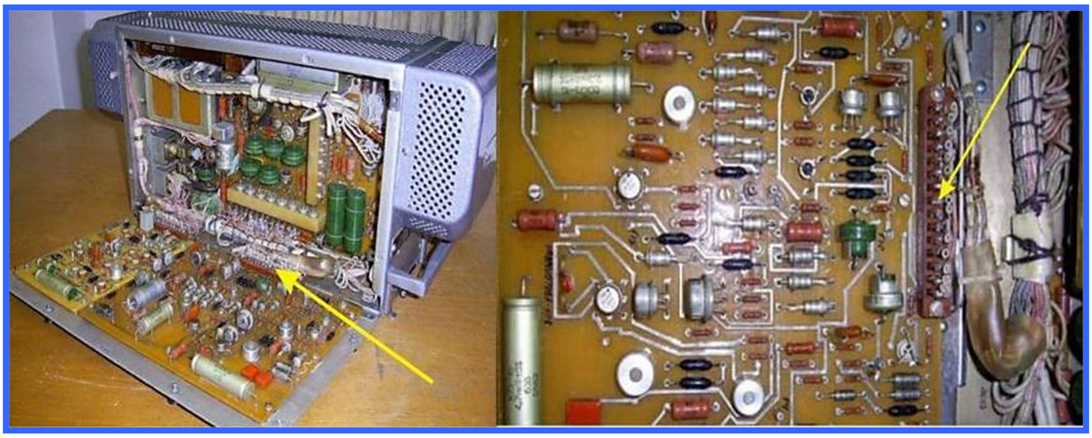

Fig. 56 Selected parts of real points in block RA AFC – 5

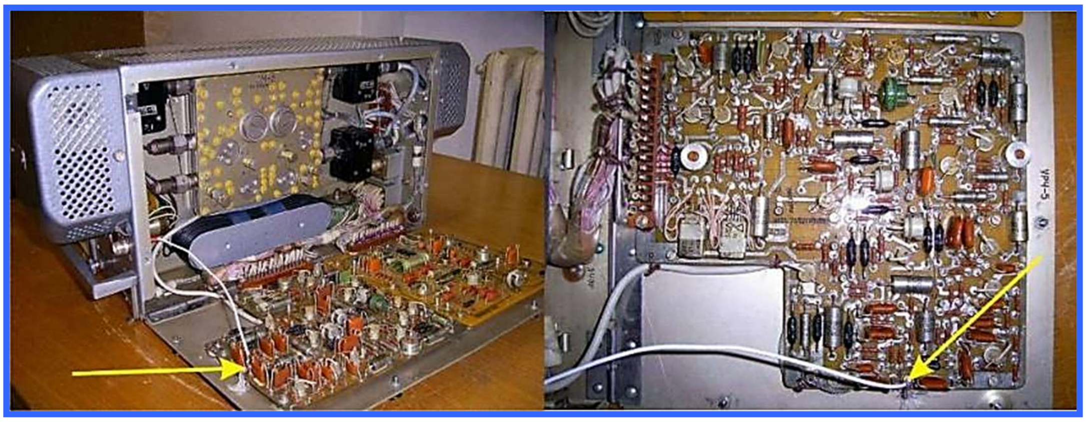

Fig. 57 Selected parts of real points in the block DFA - 5

Based on a detailed analysis of the principle of operation of the radio altimeter (RA), experimental laboratory tests were carried out to verify the correctness of the design and wiring of the system. Under the conditions of laboratory measurement (Fig. 57), the decisive electrical signals necessary for its application on the flying vehicle were recorded and subsequently evaluated (Fig. 56, 57). Despite previous verifications, repeated tests of the installed system on an aerial vehicle failed to achieve the parameters set by the equipment manufacturer. For this reason, a modification of the principle connection of the radio altimeter was carried out, the aim of which was to ensure that the required technical and operational characteristics of the measurement were met. The optimization consisted in adjusting the circuit connection in the radio frequency (RF) part of the RA. A simple resistive divider (Fig. 58) was implemented in the wiring, the function of which was to stabilize the signal level and eliminate interference effects causing fault conditions. After applying this modification, the identified anomaly, which was manifested by a periodic loss of altitude indication lasting approximately 5 seconds during the flight, was removed.

It should be emphasized that, despite its structural simplicity, the resistive divider proved to be a more efficient solution compared to previous, conceptually more complex wiring designs. Although they showed satisfactory characteristics during static measurements, there were repeated failures of information about the height in the cockpit during tests on a flying vehicle. The implemented modification thus ensured stable operation of the system in real operating conditions.

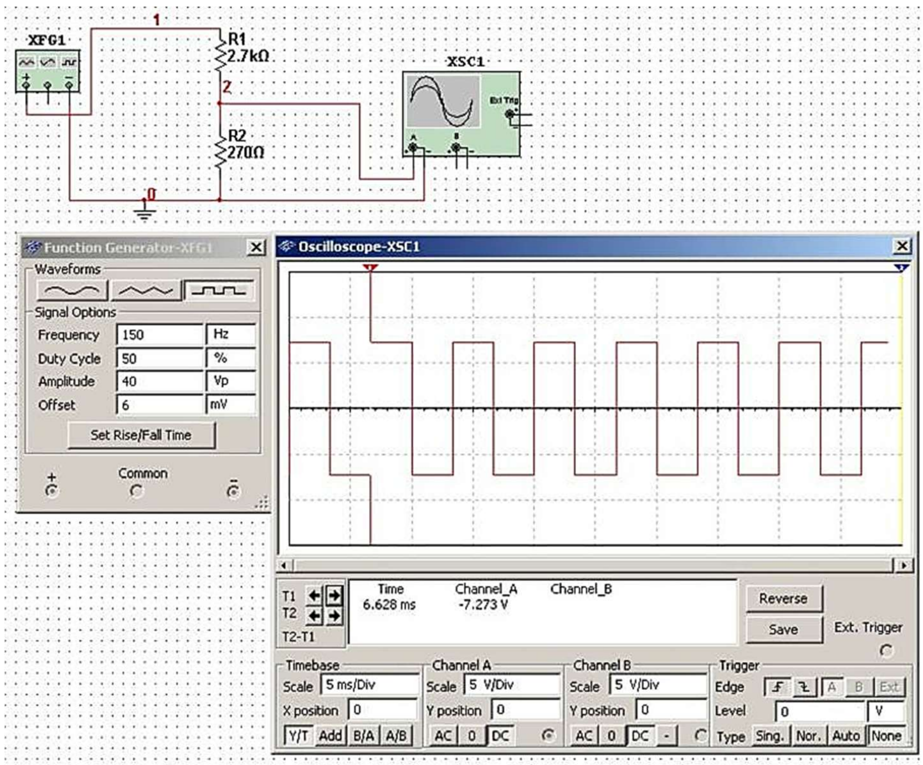

Fig. 58 Resistive divider - design in Multisim environment

The basic requirement for digital recording and recording of information from the radio altimeter is synchronous sensing of two signals, a modulating rectangular signal with a frequency of f=150Hz and a differential signal sensing with a frequency measurement requirement of f =30kHz. A specific device suitable for this purpose was a National Instruments NI USB-6210 A/D converter with a theoretical recording speed of 250kS/s (250,000 samples per second) for 8 parallel channels with differential connection and converters with a resolution of 16 bits. The wiring diagram of the device is shown in Fig.59.

The differential and rectangular signals were fed to the analogue inputs AI-1 and AI-2 of the measurement card, while the system configuration allowed for parallel sensing of both channels. The maximum sampling rate of the device was 125 kHz per channel. To record and process data, the A/D converter was connected to a portable personal computer via a high-speed USB interface.

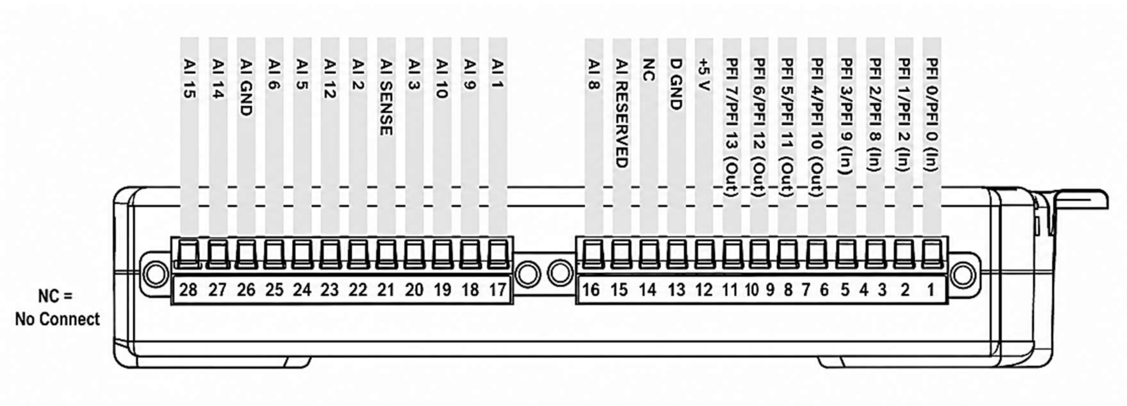

Fig. 59 Connecting Inputs and Outputs on the NI-6210

Software communication with the NI USB-6210 device was implemented in the LabVIEW 8.0 environment, which enabled the design of its own measurement application, including data acquisition management and archiving. Due to the limitations of the available hardware, it was not possible to achieve the theoretical maximum recording speed declared by the manufacturer. However, by optimizing the program architecture, especially by implementing a buffer for writing data to the hard disk and consistent synchronization of writing operations to data files, it was possible to ensure a stable transfer rate within the entire measurement loop at the level of 200 kS/s. This value represents the total sampling rate of the system, i.e. 200 kHz for both channels at the same time, which corresponds to an effective frequency of 100 kHz per channel for parallel recording and simultaneous data storage. In accordance with the Shannon–Kotelnikov sampling theorem, the sampling rate set in this way allows to analyze signals with the maximum frequency:

$$f_{max} = \frac{f_s}{2} = 50kHz \tag{107}$$

Where:

$f_s = 100$ kHz represents the sampling rate per channel.

This fulfilled the condition for a reliable frequency and time analysis of the differential signal of the examined radio altimeter without the risk of aliasing and with the maintenance of the required information value of the data measured. If you are interested, the text can be supplemented with a more detailed description of the implementation of the measurement loop (e.g. block structure VI in LabVIEW, acquisition timing, real-time data processing or statistical evaluation of measurements). Programming in the LabView system is implemented at the level of work with elementary modules in the graphical user interface and the implemented system is shown in Fig. 60.

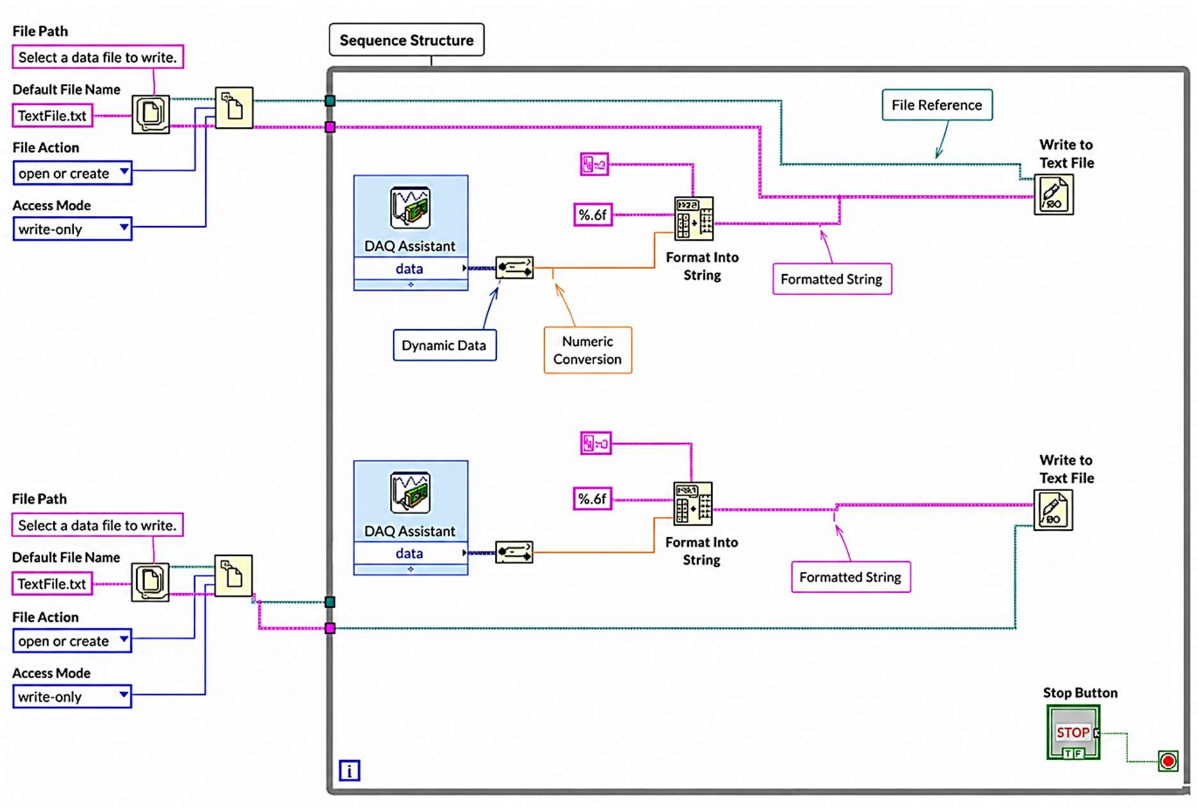

Fig. 60 Measurement scheme in LabView 8.0 software

The output of the measurements was exported in real time to two independently opened files, where the individual samples were stored along with the exact recording time of each sample from the start of the measurement. Data analysis was performed in the Matlab computational environment version 7.6 using a set of functions for signal analysis Basic analysis and data display was performed in the Matlab – Simulink simulation environment (Fig.61). where a real-time recording of a flight over a hill was played and its analysis was carried out with a display on a spectral analyzer, see Fig. 62 and 63.

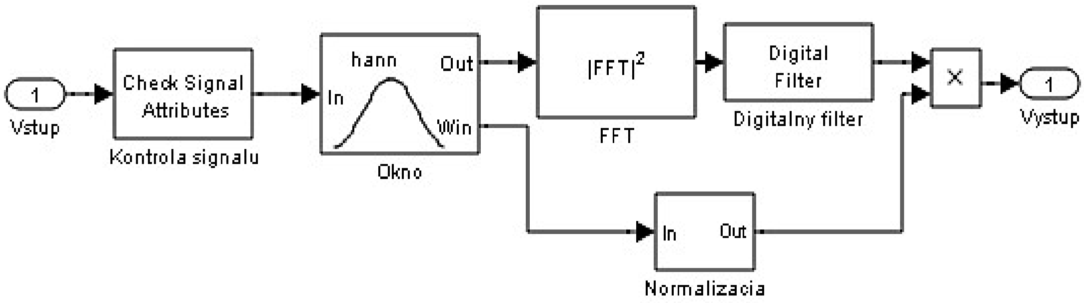

Fig.61 Model diagram in Simulink

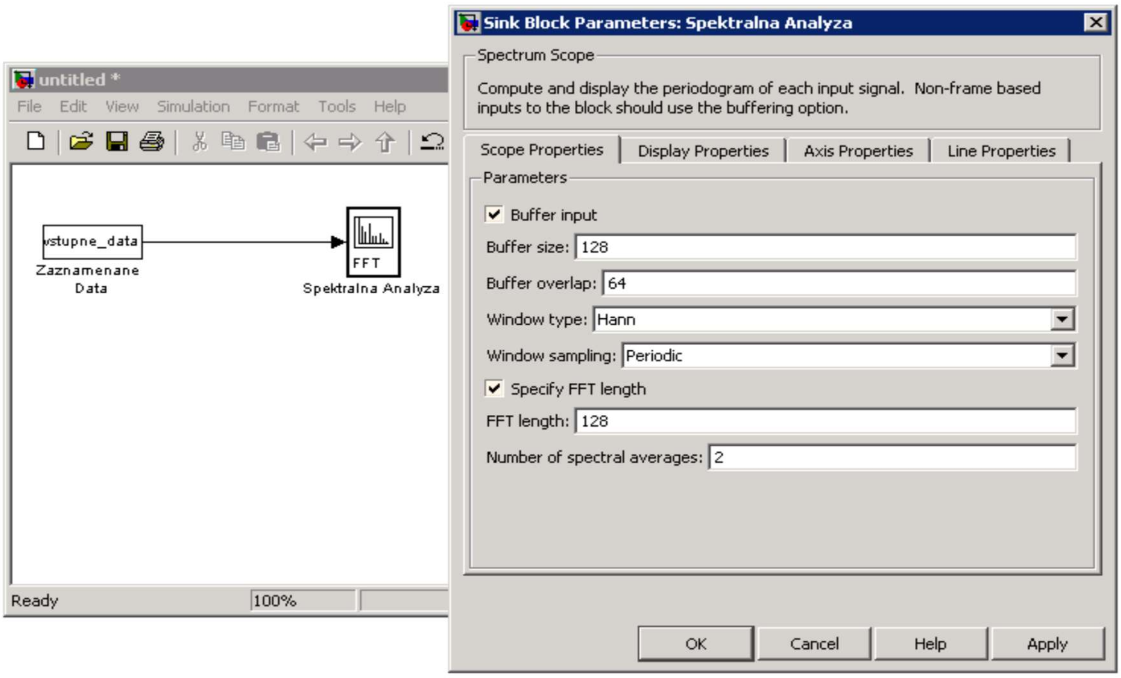

Fig. 62 Preliminary data analysis in Simulink along with setup

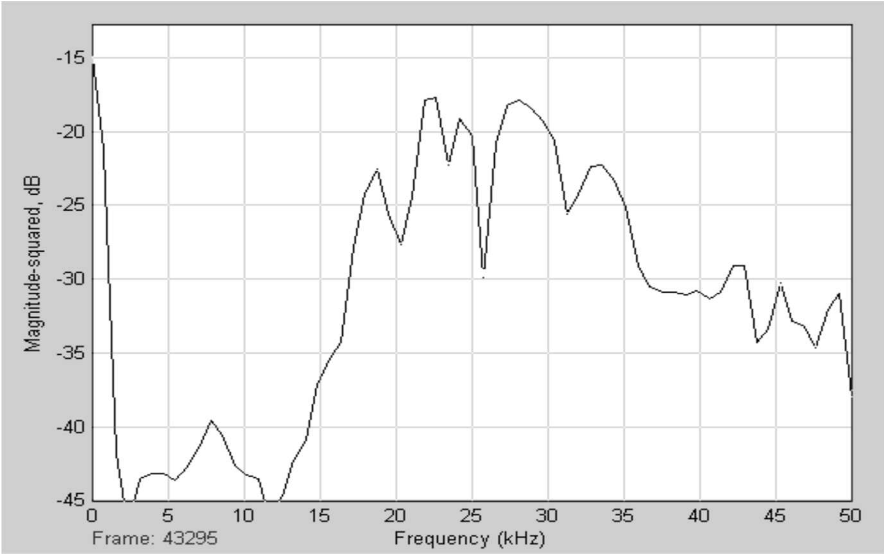

Fig. 63 Output from a survey spectrum analyzer in Simulink

Based on the output from the overview spectral analyzer implemented in the Simulink system, the entire record was divided into blocks for further batch processing in the basic MATLAB environment using the script language. The rendering of the results and the processing of the signal was carried out using the script language. Differential signal analysis was performed by functional implementation of the relationship for FFT (Fast Fourier Transform).

$$X_{(k)} = \sum_{j=1}^{N} x(j)\omega_N^{(j-1)(k-1)} \tag{108}$$

$$\omega_N = e^{(-2\pi.i)/N} \tag{109}$$

Where:

$X_{(k)}$ - k-th spectral component of the DFT output, $k = 1,2,\dots,N$

xj-th sample of the input discrete-time signal

N - Total number of samples (block length / FFT size)

ϖ_N - Complex twiddle factor (DFT kernel)

J - Sample index, $j = 1,2,\dots,N$(MATLAB 1-based indexing)

k - Frequency bin index, $k = 1,2,\dots,N$

7.7 Experimental analysis of the Doppler component of the difference signal uring flight over rising terrain

The main objective of the measurement was to analyze the formation of the Doppler effect of the radio altimeter during the horizontal flight of a flying vehicle over the terrain, the relief of which rises dangerously – approaching the flying vehicle. The situation is expressed in Fig. 80, which shows the hill over which the real measurement was made. During the flight, the flying vehicle performed a controlled flight into the terrain at such an altitude that it could safely fly over it in the last phase of the flight.
For the analysis of the formation of the Doppler signal FD, a time recording of the difference signal lasting about 75 seconds was carried out. When flying over a hill, flying in the middle of the hill, the recording of the differential frequency in front of its foot began to be recorded and continued for 40 seconds after the flight over the top of the hill. Taking into account the frequency limitation of the differential frequency recording based on the sampled recording frequency, it was possible to record the differential frequency only below 50kHz by the measuring instrument. He met this condition for about 30 seconds. recording of the writing in the time interval from 22 to 52 seconds. The differential frequency processed by the radio altimeter, the constant of which is K = 200, corresponds to the measured flight altitude of the aircraft 250 m, (50 000 : 200 = 250). The time area of the recording, which was analyzed by frequency, corresponds to the time of about 30 seconds. When the flying vehicle flew over the top of the hill, when the flight altitude was the lowest, the amplitude of the difference signal was the largest. According to the recording, the flying vehicle flew over the top of the hill in 32 seconds from the beginning of the recording. The increased amplitude of the differential signal from 0 to 10 seconds corresponds to the ramp-up of the recording equipment after it is switched on.

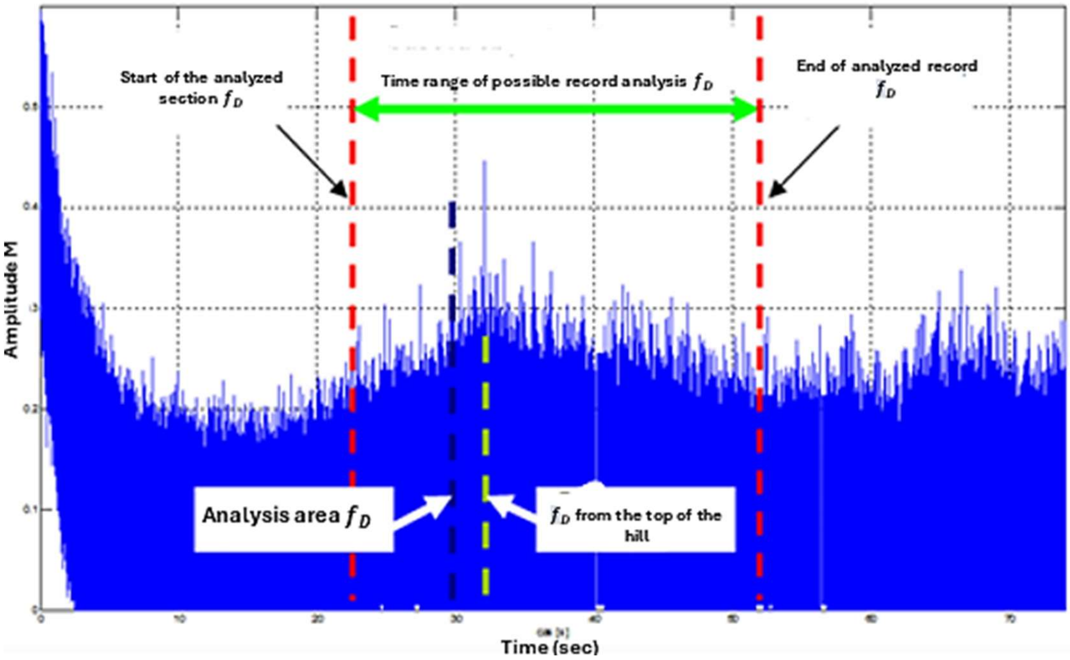

Fig. 64 Recording the difference frequency after flying over a hill

For the frequency analysis of the differential signal formation, a time period of 0.3 sec. was selected around 30 sec. of the recording, see Fig. 65. The time-amplitude record of the differential frequency Fr is highlighted in red in the figure. The blue signal of a rectangular shape represents a modulation frequency of 150Hz, which will allow us to correctly analyze the Doppler frequency.

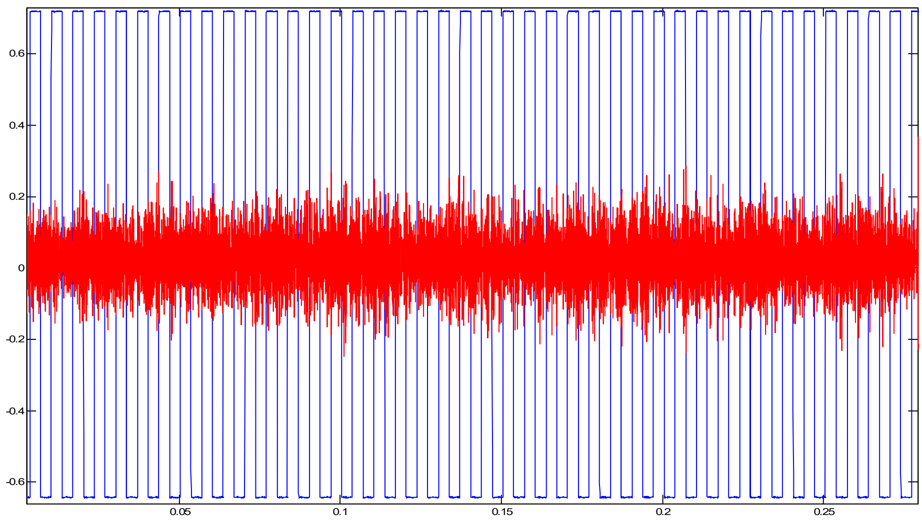

Fig. 65 Recording 0.3 sec. differential frequency

To evaluate the Doppler frequency, it is necessary to perform a frequency analysis of the differential frequency in each half-period of the modulation signal separately. Therefore, from the record in Fig. 65 Selected time period from 0.035sec. to 0.066 Fig. 66 and in it two half-periods 0.043sec. to 0.051sec. Fig. 67.

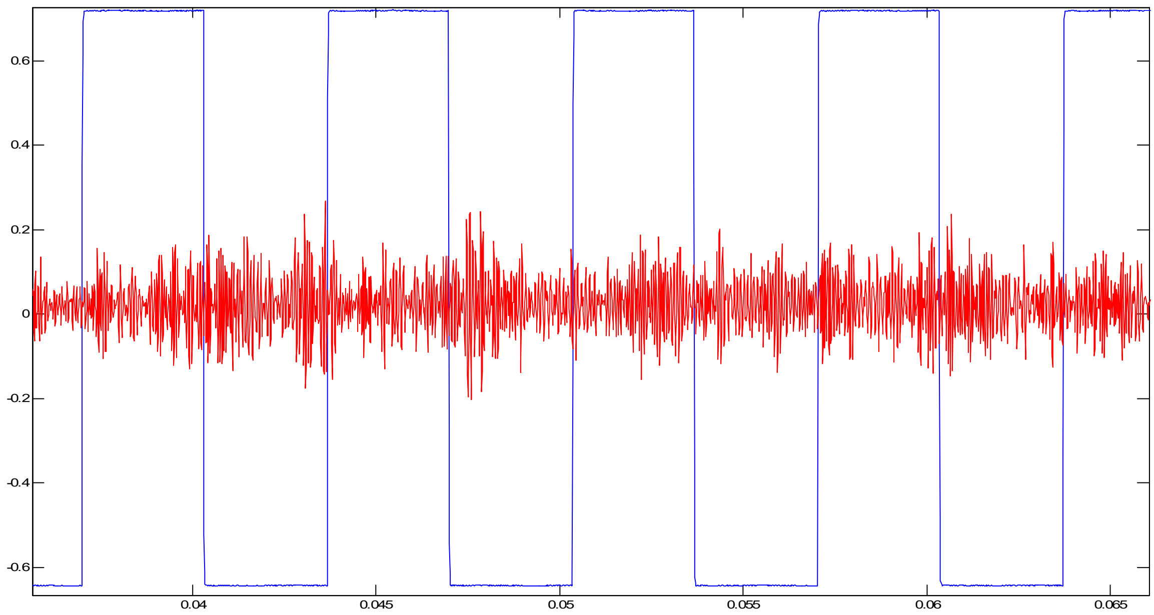

Fig. 66 Record 0.03 sec. of difference frequency

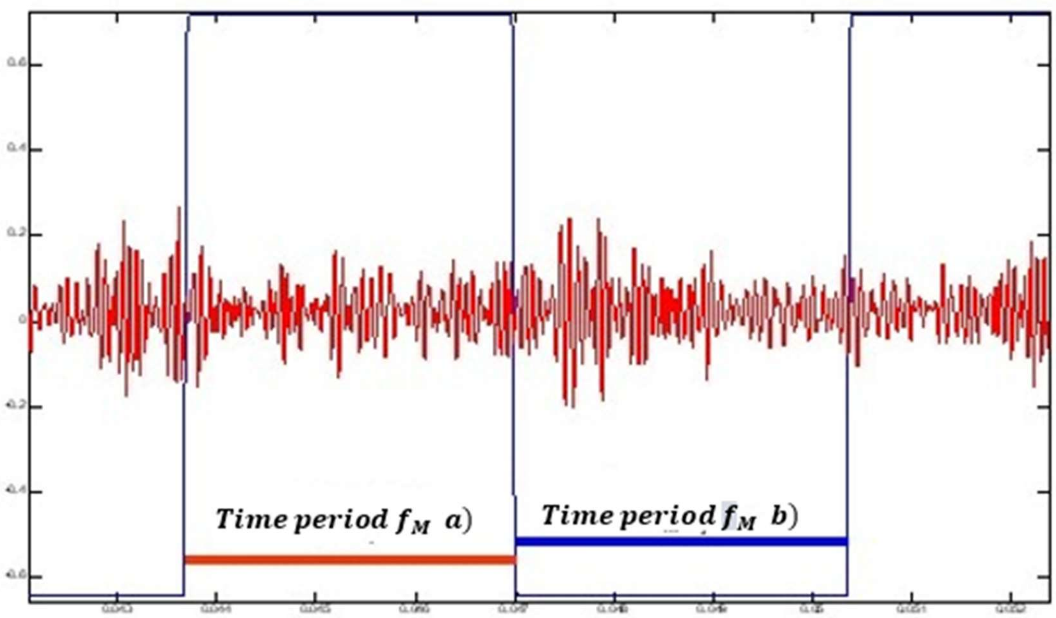

Fig. 67 Recording of the fr signal in the time period of one modulation period

The frequency analysis of the differential signal from the time period of modulation frequency a) is shown in Fig. 68. The fundamental harmonic of the differential signal in this case is at a frequency of 15.6kHz. The frequency analysis of the differential signal from the time period of modulation frequency b) is shown in Figure 69. The fundamental harmonic of the differential signal in this case is at a frequency of 13.74kHz.

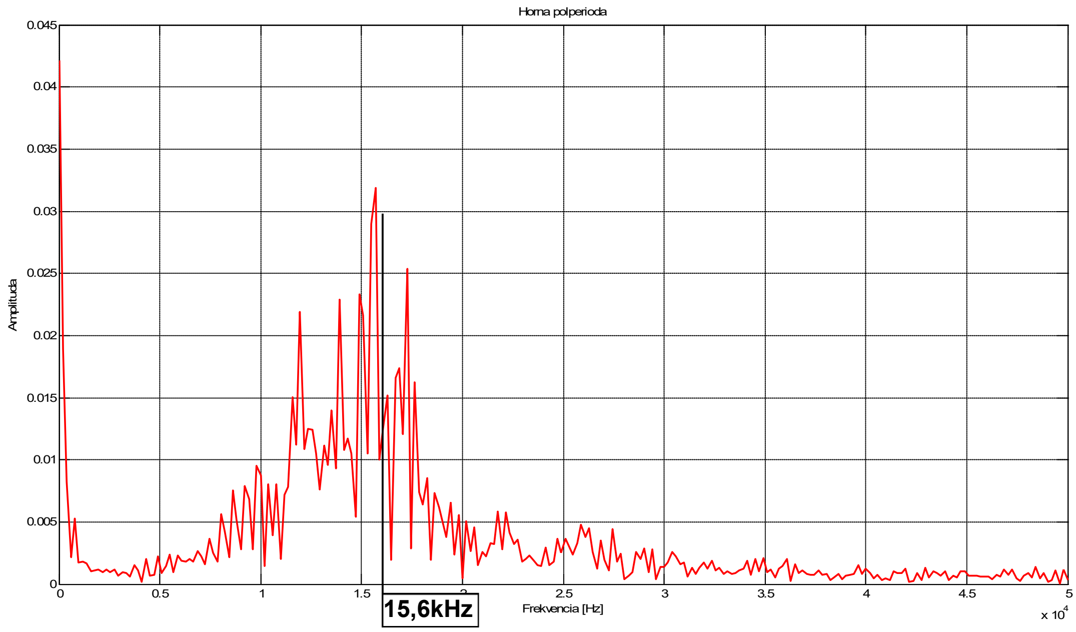

Fig. 68 Frequency analysis of the differential signal in the time period f_M

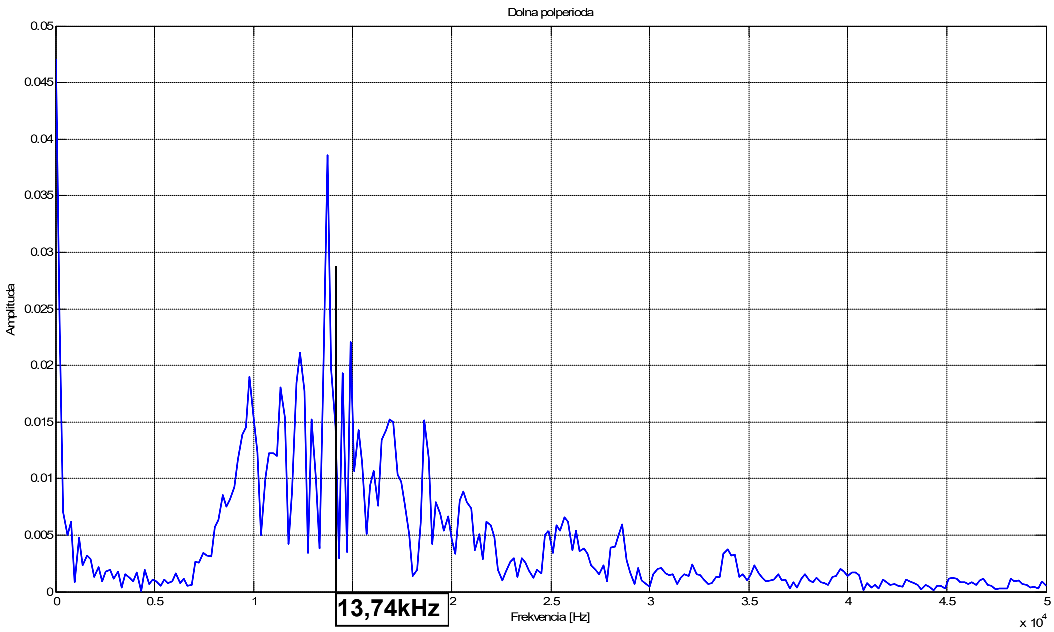

Fig. 69 Frequency analysis of the difference signal over time period (b) f_M
Frequency analysis of the difference signal over time period (b)f_M

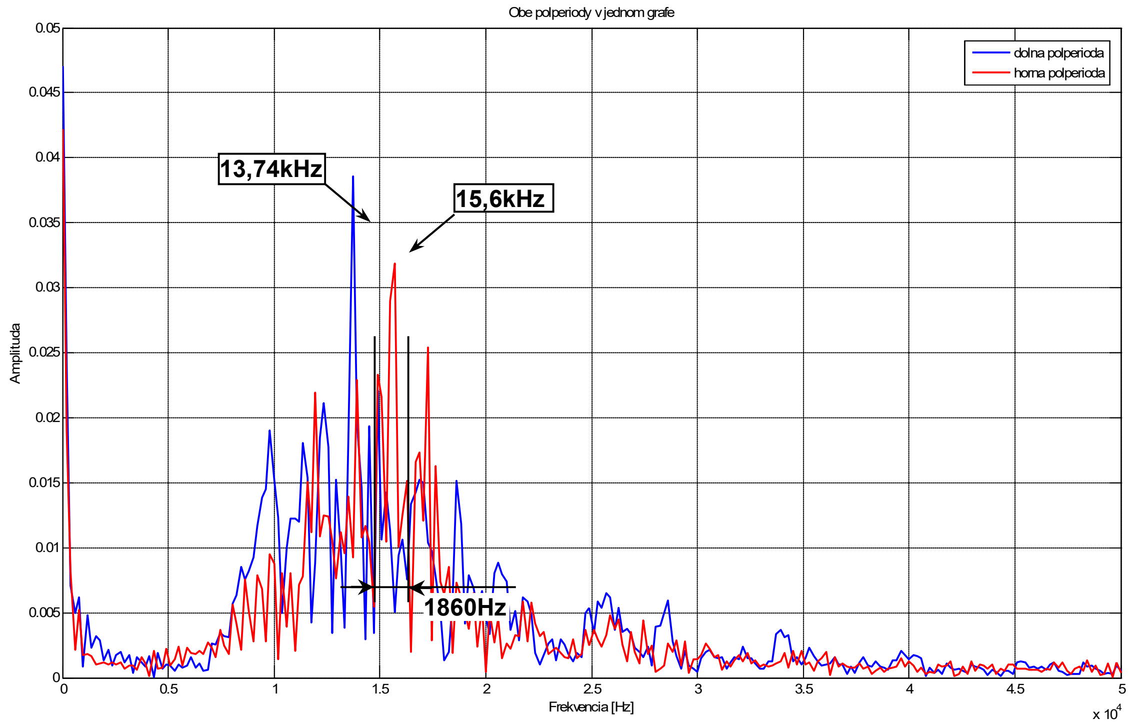

Fig. 70 Frequency analysis of F_M (a) and F_M (b) differential signals

The frequency difference of the two basic harmonics of the differential signal is 1860Hz (Fig. 70), (15600 – 13740 = 1860). The value of 1860Hz represents twice the Doppler frequency F_D = 930Hz. Substituting the measured values into the relation (108) we get:

$$F_{rD} = f_r \pm f_D = 14670 \pm 930\ Hz \qquad (110)$$

By measuring the differential signal during the flight of a flying vehicle uphill and the subsequent spectral analysis of this signal, it was concluded that the difference signal of the radio altimeter includes (under these flight conditions) in addition to the frequency proportional to the altitude of the aircraft, also the Doppler frequency. This theoretical assumption was duly confirmed by the measurements carried out. A positive conclusion of the measurement creates a prerequisite for the use of the Doppler effect of the radio altimeter to create a suitable anti-impact system for flying vehicles. To verify the measured results, it is necessary to assess them from theoretically derived values.

For this purpose, the image of the measured hill (Fig. 80) supplemented by known quantities so that they can be used in the calculation.

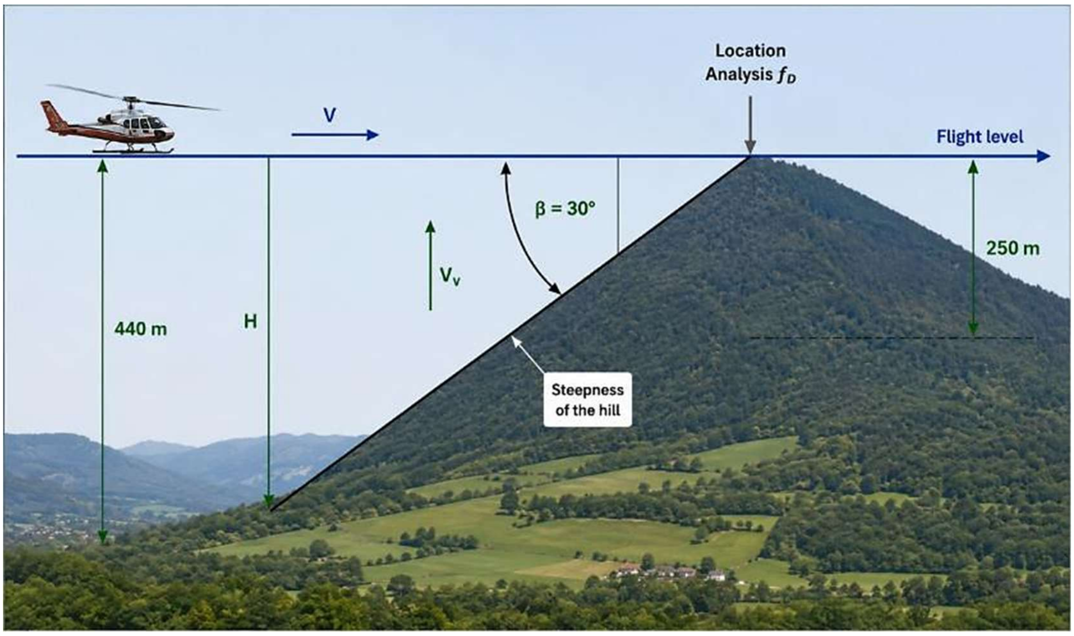

Fig. 80 Hill relief used in FD measurement

The Doppler frequency, as part of the radio altimeter's differential signal, is produced due to the vertical component of velocity vF_D v as the terrain approaches the flying vehicle during its horizontal flight. Therefore, to determine the value of the Doppler frequency, it is necessary to determine the value of the vertical component of velocity. We determine this value using the function tg β using the horizontal component of velocity v.$F_D v_v$. The flight speed of the flying vehicle during the experiment was 150 km/h. This value corresponds to the horizontal component of velocity v = 41.67m.s-1. Using the function tg of the known value of the angle β and the horizontal component of velocity v, the vertical component of velocity v_v can be calculated.

$$tg\beta = tg\ 36{,}5 = 0{,}74 \tag{111}$$

$$tg\beta = \frac{v_v}{v}\ v_v = tg\beta\ .v = 0.74.41{,}67 = 30{,}84ms^{-1} \tag{112}$$

The calculated value of the vertical component of velocity is vv = 30.84m.s-1. By introducing this value into the relation (112), we can calculate the Doppler frequency of f_D. At the same time, the value of the carrier frequency of the radio altimeter is 4.4.109 Hz.

$$f_D = \pm f_0 \frac{2v_v}{c} = \pm 4{,}4.\,10^9 \frac{2.\,30{,}84}{3\,.\,10^8} \doteq \pm 905\,Hz \tag{113}$$

The calculated Doppler frequency value of 905Hz is comparable to the measured Doppler frequency value of 930Hz.

7.8 Linking a dynamic flight model with a radio altimeter measurement chain

A flying vehicle controlled by collective and cyclic control can be described by differential equations, where these are differential equations with constant coefficients. By transforming the differential equations into the Laplace pattern, which is also a symbol of the Matlab computing environment, it is necessary to describe the flying means by symbolic equations of motion, the image of which in the program scheme for the Matlab language is shown in Fig.81 .

- V_x *flight parameters (forward speed)*
- V_y *flight parameters (vertical speed)*
- *υ – is the position parameter of the flying vehicle (longitudinal inclination)*

The flight experiments were conducted using a Mi-8MTV helicopter and an Agusta 102 helicopter. The equations describe a generic light helicopter. The Agusta A109K (the basis for the K102) is characterized by the following parameters:

- Gross Weight: ~2,850 kg
- Main Rotor: 4-bladed, 11 m diameter
- Powerplant: 2 × Turbomeca Arrius 2K2 engines

$$v_x(s) = -\frac{3{,}1}{s + 0{,}028}\left[s + 2{,}65)\,\upsilon - 0{,}29\,\delta_{col.} - 0{,}95\,\delta_{cycl.}\right] \tag{114}$$

For the Agusta K102 (larger rotor disk area → increased aerodynamic drag, stronger velocity-tilt coupling):

$$V_y(s) = -\frac{1}{s+0{,}58}\,[s0{,}052\,V_x - 0{,}28\upsilon - 7482 - 4751] \tag{115}$$

$$\upsilon(s) = \frac{1}{s(s0{,}28)} = -0{,}85\,\delta_{col.} - 3{,}1\delta_{cycl.} \tag{116}$$

The quantities given are the output quantities of the flying vehicle - helicopter. The input quantities for the flying vehicle are the deflection of the handlebars, where the deflection of the cyclic and collective control is (Fig. 81). From the point of view of control theory, it is an object (Multi-Input – Multi-Output). [56] [28][16]. The circuit is limited to 2 inputs and 3 outputs (Fig. 81), the influences of the external environment that allow both inputs and outputs are omitted. In the case of variables, constants in numerical form appear, which represent aerodynamic coefficients for the flying vehicle (generally in airplanes). Aerodynamic coefficients accept aerodynamic quantities where we assume that they will not change in a given range, i.e. 10 % deviation from the specified quantity. The linearization of differential equations, which are generally non-linear, makes it possible to work with aerodynamic coefficients, which also do not change in the indicated band.

Their origin is obtained by calculation on the basis of aerodynamic characteristics supplied by the manufacturer, which are verified by practical measurements.
In the aerodynamic coefficients are encoded:

1. *static and dynamic values of buoyancy coefficients C_y and C_x,*
2. *changes in the angle of inclination and their derivatives.*

Other important parameters for the calculation are the moment coefficients in the given case, as well as the axial moments of inertia. The notation and the corresponding scheme do not accept the influence of lateral deviations. This simplification can be accepted because the radio altimeter was monitored only during horizontal flight with longitudinal inclination. The output quantities for the RA are shown in Fig. 81. The issue would be considerably more complicated if we considered the large deviations in each coordinate axis. The scheme neglects quantities of smallness of the second order. The reason is that it is a flying vehicle with great potential energy, where the relaxation of the release of the control forces requires time in the airborne environment. The delay between entering the control and responding to a flying vehicle is up to 3 seconds. For this reason, we can consider the speed to be highly inertial, which is advantageous from the point of view of control, since the pilot can comfortably control kinematic quantities. The conditional equation for height tracking is:

$$V_y = \dot{H} \tag{117}$$

When transferred to the Laplace transform:

$$V_y(s) = s\,.H(s) \tag{118}$$

Where:

$$H = \frac{1}{s}\,V_y(s), \quad \omega_z = \dot{\sigma}_H \qquad V_y(t) = \frac{dH(t)}{dt} \tag{119}$$

The abstract analysis of the above problem should result in the simulation of a radio altimeter model, which can have the form of a differential equation for unit observation of the input quantity:

$$\ddot{H}_{REL} + 2d_{REL}\omega_{REL}\dot{H}_{REL} + \omega_{REL}^2 H_{REL} = \varsigma_{REL} \tag{120}$$

Where:

$\ddot{H}_{REL}$ - second derivative of the relief height

d_c – damping constant of the altimeter measurement system

$\dot{H}_{REL}$ - relief derivation

ξ_{rel} - white noise

In general, however, the input quantity is the relief, which can be replaced by white noise. Further considerations about the possibilities of altitude tracking solutions can be found in Fig. 82:

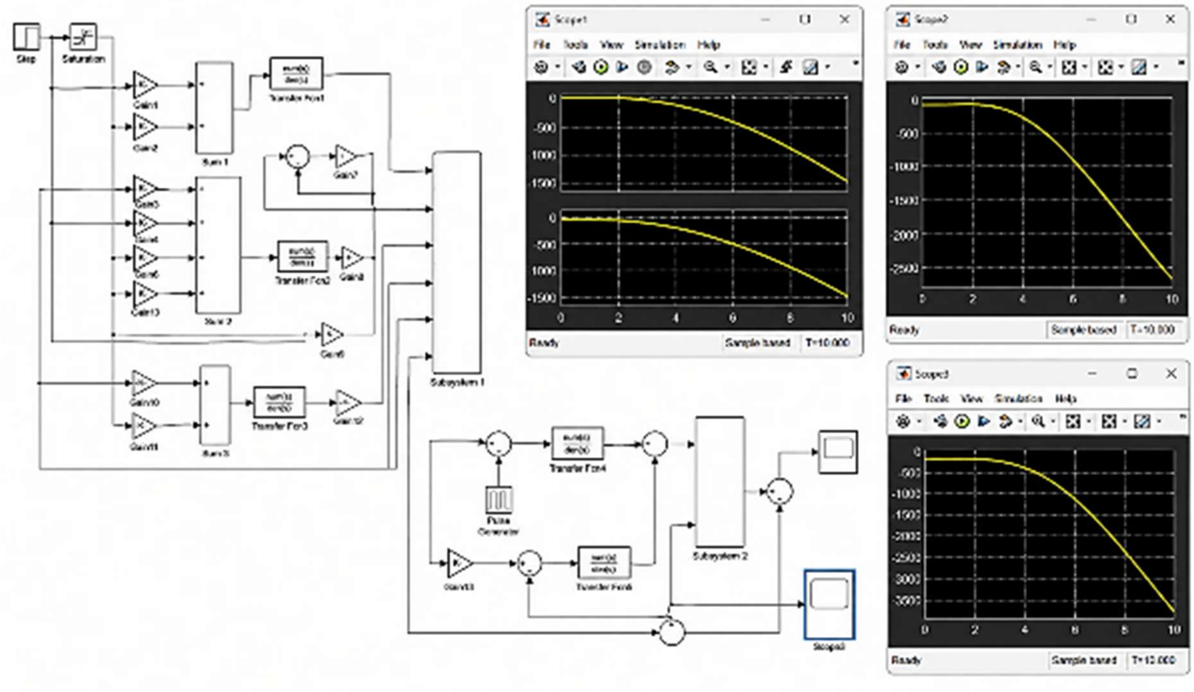

Fig. 81 Model of a flying vehicle with RA in the forward direction of flight Matlab-simulink

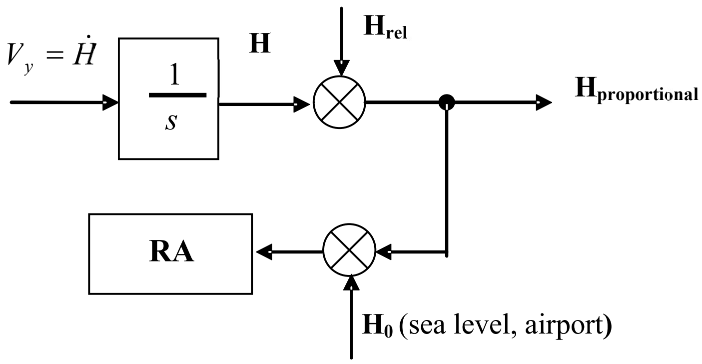

Fig. 82 Detail of the simulation mathematical model with RA output

7.9 Model of aircraft-terrain interaction in the context of flight safety

Following the previous considerations about the influence of the Doppler component of the signal and the need for predictive evaluation of the risk of collision with the terrain, it is necessary to extend the analysis to model the situational dynamics of flight. The measurement of altitude or vertical speed alone does not provide a complete picture of the safety status of the system, unless it is placed in the broader context of the interaction of the flying vehicle with the environment. Modelling situational dynamics in aviation requires an appropriate degree of abstraction and simplification.

Simplified mathematical models allow for an analytical grasp of the problem and the identification of decisive parameters, but they usually do not capture all the interaction links between objects in space. When evaluating flight safety, it is therefore necessary to consider the interaction of several bodies, especially the flying vehicle and the terrain below it. This fact leads to the need to extend the dynamic description of the system into a broader context and to create a simplified but relationally correct mathematical model of their interaction. Situational dynamics can be considered ideally describable only under the assumption of a physically undisturbed environment without random disturbances and unpredictable influences. However, in real conditions, there are deviations caused by changes in terrain, meteorological influences, measurement errors or reaction time of the crew. Even when using a simplified model, which represents, for example, the presence of an isolated terrain obstacle, it is clear from the point of view of flight safety that it is necessary to consider the mutual situational dynamics of the flying vehicle and the terrain as a common system. The complexity of this problem can be partially formalized by introducing the concept of situational uncertainty, which expresses the degree of uncertainty in estimating the future evolution of the flight situation. This uncertainty is an important, often difficult to quantify, factor in the assessment of air traffic safety and in the analysis of the causes of air accidents. Reducing situational uncertainty is one of the main goals of modern on-board systems.
The concept of cognitiveness, i.e. the cognitive ability of a system consisting of a pilot and on-board equipment, is closely related to the above. The pilot must continuously evaluate the development of the situation, interpret the available information and appropriately adapt the flight dynamics to the current conditions. The technical equipment of the flying vehicle, including the radio altimeter and related warning systems, is designed not only to react to a critical condition, but above all to predict the

potential risk of collision with the terrain. By implementing the measurement of the Doppler component and evaluating the ratio of altitude to vertical velocity, the prerequisites are created for providing information that reduces the entropy of the programmed situational dynamics of flight. In other words, the system becomes more information-rich and able to predict the development of critical states. A graphical interpretation of the problem considered is shown in Fig. 83 and 84.

The situational dynamics model formulated in this way builds on previous experimental and theoretical considerations and represents a logical extension of the analysis towards an integrated flight safety assessment. In the following, we consider the flight of a flying vehicle, the purpose of which is determined by the pilot's activity. It is generally impossible to determine the degree of freedom of its situational dynamics.

The common abstract airspace of both situational dynamics realized by the pilot through a flying vehicle in the Pilot-Aircraft cybernetic link is situational space D, which simply represents physical space for the aircraft and for the pilot.

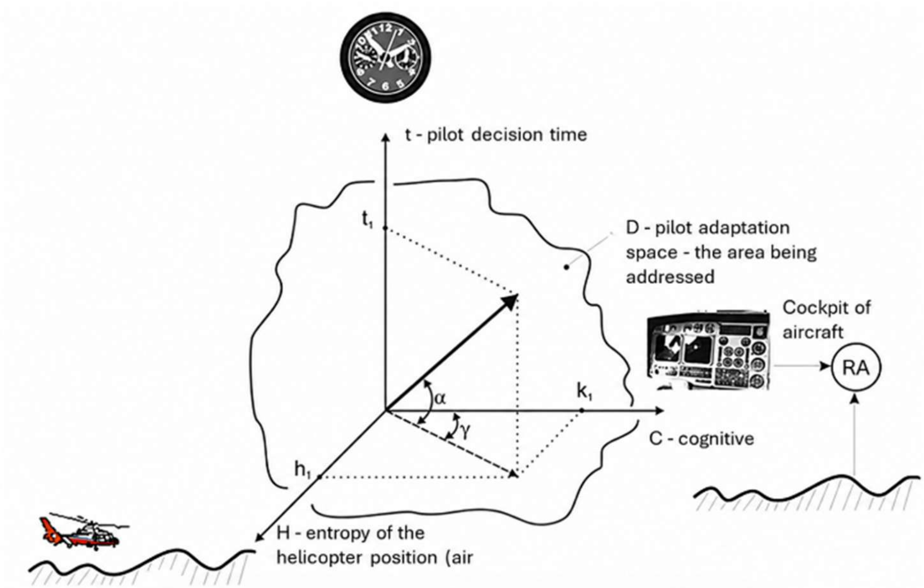

Fig. 83 Model situational flight dynamics in the space of physical adaptation

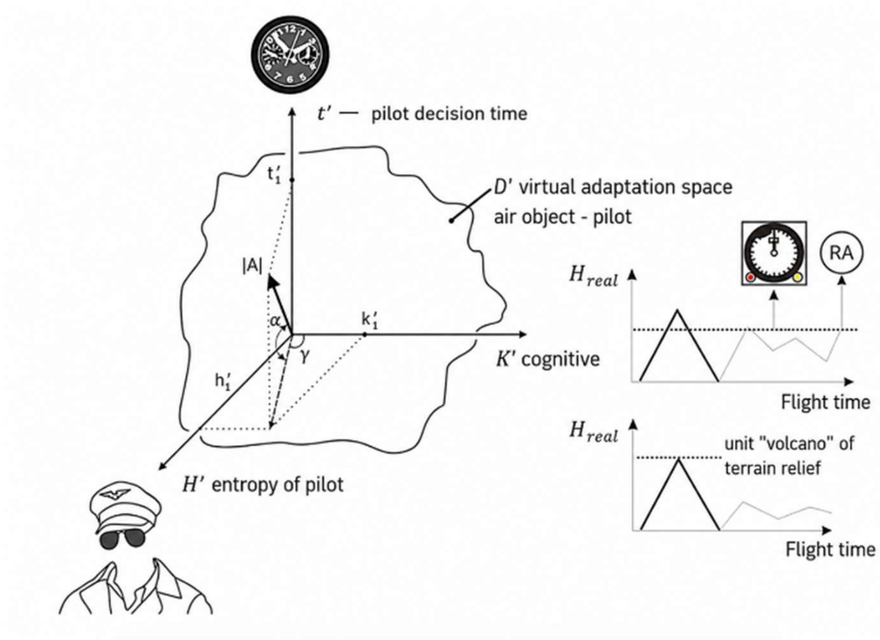

Fig. 84 Model situational flight dynamics in the space of virtual pilot adaptation

Each of the mentioned spaces is limited by information that represents the intelligent characteristics of the aircraft and the learned, trained skills of the pilot. Another non-binding D'fact in creating an idea of situational dynamics is virtual and physical knowledge, which is fixed in his consciousness by real practical experiences from flight, which complete the content of the adaptation scene. The complexity of the considerations can be further increased, e.g. by disinformation with dominant interference influences, operating in the sphere of adaptation D and the adaptation scene $D'D'$. For safe flight, the equality D, shall be reflected in the new representation D', which represents the new safety coordinate system, approximated in Fig. 85.

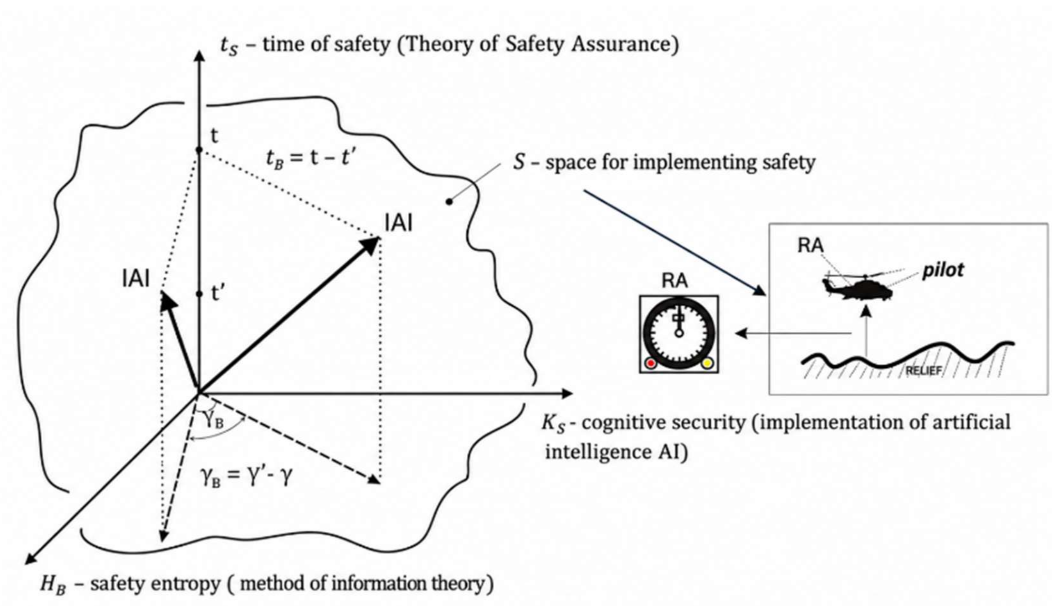

Fig. 85 Flight safety coordinate system

For $t_S > t - t'$ → *forecast of decision-making on the perception of the situation from information systems and from possible visualization of the terrain,*
for $t_S < t - t'$ → *pilot intervention,*
for $t = t'$ → *balanced safe flight.*

Building on the previous considerations of the situational dynamics of flight and the reduction of uncertainty by means of additional information variables, it is also possible to analyze the situation when there is a deviation between the desired and actual trajectory of the system. With a difference (D D' Fig..84) new flight conditions arise that change the character of the current flight situation in front of the pilot. This difference represents a shift of the resulting IAI module towards the coordinate, which is desirable from the point of view of control, but may not correspond to the real dynamic capabilities of the flying vehicle-terrain system. The deviation thus created modifies the pilot's decision-making framework and creates a new quality of situational dynamics. Negative value of the distance between modules (|AD|) and (||) represents a condition in which pilot intervention (S) is necessary. Although this intervention is aimed at stabilizing the flight, it also increases the burden on the decision-making process and reduces the cognitive reserve of the entire human-flying system. AD_1.

As a result, there is a gradual reduction of the safety margin and a limitation of flight safety as a dynamic quantity. The validity of the above considerations can be documented by analyzing real flight data records (FDR – "black box") from air accidents.

The time course of the recorded parameters indicates a gradual change in the dynamic characteristics of the aircraft and the development of the crew's decision-making process. Control interventions often show the character of divergent control functions, which ultimately lead to the loss of stability of the system and to the termination of the flight in a catastrophic, irregular manner. Further research in this area is aimed at determining the critical angle of inclination), the exceeding of which does not allow return to the safe flight zone. The identification of this limit is essential for defining the limit states of the system and for the design of preventive or warning algorithms. The aim of a transparent interpretation of the issue of degradation of flight safety is to point out the un justification of an isolated assessment of individual safety factors. An unambiguous designation of the cause of degradation of the safety of a complex man-a-vehicle system is almost always based on an isolated assessment of the final consequences, without taking into account their dynamic development over time. In the context of this monograph, it should be emphasized that the activity of the radio altimeter itself cannot be evaluated in isolation in a similar way. The accuracy of the altitude measurement, the influence of the Doppler component of the differential signal, the dynamic error in vertical movement, and the pilot's response to the indicated altitude are not separate phenomena. They form an interconnected information-control chain, in which a measurement error can lead to an incorrect interpretation of the situation by the pilot and subsequently to inadequate intervention in the control. Therefore, the radio altimeter cannot be understood merely as a stand-alone measuring instrument, but as an integral part of the aircraft safety system, significantly affecting the situational dynamics of flight, especially at low altitudes. The dynamics of causes and the statistical occurrence of aviation accidents indicate various sources of their origin, whether caused by the human factor (operator) or by technical failures of aviation technology. In real operating conditions, however, these events are the result of the interaction of both subsystems within a single integrated safety unit. In the case of CFIT (Controlled Flight Into Terrain) events, the quality of altitude information and its dynamic variation provided by the radio altimeter play a decisive role. If this information is distorted or misinterpreted, it may become the trigger for a chain of events leading to the loss of a safe flight trajectory.

8 THE EXPERIMENTAL SETUP OF TWO CHANNEL RADIO ALTIMETER

The experimental dual-channel radio altimeter was implemented under laboratory conditions using two older, conventional single-channel radio altimeters. These units were available and could be irreversibly mechanically disassembled for the purposes of experimental measurements, and their electrical circuitry could be purposefully reconfigured. For these reasons, decommissioned yet fully functional FMCW radio altimeters were used, operating at a carrier frequency of $f_0 = 444$ MHz with a frequency deviation $\Delta f = 17$ MHz, a modulation frequency $F_M = 75$ Hz, and a measurement accuracy of $\Delta H = 2.2$ m. One of the radio altimeters (Channel 1) remained entirely in its original configuration. From the second unit, which was disassembled, the following circuits were reused: the high-frequency balanced mixer, the low-frequency amplifier, the difference-frequency shaping circuit, and the evaluation circuit for height pulses (Channel 2). Both channels shared a common transmitter, a common output to the transmit antenna, and a common input from the receive antenna. To implement the dual-channel radio altimeter, an RF splitter for the receive-antenna signal was built, including a delay line in one of the channels, along with an RF splitter for the transmitter signal and an adder/combiner for the low-frequency beat (difference) signal. However, height measurements were not performed between the transmit and receive antennas via propagation of electromagnetic waves in free space. Instead, the RF path was emulated using a coaxial line, connected at one end in place of the transmit antenna and at the other end in place of the receive antenna. An attenuator was also inserted into this RF path, enabling emulation of the required signal attenuation under real operating conditions. The basic minimum—so-called residual—height of the radio altimeter, i.e., the height from which the measurement started, was created by coaxial sections on the transmit and receive sides, corresponding to a baseline height of 7.54 m; the attenuator was included in this baseline height. Because a radio altimeter operates at a relatively high frequency (approximately 4.2–4.4 GHz), a coaxial cable rated for at least 5 GHz was used. These requirements were met by the NORDIX coaxial cable type MWC6/50. Each section consisted of a specified length of NORDIX MWC 6/50 cable and two RF connectors/feedthroughs of type F. During laboratory measurements, changes in the measured height were implemented by extending the baseline height (7.54 m) with additional coaxial sections of 0.5 m length. For this purpose, six coaxial-line sections were fabricated with lengths of 0.5 m, 1 m, 2 m, 4 m, 8 m, and 16 m. By interconnecting these sections, a physical maximum additional measured path length of 31.5 m could be achieved.

In terms of electrical properties, the measured RF-path values had to be recalculated taking into account the velocity factor (shortening factor) of 0.8 for the coaxial cable used. Consequently, an additional RF path with an electrical length of 25.2 m was implemented, which could be adjusted discretely in 0.4 m steps.

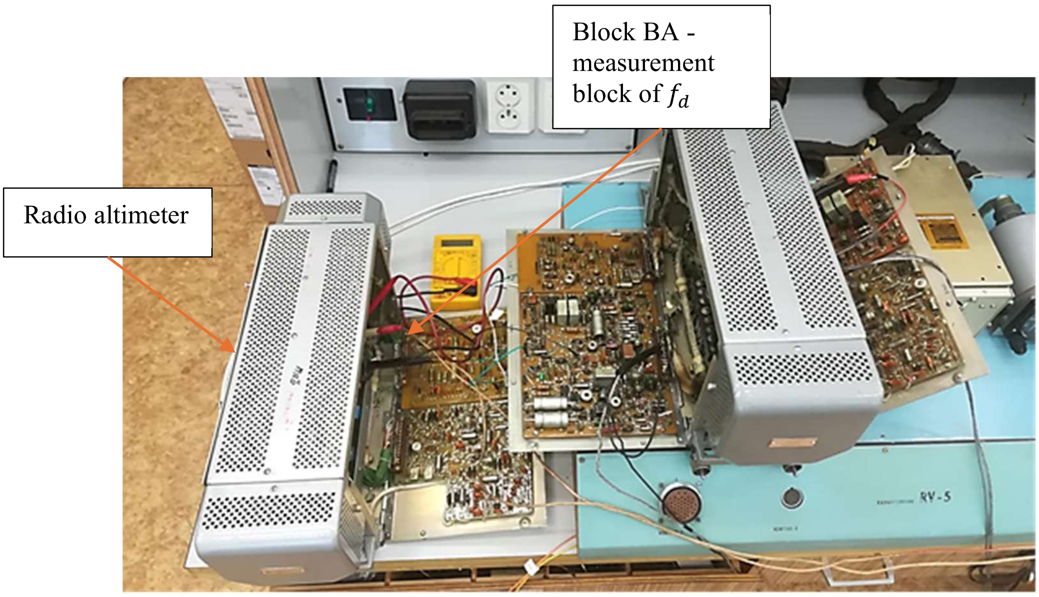

Fig. 86 Mutual interconnection and cooperation of two RV5 radio altimeters in a dual-channel configuration

For improved visualization of the measured values and a more objective evaluation of the achieved results of all three outputs within a single graph, the doubled value of the beat (difference) frequency at the common output of both channels was divided by two. To convert the beat-frequency value to the measured height, the fundamental radio-altimeter equation can be used. For an FMCW radio altimeter with a frequency sweep $\Delta f = 17$ MHz and a modulation frequency $F_M = 75$ Hz, the radio-altimeter constant is

$K = 34$. Therefore, if the measured beat frequency F_d[Hz] is divided by the constant 34, the measured height H[m] is obtained.

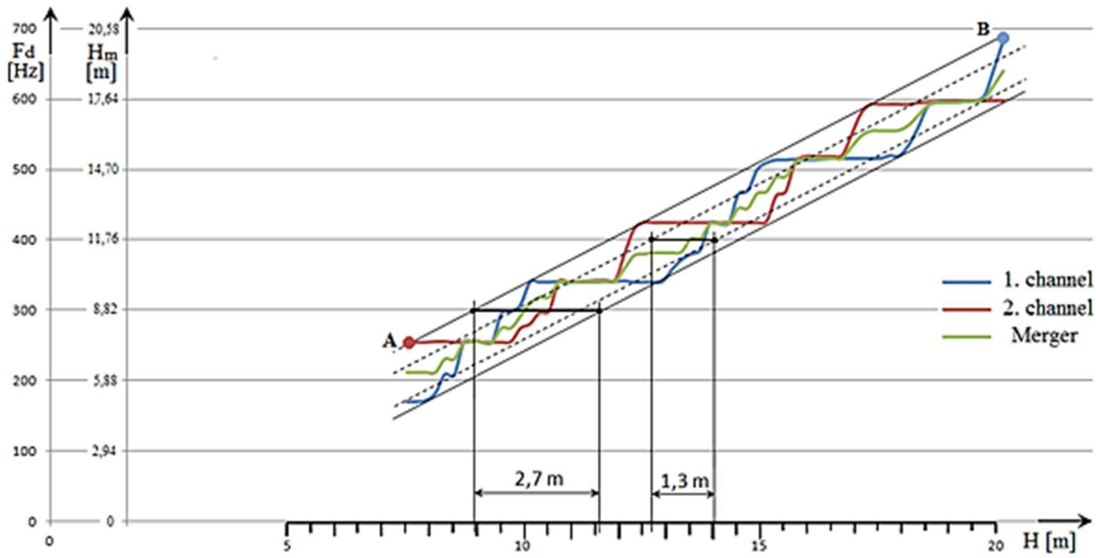

Fig. 87 Results of experimental measurements of the dual-channel radio altimeter

8.1 Results of the experimental measurement

The aim of the laboratory measurements was to practically verify the theoretical analysis of a dual-channel radio altimeter, with a focus on improving height-measurement accuracy. For this reason, the results of the experimental measurements of the dual-channel radio altimeter are discussed below. Three traces of the measured beat (difference) frequency were evaluated: Channel 1, Channel 2, and the combined channel. The beat frequency (F {dis}) is proportional to height, such that the number of height pulses (N - shaped) generated during one modulation period (T_M) is multiplied by the number of modulation periods per second, i.e., the modulation frequency (F_M)). A discrete increase by one pulse within a single modulation period corresponds to a discrete increase of the beat frequency by the value of the modulation frequency. Consequently, the beat frequency exhibits a staircase-like increase, which can be observed in the measured results. On the “steps” of each trace, two straight lines can be constructed. The first connects the peaks -i.e., the “tips” - corresponding to the minimum height values at a constant beat-frequency level (upper line). The second connects the peaks - i.e., the "feet" corresponding to the maximum height values at a constant beat-frequency level (lower line). For any constant beat-frequency value, these two solid lines can be connected by a horizontal line. The projection of the two intersection points of this horizontal line with the two solid lines onto the horizontal height axis represents the measured systematic (method) error ΔH(critical height) of the classical single-channel radio altimeter under test. For the method error of one channel of the dual-channel radio altimeter, the evaluated value was $\Delta H = 2.7$ m. The theoretical method error of the radio altimeters used is 2.2 m. From this it can be concluded that the mechanical and electrical modifications applied to the original radio altimeter degraded its method error from 2.2 m to 2.7 m.

The "stairs" formed by the height pulses of Channel 1 and Channel 2 are mutually shifted such that the sum of the height pulses from both channels can be formed. The resulting sum of the beat-frequency pulses of both channels has twice the value, and the plotted characteristic would extend beyond the range of the single-channel dependencies. Therefore, each summed beat-frequency pulse value of both channels was subsequently divided by two and is shown as the green height-dependent trace positioned between the traces of the two channels. This combined trace also exhibits a staircase characteristic, for which two analogous dashed straight lines can likewise be constructed. In this case as well, for any constant beat-frequency value, these two dashed lines can be connected by a horizontal line. The projection of the two intersection points of the horizontal line with the two dashed lines onto the horizontal height axis represents the measured method error ΔH(critical height) of the dual-channel radio altimeter under test.

For the method error of the dual-channel radio altimeter, the evaluated value was $\Delta H = 1.3$ m. The theoretical method error of the radio altimeters used is 2.2 m; accordingly, the theoretical method error of the dual-channel radio altimeter should be 1.1 m. From this it can be concluded that the mechanical and electrical modifications of the two original single-channel radio altimeters slightly degraded the method error of the resulting dual-channel radio altimeter from 1.1 m to 1.3 m.

However, if the measured method error of the real, classical, mechanically modified laboratory radio altimeter, $\Delta H = 2.7$ m, is compared with the achieved method error of the implemented laboratory dual-channel radio altimeter, $\Delta H = 1.3$ m, it can be stated that the theoretical analysis presented in the introductory chapters has real and practical significance.

8.2 Test bench for measuring the systematic (method) error of radio altimeter

To achieve the required accuracy of any measurement, it is advisable to optimize the measurement test bench and thereby eliminate factors that could significantly affect the measured results. One way to improve measurement quality is to implement an automated test bench for measuring radio-altimeter parameters. The use of an automated test bench for measuring the parameters of FMCW radio altimeters lies in simplifying the recording of measured data, reducing the total measurement time, minimizing the possibility of incorrect reading of measured values from the indicator through automatic data logging to a storage medium, and facilitating subsequent processing of the measured data. In addition, this type of test bench minimizes the presence of personnel during the measurement itself, thereby also reducing exposure to the harmful effects of electromagnetic radiation. For driving the antenna system, a cable-driven motion mechanism was selected, consisting of:

- *the drive unit (electric motor with a drive wheel),*
- *the driven wheel (a wheel located on the opposite side from the drive unit), and*
- *a guiding mechanism.*

Antenna-system drive

The drive unit consists of a stand in which the drive wheel is mounted. The wheel is connected to the electric motor via a shaft. In order to minimize friction, the shaft is supported by two low-viscosity bearings housed in bearing blocks. A clamping ring is bolted to the drive wheel, rigidly fixing the drive wheel to the shaft by means of a locking screw. The guiding mechanism consists of a robust metal structure attached to the antenna stand and two nylon rollers arranged in series. Each nylon roller is mounted on a pair of low-viscosity bearings in order to minimize friction between the roller and the axle, which would otherwise introduce a braking effect on the antenna stand. The mounting of the individual parts of the motion mechanism was designed to allow fast and simple installation and subsequent removal.

This was achieved using a U-shaped steel profile with two threaded holes and clamping screws. Such a mounting system is advantageous due to its high flexibility with respect to mounting locations.

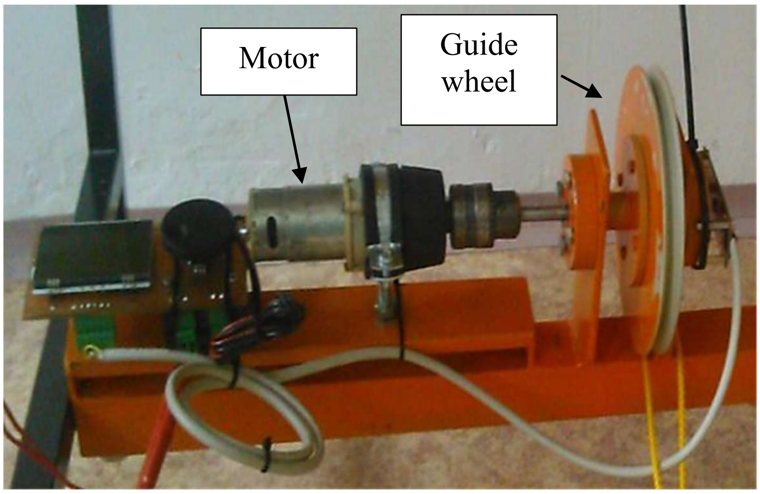

Fig. 88 Drive motor for the antenna system, including the service panel

Fig. 89 End point of the cable travel path for driving antenna displacement

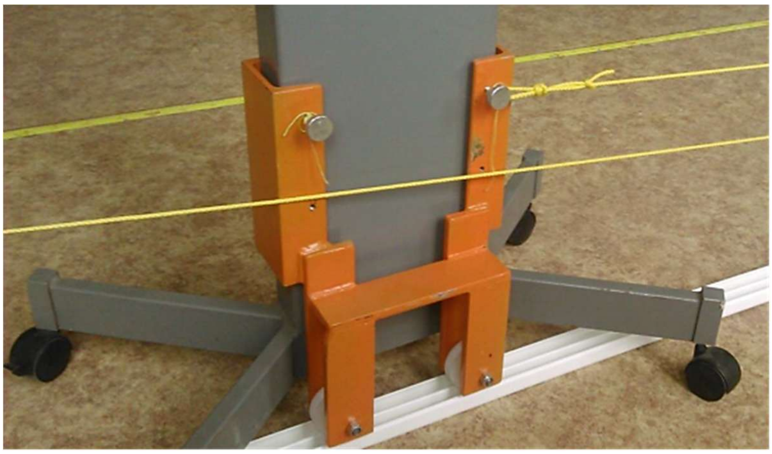

Fig. 90 Antenna-system carriage (undercarriage)

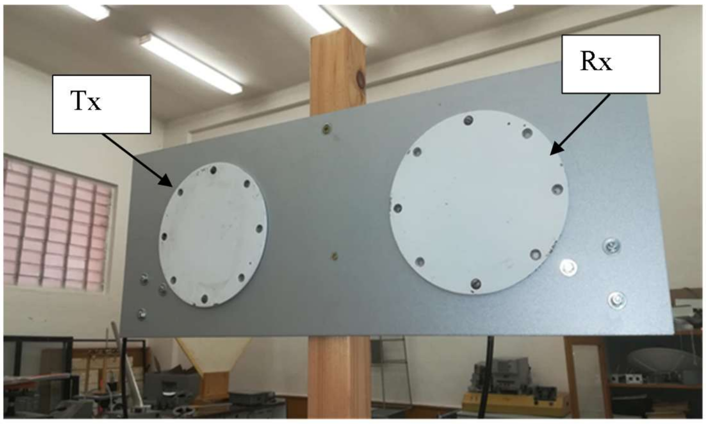

Fig. 91 Radio altimeter receive and transmit antennas

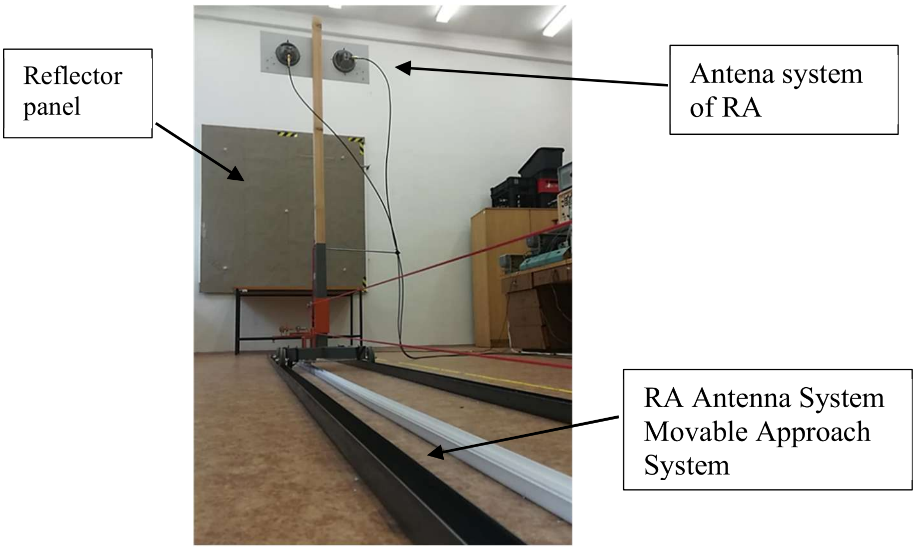

Fig. 92 Antenna-system guide rails and the depolarizing panel

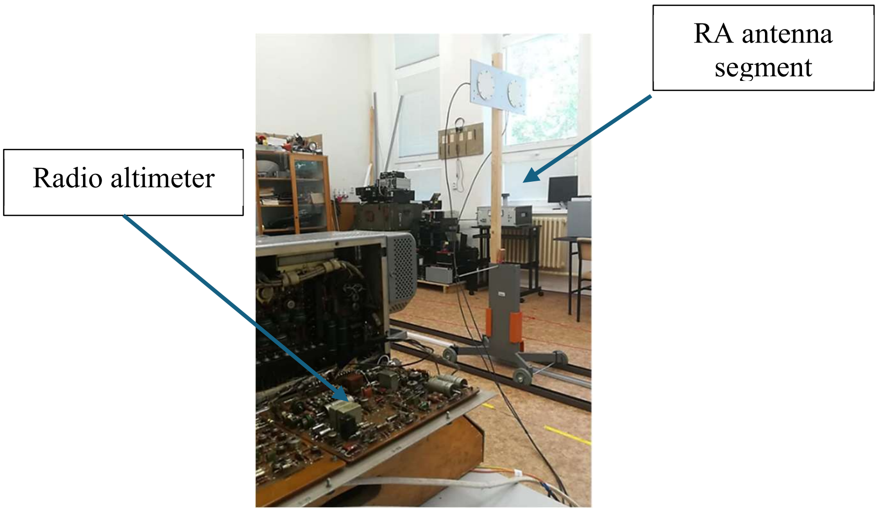

Fig. 93 View of the “experimental” radio altimeter and its antennas

Test-bench control and data acquisition

Because the entire test bench has to be electronically controlled—both the drive system and the acquisition of measured data—it was necessary to design the electrical interconnections between the individual subsystems. The overall electrical system consists of two parts: the electrical drive subsystem and the electrical measurement and data-logging subsystem. LabVIEW was used for test-bench control, data display, and data recording. Using this graphical programming environment, the motion mechanism can also be controlled. The radio altimeter is connected to the PC via a DAQ (data acquisition) converter, which converts the measured voltage taken from the RV-5 radio altimeter into a digital signal. However, the DAQ converter accepts a maximum input of ±10 V, whereas the radio altimeter output is in the form of a voltage of up to ±30 V. For this reason, resistive voltage dividers had to be inserted in the input leads to the converter to prevent damage. Test-bench control, data acquisition, and storage of measured data are implemented using a personal computer and a control application running on the LabVIEW platform. Within this platform, a virtual control panel is created that controls the electric motor driving the antenna motion, senses the antenna position using an optical gate at the terminal turning point and end switches, controls the direction and speed of antenna-system motion thus simulating a dynamic change in height as measured by the radio altimeter. At the same time, it starts and stops the recording of measured data obtained from the radio altimeter (modulation frequency and beat/difference frequency) as well as the antenna-system distance from the reflecting depolarizing wall.

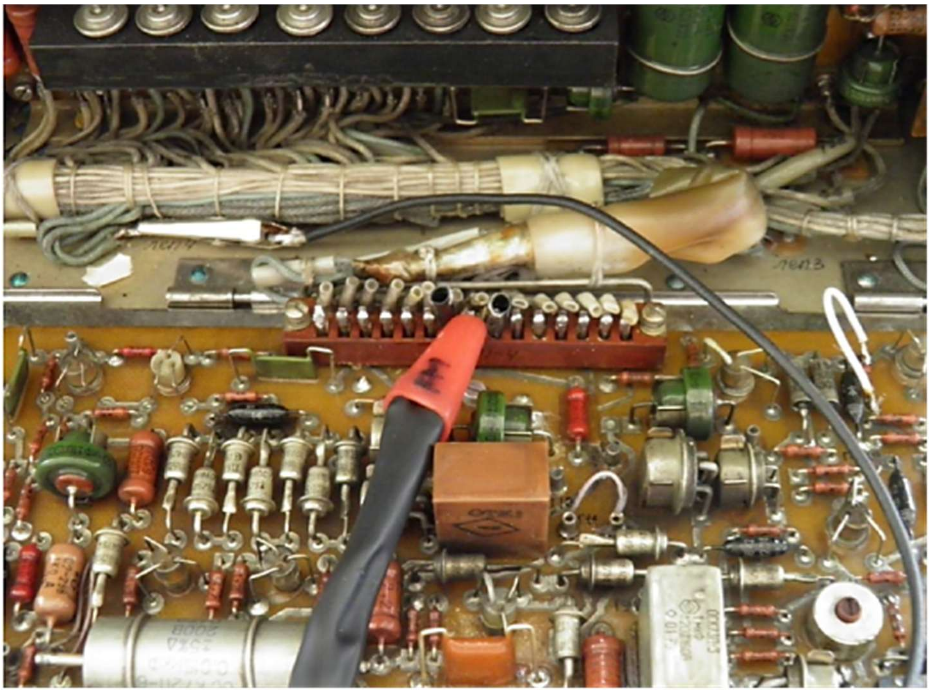

Fig. 94 Connection of the probe for measuring the method error of FMCW radio altimeters

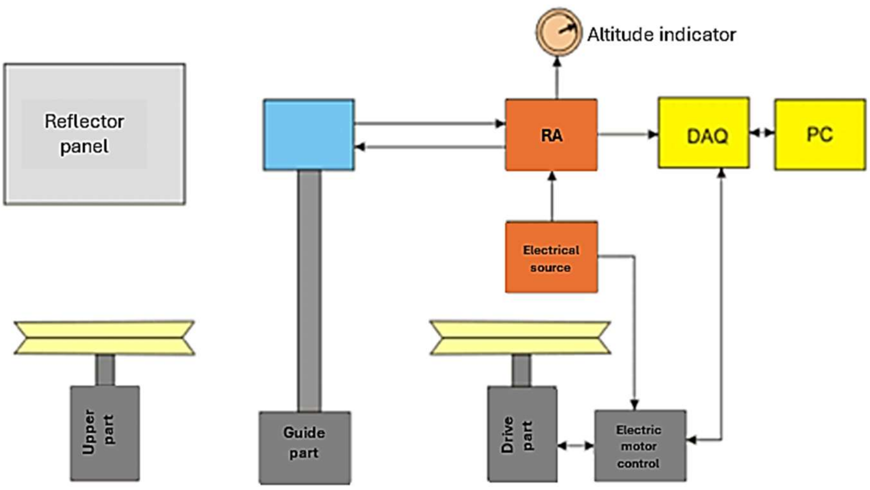

Fig. 95 Block diagram of the test bench for measuring the method error of radio altimeters

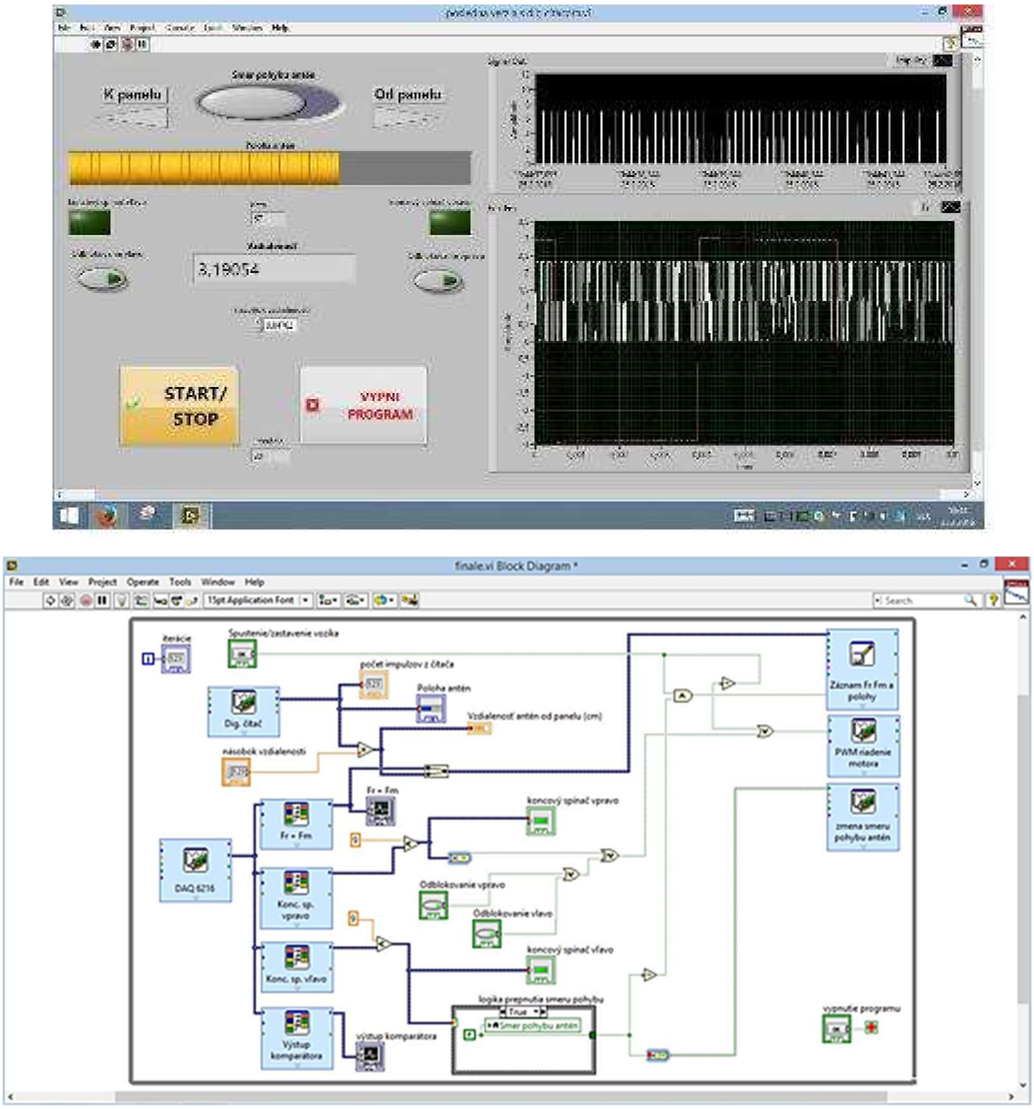

Fig. 96 User interface and block diagram of the program for measuring the method error of RA

8.3 Analysis of radio-altimeter method-error measurements

From the perspective of qualitative evaluation of the height-measurement accuracy of airborne radio altimeters, it is essential to know the method error. The method error of a radio altimeter is the most important parameter, and its value is defined by the manufacturer already during the design phase.

After long-term operation of a radio altimeter, or after fault rectification, its height-measurement accuracy is typically assessed only in a static mode at several predefined discrete heights using calibrated test equipment. This static method is commonly applied to all types of radio altimeters because, until now, dynamic height measurement under laboratory conditions has not been feasible. There are certain possibilities for measuring height during flight, but only on specially modified experimental aircraft operated by aviation authorities or manufacturing facilities. Under laboratory conditions, continuous height measurement over a wider height range could only be achieved by progressively changing height in discrete steps by varying the length of the RF coaxial line. In this way, the RF signal path present in real flight conditions—aircraft–ground–aircraft—was replaced by a dedicated set of coaxial cables. In any case, however, this did not represent a dynamic height change, but rather discrete, static, incremental height measurements over a certain altitude range with a defined step size. The outcome of this measurement approach is shown in Fig. 60. Such conventional measurements allow only an approximate evaluation of the radio altimeter method error, because it is not possible to capture the formation of combinations of stable and unstable pulses that determine the method error of a radio altimeter.

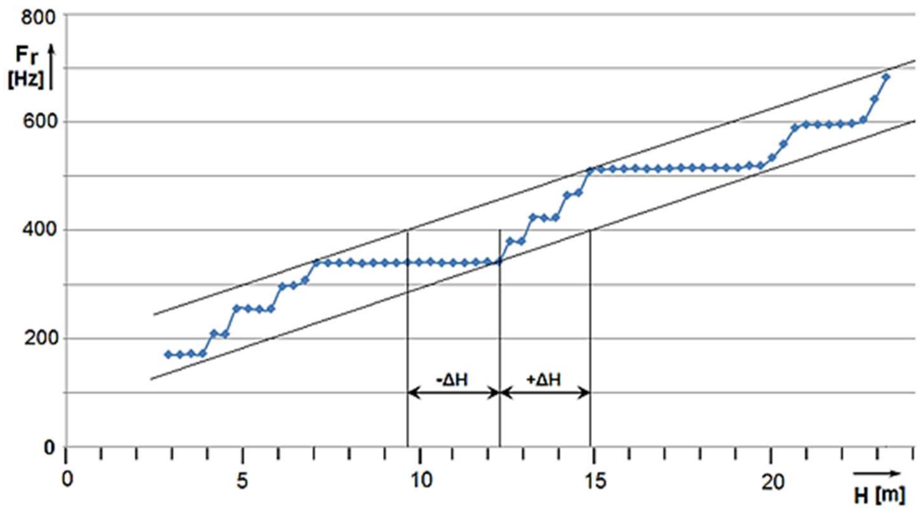

Fig. 97 Measurements using the conventional method

In Fig. 97, the measured results can be used to evaluate the method error $\pm\Delta H$ of the RVUM radio altimeter obtained by the conventional approach employing coaxial cables. If a measured height of 12.3 m is considered, then the value $+\Delta H$ corresponds to the height level of 14.9 m and the value $-\Delta H$ corresponds to the height level of 9.7 m.

In this case, the method error measured and evaluated by the conventional approach is $\pm\Delta H = \pm 2.6$ m, whereas— as is generally known—the RV-UM radio altimeter should have a method error of $\pm\Delta H = \pm 2.2$ m. From the results obtained by the conventional method, it is not possible to determine whether this discrepancy is caused by the measurement/evaluation method used to assess the radio-altimeter method error, or whether the radio altimeter itself is inaccurate. In any case, although this simple method has certain advantages, it cannot be used to demonstrate the theoretical conclusions regarding radio-altimeter operation, i.e., the discrete appearance and disappearance of stable and unstable height pulses. In addition, the use of coaxial cables results in repeated interruptions of the RF signal path between the transmitter and the receiver during the measurement. This abrupt change in transmitter load can lead to transmitter damage; therefore, the method cannot be applied to every type of radio altimeter. Furthermore, height measurement requires a coaxial cable of twice the length of the measured height, because a coaxial cable does not emulate the reflection from the ground.

For these reasons, an alternative method for measuring the radio-altimeter method error was developed to provide higher accuracy, broader applicability, and to eliminate the limitations of the existing approaches. As part of research activities at the Department of Avionics, a patented depolarizing panel was developed for measuring antenna directional characteristics; it was subsequently found that this panel could also be used for height (range) measurements in an enclosed space. The panel enables range measurement via an RF path, i.e., using a conventional TEM electromagnetic field generated by the transmit antenna and, after reflection from the panel, processed by the receive antenna.

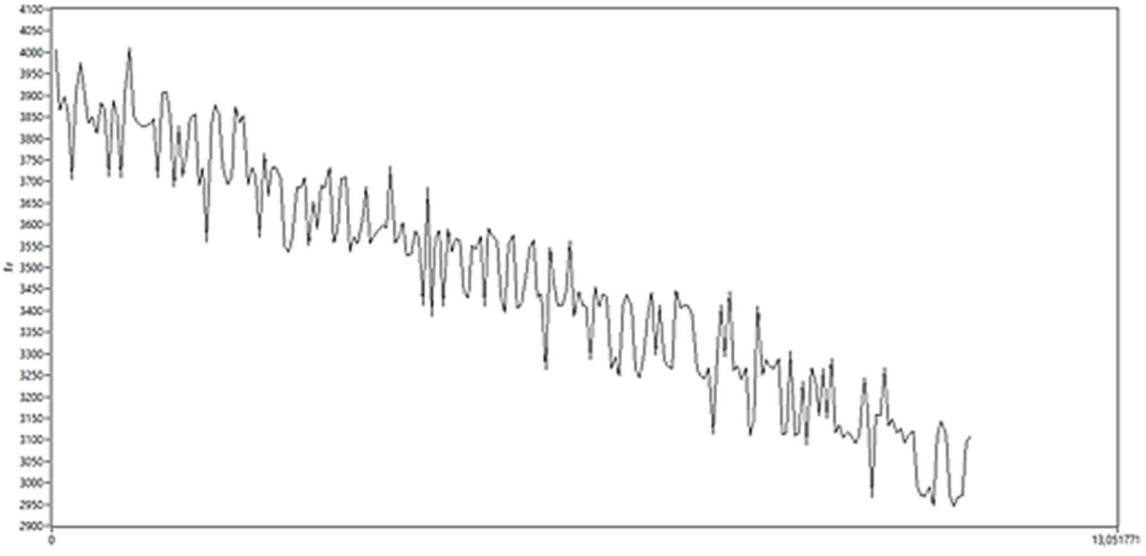

Fig. 98 Rapid measurements on the RV-5 using the patented method

As part of the research, experimental measurements were carried out using this method on the RV-5 radio altimeter, which is a newer-generation radio altimeter with a height-measurement accuracy of $\pm\Delta H = \pm 0.75$ m. The first measurement results are shown in Fig. 61. These results are far more convincing than in the previous case; however, the method error is still not clearly discernible. It was later determined that this was due to an improperly selected rate of dynamic height change during the automated measurement. A subsequent measurement performed at an appropriate speed captured a more detailed variation of the beat (difference) frequency during dynamic height changes. As a result, the contours of the “steps” appeared in the final plot, which is the fundamental signature of radio-altimeter method error. In addition to the basic height-dependent beat-frequency trace, the measurement output also contains a series of narrow interference spikes. The source of these interference spikes is the surrounding laboratory environment in which the radio altimeter evaluates the measured height. In the patented measurement method, the reflection from the depolarizing panel is used. The radio altimeter tracks this dominant reflection, from which the staircase-shaped method-error characteristic is obtained. However, during dynamic changes in antenna height, it is not possible to prevent parasitic reflections from surrounding walls and other metallic objects from reaching the receiver. Their distances from the antennas are typically greater or smaller than the distance to the depolarizing panel, and therefore, at certain instants, a larger or smaller number of height pulses is produced. This effect generates the interference spikes in the measured plot. Their number is then either greater or smaller than would correspond to the actual measured height.

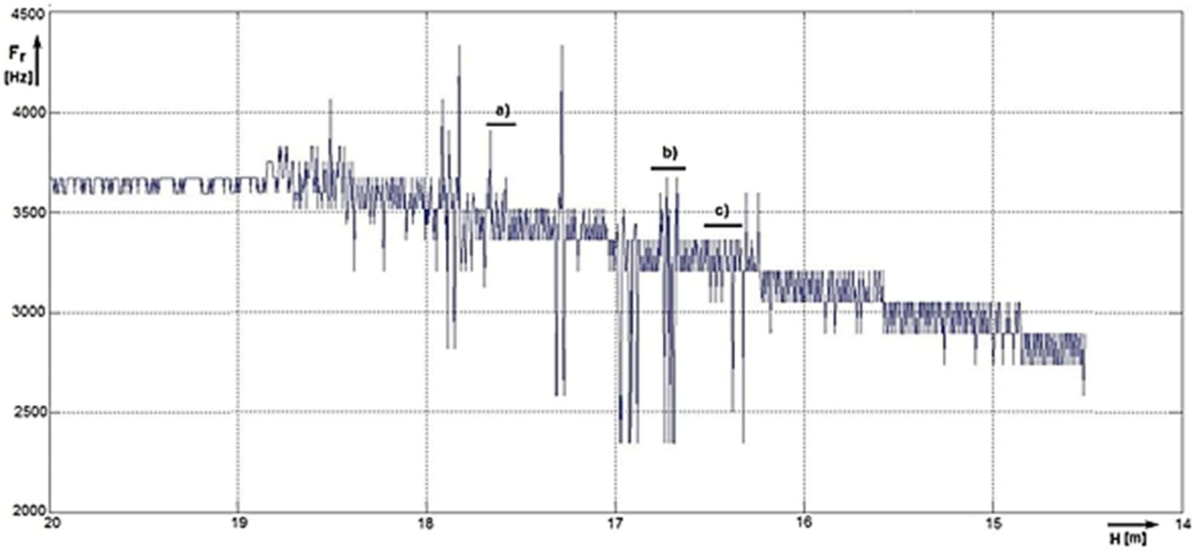

Fig. 99 Slow measurements on the RV-5 using the patented method

In Fig. 99, the height-pulse train contains very narrow interference height pulses, which are a concomitant effect observed when measuring the radio-altimeter method-error characteristic. These are manifestations of spurious height-related signals that undesirably contaminate the final method-error measurement plot. Three representative samples of such interference pulses are marked as [a), b), c)].

The three selected samples of interference height pulses are:

a) interference height pulses reflected from a greater distance than the measured height,

b) interference pulses simultaneously reflected from both a greater and a smaller distance than the measured height,

c) interference height pulses reflected from a smaller distance than the measured height.

Such interference height pulses cannot be removed by filtering (i.e., by a software-based approach), because they are part of the actual measured results not in the time domain but in the height domain. Suppression of this type of interference would require a dedicated investigation.

Figure 100 shows, side by side, three short segments [a), b), c)] representing different types of interference height pulses. These segments were extracted from the plot and inserted into a separate. All three pulse types are "aligned" at a frequency of 3500 Hz in Fig.100 to enable direct comparison of the frequency values of the interference height pulses. These pulses adversely affect the method-error measurement results, with each type influencing the outcome in a different way.

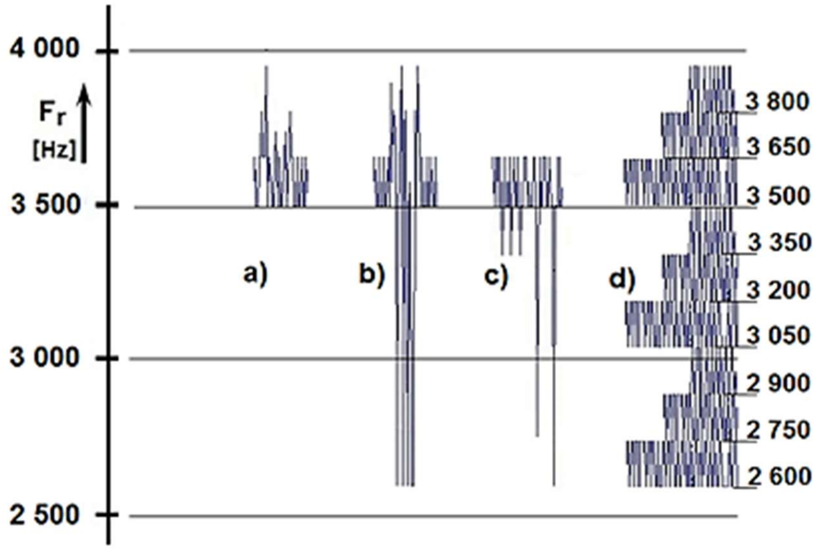

Fig. 100 Types of interference height pulses observed during measurement

Each of the three selected interference-signal traces in Fig. 63 contains several spurious signals.

Trace 100 a) represents interference height pulses generated by a parasitic reflection from a greater distance than the actual measured height.

If the nominal measured height corresponds to a radio-altimeter beat frequency cantered at 3500 Hz, then in this case it is contaminated by five interference signals (pulses) with a higher beat-frequency value, as follows:

- *four interference signals with a frequency 150 Hz higher, i.e., 3650 Hz,*
- *one interference signal with a frequency 300 Hz higher, i.e., 3800 Hz.*

Trace 100 b) represents interference height pulses generated by parasitic reflections both from a greater distance and from a smaller distance than the actual measured height. If the nominal measured height corresponds to a radio-altimeter beat frequency cantered at 3500 Hz, then:

- on the higher beat-frequency side, it is contaminated by a total of six interference signals (pulses) with higher beat-frequency values, as follows:
    - *three interference signals with a frequency 150 Hz higher, i.e., 3650 Hz,*
    - *three interference signals with a frequency 300 Hz higher, i.e., 3800 Hz;*
- on the lower beat-frequency side, it is contaminated by a total of six interference signals (pulses) with lower beat-frequency values, as follows:
    - *four interference signals with a frequency 900 Hz lower, i.e., 2660 Hz.*

Trace 100 c) represents interference height pulses generated by a parasitic reflection from a smaller distance than the actual measured height. If the nominal measured height corresponds to a radio-altimeter beat frequency cantered at 3500 Hz, then in this case it is contaminated by five interference signals (pulses) with lower beat-frequency values, as follows:

- *three interference signals with a frequency 150 Hz lower, i.e., 3350 Hz,*
- *one interference signal with a frequency 750 Hz lower, i.e., 2750 Hz,*
- *one interference signal with a frequency 900 Hz lower, i.e., 2600 Hz.*

Trace 100 d) is only an artificial illustration of the magnitude of discrete beat-frequency changes in 150 Hz steps. From individual beat-frequency “packs,” discrete values—i.e., beat-frequency “floors/levels”—are formed, making it possible to see which frequency “levels” are reached by the interfering beat-frequency values.

To evaluate the radio-altimeter method error from measured data using the presented new patented method, it is necessary to remove the parasitic reflections described above. At present, their suppression can only be achieved by simple removal from the plotted trace. This manipulation is enabled by the discrete and unambiguous values of the interfering beat-frequency signals, as described above. After their removal (filtering), a clean beat-frequency trace is obtained, in which the staircase-like progression of the measured values is clearly visible (Fig. 101).

The practical measurement results of the beat frequency obtained during dynamic height changes provide an objective basis for evaluating the radio-altimeter method error.

A dynamic height-change profile created by real measurement under standard laboratory conditions had not previously been achievable. Such a truly measured trace (Fig. 102) has not, to the best of our knowledge, been published in accessible international literature; only simulation results or other forms of mathematical interpretation of the problem have been presented. It is therefore an original, breakthrough record that may significantly advance the objective evaluation of height-measurement accuracy of airborne radio altimeters.

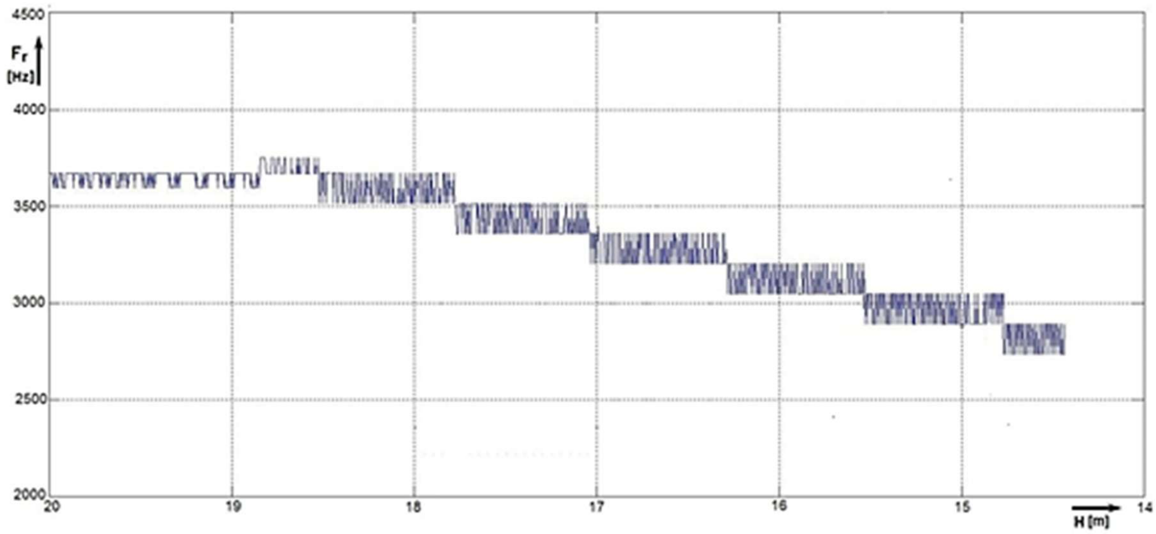

Fig. 101 Filtering out interference pulses in RV-5 measurements using the patented method

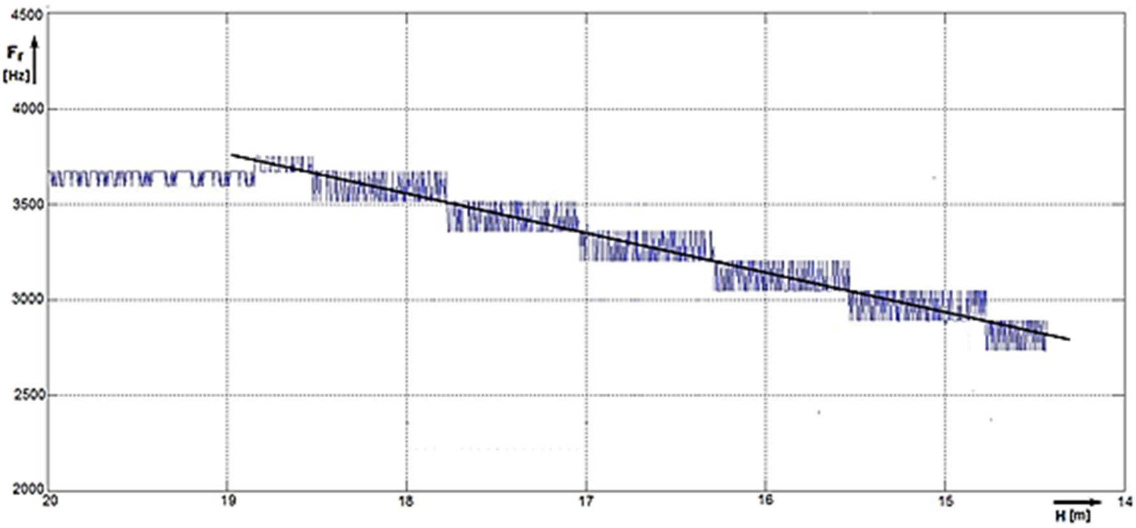

Fig. 102 Linear dependence of RV-5 measurements using the patented method

The description of the measurement results so far has focused only on confirming the obtained measurement outcomes and on the way they are visualized and interpreted from their graphical representation.

Next, attention is directed to what information can be extracted from this plotted trace. By simply fitting a straight line to the staircase-shaped characteristic (Fig. 102), it is possible to assess the extent to which the height-measurement response is linear. This is an important indicator of height-measurement accuracy, particularly at low heights during the approach-to-land phase and during touchdown itself.
Another - and the most significant - measurement outcome is the ability to evaluate the critical height ΔH of the radio altimeter under test as the key parameter for determining the method error $\pm\Delta H$ of the radio altimeter (Fig. 103). This parameter defines the objective height-measurement accuracy of airborne radio altimeters. At present, this measurement accuracy is derived from theoretical considerations, and it is assumed that it is measured in some manner at the manufacturing facility. Once the radio altimeter enters service, the only objective verification of height-measurement accuracy is typically possible only at a single discrete height using a coaxial cable. Measurement of a radio altimeter using an RF path via electromagnetic-wave propagation is currently not possible.

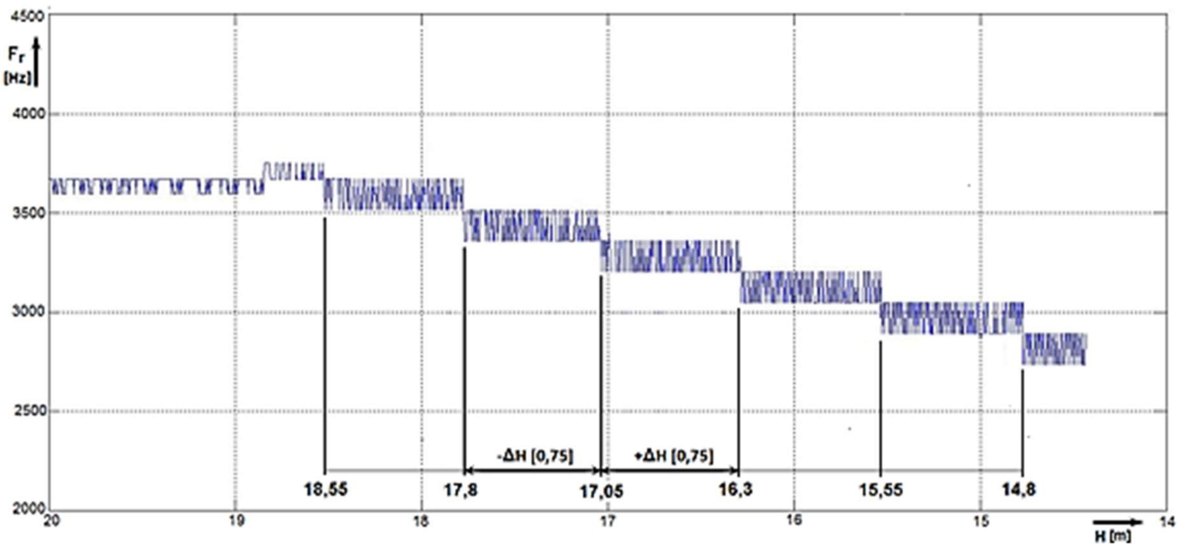

Fig. 103 RV-5 method error evaluated using the patented measurement method

Figure 103 shows the height-measurement trace obtained on the RV-5 radio altimeter. This is a radio altimeter operating with parameters comparable to those of current modern radio-altimeter types:

- *operating carrier frequency* $f_0 = 4.4$ *GHz,*
- *frequency sweep* $\pm\Delta f = 25$ *MHz,*
- *modulation frequency* $f_M = 150$ *Hz,*
- *height-measurement accuracy* $\pm\Delta H = \pm 0.75$ *m.*

By graphically processing the measured results in Fig. 103 - specifically by evaluating the critical height ΔH—the method error of this radio altimeter can also be determined as $\pm\Delta H = \pm 0.75$ m. Based on the measured data, it can be stated that the radio altimeter under test meets the specified height-measurement accuracy requirement of ± 0.75 m within the defined range.

For the above radio altimeter, measurements were performed over a height (range) interval of 4 m, i.e., from 18.5 m down to 14.5 m. This measurement span was dictated by the technical constraints of the laboratory environment. Although this is a height measurement, the actual change in distance between the radio-altimeter antennas and the reflecting panel—representing the ground surface—was implemented in the horizontal plane. From this perspective, the height measurement was effectively realized as a distance (range) measurement. The distance measurement was performed in a descending direction, i.e., the range decreased, and the measurement thus simulated aircraft descent. From the measurement results, $5+\frac{1}{3}$ (Fig. 104) critical height intervals ΔH were obtained $(5\times 0.75+0.25=4\,\mathrm{m})$. Within the experimental campaign, a second measurement was also performed on the same radio altimeter, over a height/range interval of 4.8 m, i.e., from 6.4 m to 11.2 m. In this case, the distance measurement was performed in an ascending direction, i.e., the range increased. From these measurement results, $6+\frac{1}{3}$ (Fig. 104) critical height intervals ΔH were obtained $(6\times 0.75+0.3=4.8\,\mathrm{m})$.

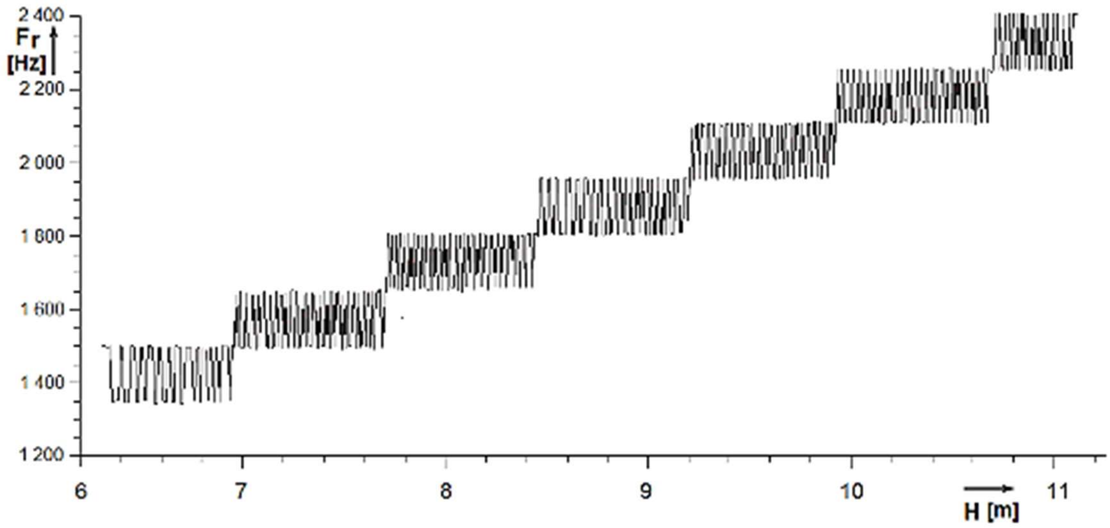

Fig. 104 Ascending RV measurements using the new patented method

Subsequently, the second measurement performed on the same radio altimeter had a more verification-oriented character, intended to confirm that the measurement results are reciprocal even though the measurement was carried out in a different manner, i.e., it simulated aircraft climb.

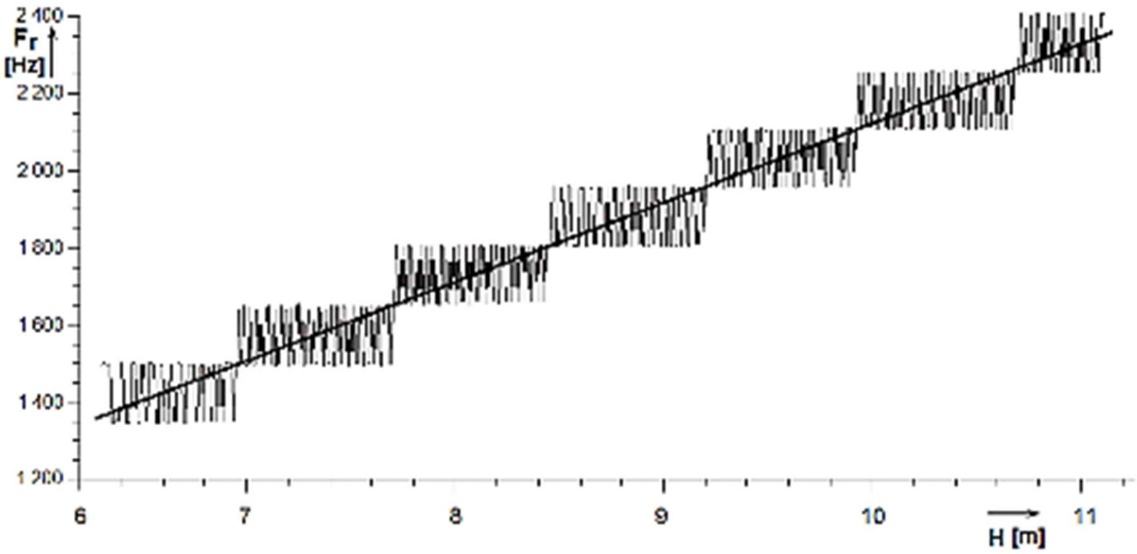

Fig. 105 Linear dependence of the ascending height measuremen
using the patented method

In Fig. 105, the linearity of the height-response measurement is again assessed by fitting a straight line to the staircase-shaped characteristic. From the figure, it can be concluded that the height-measurement response is linear also in this case. This is an important indicator of height-measurement accuracy at low heights—here, above the runway (RWY) during the take-off phase. The second evaluated parameter is the critical height ΔH obtained when measuring the same radio altimeter. This represents the key parameter used to determine the method error $\pm\Delta H$ from Fig. 106. In this case as well, the measurement produced satisfactory results, which means that the method error did not change during the simulated aircraft climb.

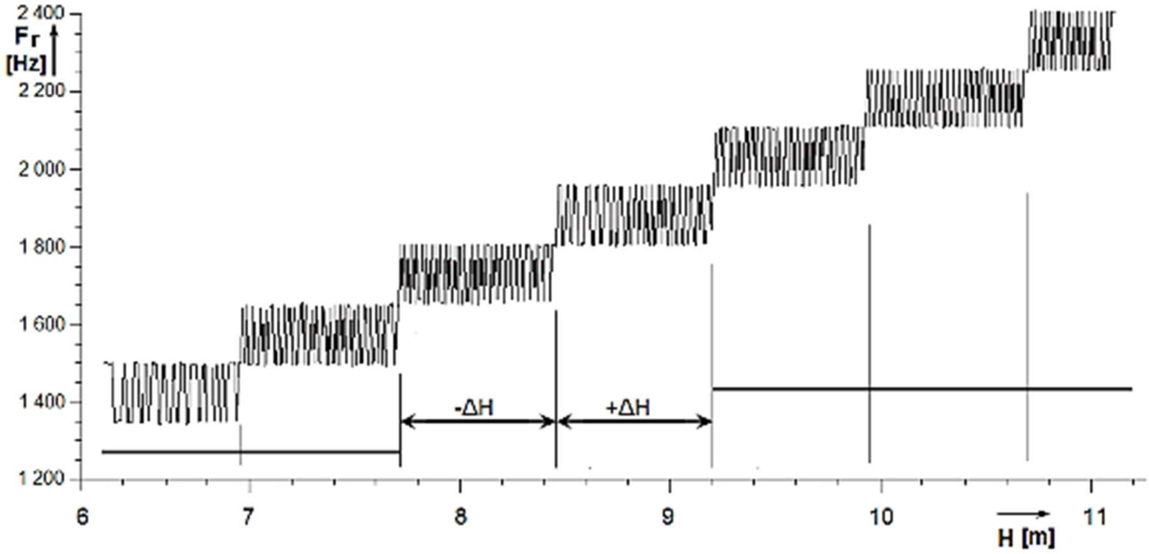

Fig. 106 Radio-altimeter method error evaluated from the ascending height measurement

By evaluating these two radio-altimeter measurement parameters—namely, the linearity of the response and the method-error value—it is possible to assess, in the most objective manner, the measurement accuracy, technical condition, and overall quality of the radio altimeter. Both parameters can be combined into a single graph (Fig. 107).

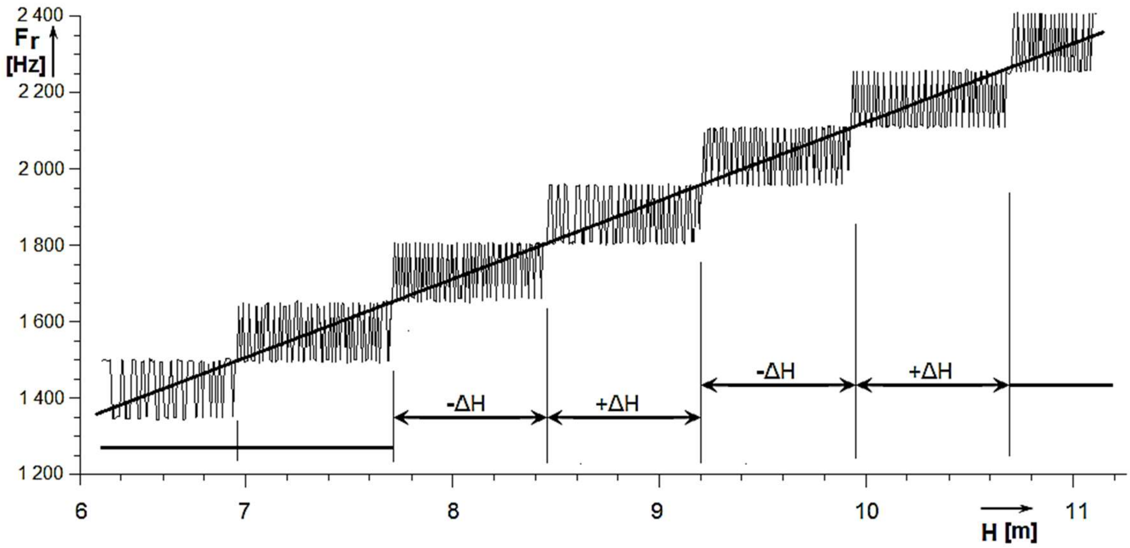

Fig. 107 Height-measurement accuracy evaluated using the new patented method

Such a plot can be viewed as a kind of quasi "X-ray image" of the radio altimeter, in which any inaccuracy in the setting of its parameters or any imperfection in the operation of a particular circuit can be detected. If the radio altimeter exhibits even a minor deviation from the required parameters in any respect, the beat-frequency growth characteristic will not be linear and, in terms of method error, it will not be symmetrical. Using this sophisticated yet straightforward approach, it is possible to compare qualitative indicators not only among units of the same radio-altimeter type, but also across different radio-altimeter types.

9 CONCLUSIONS

Since the changes in former Eastern Europe in 1989 and 1990, new trends in regulating production processes and evaluating machines, production processes, and gauges have now impacted our society. In some cases, it has been the result of customer demand and in other cases, it has been to attain a prestigious level, which these methods have certainly facilitated. It is impossible to deal precisely with the analysis of production processes based on the information provided by these methods. It is essential to acknowledge that enhancing the capacity of manufacturing processes, machines, and measuring devices is an economic category, including expensive new machines, active gauges, computer-supported production processes, software equipment, and staff training. A problem may occur when we lack the means to implement, even when we know what we want and need. However, these investments are returned swiftly and therefore, it is profitable to invest in this field. These savings will be prevalent across all domains: This includes savings in the financial area, staff, and material cost due to fewer rejects, and other operational areas. However, the result will also appear in the domain that cannot be purchased but still has a high resale value. The company's image has been growing rapidly in the eyes of its customers. The customer can greatly appreciate it when preventive measures and methods replace the classic final control, which enables high-quality product production rather than control.

The designated goals that we had established prior to the onset of practical implementation in the particular conditions of the unnamed production company have been achieved. For the first time in the history of this company, the production processes, machines, and measuring devices have been evaluated using methods that a serious customer, such as the automotive industry, can easily comprehend. Spatial has been implemented for all production operations to regulate the manufacturing processes, machines, and gauges capabilities. In this manner, we have acquired and will continue to obtain numerous records for conducting a thorough examination of processes, machines and gauges that were previously unavailable.

The monograph has expanded the area of knowledge on the specific manufacturing processes, machines, and measuring devices. Further analysis is now possible, leading to better quality and more sophisticated products, including bearings in the engineering industry.

10 REFERENCES

[1] Labun J.: Vplyv pásma otočenia fázy na presnosť merania výšky u rádiovýškomerov s frekvenčnou moduláciou, PGŠ, ČVUT, Praha, 1989.

[2] Labun J.: Analýza chýb rádiovýškomerov malých výšok, RS, VLA, Košice, 1996.

[3] Labun J.: Zvýšenie presnosti merania malých výšok u leteckých rádiovýškomerov, KDP, VLA, Košice, 1998.

[3] Odincov B. A.: Rádionavigacija letateľnych apparatov, Mašinostrojenie, Moskva, 1968.

[4] Pečinka R.: Letecké rádionavigační systémy, LaK, Radar č. 16, 1996.

[5] Powell J.: Aircraft radio systems, USA, 1981.

[6] Labun J.,: Zvýšenie presnosti merania malých výšok u leteckých rádiovýškomerov. Košice 1998

[7] Labun J.: Analýza chýb rádiovýškomerov malých výšok. Košice 1996

[8] Beneš L.: Učebnice pro piloty vrtuľníku, Bratislava 1985, ALFA n.p. Bratislava

[9] Vejražka F, Vičan M.: Aerodynamika, konstrukce a systémy letadel, Brno 2004, CERM s.r.o.,

[10] Kurdel, P.; Češkovič, M.; Gecejová, N.; Labun, J.; Gamec, J.: The Method of Evaluation of Radio Altimeter Methodological Error in Laboratory Environment. Sensors 22(14), 5394 (2022)

[11] Labun, J.; Kurdel, P.: Radar-altimeter in the Function of Anticollision System. Deutscher Luft- und Raumfahrtkongress (2010)

[12] Češkovič, M.; Kurdel, P.; Gecejová, N.; Labun, J.; Laššák, M.: Evaluation of Doppler Effect Error Affecting the Radio Altimeter Altitude Measurements. Sensors 23(1), 177 (2023)

[13] Pečinka, R.: Letecké rádionavigační systémy. LaK, Radar č. 16 (1996).

[14] Prokop, V., Vokurka, J.: Šíření elektromagnetických vln a antény. SNTL/ALFA, Praha (1982).

[15] Hoggan, D.: Challenges, Strategies, and Tools for Research Scientists. Electron. J. Acad. Spec. [16] Librariansh. 3(3) (2002).

[17] Kurdel, P.: Helicopter accidents statistics. HAI Magazine ROTOR (2010).

[18] GEC-Marconi: Technical Documentation for Aircraft Altimeters. UK.

[19] Honeywell: Technical Specifications for Altitude Sensors. USA.
[20] Collins Radio Co.: Operating Principles of Pulse Radio Altimeters. USA.
[21] TRT/Thomson-CSF: AHV series radio altimeters manual. France.
[22] Canadian Marconi: CMA series airborne systems documentation. Canada.
[23] Bendix/King: KRA series radio altimeter specifications. USA.
[24] Smiths Industries Aerospace: RA 3000 series technical manual. UK.
[25] Teledyne Ryan Electronics: Frequency modulation altimetry systems. USA.
[26] MATLAB. (2023). *version 9.15.0 (R2023b)*. Natick, Massachusetts: The MathWorks, Inc.
[27] Moir, I., Seabridge, A.: *Civil Avionics Systems*. Wiley-IEEE Press, Chichester (2013)
[28] Spitzer, C.R., Spitzer, C.R., Ferrell, U., Ferrell, T.: *Digital Avionics Handbook*. CRC Press, Boca Raton (2014)
[29] Collinson, R.P.G.: *Introduction to Avionics Systems*. Springer, Dordrecht (2011)
[30] Tooley, M.: *Aircraft Communications and Navigation Systems*. Routledge, London (2017)
[31] Helfrick, A.: *Principles of Modern Avionics*. Avionics Communications Inc., Leesburg (2010)
[32] Kayton, M., Fried, W.R.: *Avionics Navigation Systems*. John Wiley & Sons, New York (1997) –
[33] RTCA DO-178C: *Software Considerations in Airborne Systems and Equipment Certification*.
[34] RTCA Inc., Washington (2011)
[35] RTCA DO-254: *Design Assurance Guidance for Airborne Electronic Hardware*. RTCA Inc., Washington (2000)
[36] SAE ARP4754A: *Guidelines for Development of Civil Aircraft and Systems*. SAE International, Warrendale (2010)
[37] Rushby, J.: *Formal Methods and Digital Systems Validation for Airborne Systems*. NASA Contractor Report, Langley Research Center (1993)

[38] Watkins, C.B., Walter, R.: *Transitioning from Federated Avionics Subsystems to Integrated Modular Avionics*. In: IEEE/AIAA 26th Digital Avionics Systems Conference (2007)

[39] ARINC 664P7: *Aircraft Data Network, Part 7: Deterministic Networks*. Aeronautical Radio Inc., Annapolis (2009) – *Základ pre AFDX protokoly.*

[40] Gaska, T., Gaska, J.: *Next Generation Integrated Modular Avionics*. In: 30th Digital Avionics Systems Conference (DASC) (2011)

[41] Biniet, P., et al.: *AFDX and Ethernet: The New Standard for On-board Networks*. In: International Journal of Computer Science (2012)

[42] McLean, D.: *Automatic Flight Control Systems*. Prentice Hall, New York (1990)

[43] Pratt, R.: *Flight Control Systems: Practical Issues in Design and Implementation*. Institution of Engineering and Technology, London (2000)

[44] Stevens, B.L., Lewis, F.L., Johnson, E.N.: *Aircraft Control and Simulation: Dynamics, Controls Design, and Autonomous Systems*. Wiley, Hoboken (2015)

[45] Sampigethaya, K., et al.: *Future Arinc 811: Communication, Security and Network Management*. IEEE Aerospace and Electronic Systems Magazine (2011)

[46] Kurd, Z., Kelly, T.P.: *Establishing Safety Arguments for Artificial Neural Networks in Product Certification*. Springer, Berlin (2007)

[47] Lykou, G., Gritzalis, D.: *A Cyber-Security Risk Assessment Strategy for Modern Aviation*. In: International Conference on Critical Infrastructure Protection (2016)

Applied Technologies of FMCW Radio Altimeters
for Next-Generation Aviation and Automotive Systems

Pavol Kurdel, Marek Češkovič, Anton Panda

Edition of scientific and technical literature: Monograph

Authors: prof.Ing. Pavol Kurdel, PhD.
assoc.prof. Ing. Marek Češkovič, PhD.
Dr.h.c.,prof. Ing. Anton Panda, PhD.

Title: Applied Technologies of FMCW Radio Altimeters
for Next-Generation Aviation and Automotive Systems

Year of publication: 2026

Edition: Fist edition

Number of pages: 160

Publisher: RAM-Verlag

ISBN 978-3-96595-57-3

Authors:

***Pavol Kurdel,* Prof., Ing., PhD.:** University studies – Faculty of Aeronautics of Technical University of Košice (PhD. - 2011 and associate professor of study branch electronics). 18 – years of experience in military forces as technician of radiotechnology aviation systems. Since 2011 operates as pedagogue and scientist at the Faculty Aerospace TU Košice. He is the author (co-author) of 2 monographs, 5 university lecture notes, patents and discoveries (3), several domestic and foreign original scientific papers in scientific and professional journals, in impact factored. Current Contents Connect journals of WoS (33). Solver of several research projects and grant projects.

***Marek Češkovič,* Assoc.prof. Ing., PhD**.: University studies – Faculty of Aeronautics of Technical University of Košice (PhD.-2014); 12 – years of experience as a member of research team of the laboratories of Aircraft antenna measurements and Laboratory of Intelligent Control Systems of Aircraft Engines (LIRSLM). Since 2014 works as pedagogue and scientist at the Faculty of Aeronautics of TU Košice. He is the author (co-author) of 2 monographs, 3 university lecture notes, patents and discoveries (3), several domestic and foreign original scientific papers in the scientific and professional journals, in impact factored Current Contents Connect journals of WoS (13). Solver of several research projects and grant projects.

Anton Panda, Dr.h.c. prof. Ing., PhD.: University studies – Faculty of Mechanical Engineering TU Košice (Ing.-1987); terminated doctoral studies –Faculty of manufacturing technologies TU Košice (PhD.-2002), associate professor of study branch 5.2.51 manufacturing technologies, FMT TU Košice (assoc. prof.-2008), professor of study branch 5.2.51 manufacturing technologies, FMT TU Košice (prof.-2015). 29 – years of experience in the engineering company supplying the products for demanding automotive, also farm and agricultural industry (constructor of special purpose machinery and equipment, systems analyst, head the department of development and technical preparation of production, methodist of statistical methods, commercial and technical director, director of quality). In the present expertise and design activities in the area of development, production and verification of rolling bearings, in the area of deposition with rolling bearings for various domestic and foreign customers. Since 2008 (since 1994 external) operates as pedagogue and scientist at the faculty of manufacturing technologies TU Košice with the seat in Prešov, as well as an expert - coordinator (auditor) of quality management systems. He is the author (co-author) of 17 monographs (11 foreign, 6 domestic) – of it 3 monograph in Springer publishing, 2 university textbooks (1 foreign, 1 domestic), 16 university lecture notes, author's certificates (16), patents and discoveries (15), catalogs of bearings (2), several domestic and foreign original scientific papers in the scientific and professional journals, in Current Contents Connect journals in Web of Science (21), in impacted journals and publications led in the world renowned databases (Web of Science - 117, Scopus - 148) and in proceedings from domestic and foreign scientific conferences from the following areas: Automobile production, manufacturing technologies, experimental methods in the manufacturing technologies, machining, development, manufacturing and verific-ation of new products in accordance with the standards EN ISO 9001 and in accordance to the specific requirements of automobile manufacturers IATF 16 949, quality control, statistical methods and techniques of quality for the production of parts, capability of machine, capability of manufacturing processes, capability of gauges and measuring equipment, technical preparation of production, product audits, system audits of quality management system, analysis of potential errors and their effects on construction (FMEA-K) and on manufacturing process/technology (FMEA-V), statistical regulation of manufacturing processes SPC, process of approval of parts to the production PPAP, modern quality planning of product APQP, control plans and regulation, requirements the association of automobile manufacturers in Germany VDA 6.1, quality system requirements for suppliers of Ford, Chrysler, GM, specific requirements the using of EN ISO 9001:2015 inorganizations ensuring the mass production in automotive industry IATF 16949, method of Poka-Yoke, quality assurance before the mass production for suppliers of automobile manufacturers in Germany VDA 4.3, quality assurance of supplies for suppliers of automobile manufacturers in Germany VDA 2, product liability, method of Global 8D (8-step method for solving of problems), etc. At these works are registered the various domestic and foreign quotations and testimonials in the worldwide databases. He is auditor of quality system management on TU Košice, Slovakia. Active collaboration with the university workplaces at home and abroad. He is recognized as an expert for the production of bearings in companies in Germany, Italy, China, Slovakia and Czech Republic. As the coordinator of research collective and co-author of documentation EFQM has won the Award for improvement of performance in the competition National award of Slovak Republic for quality in the year 2010 for the TU Košice. In the same competition, he has won the same award in year 2012, when the TU Košice has obtained the highest score in its category. Since 2014 he has a member of the Polish Academy of Sciences. Since 2014 he has been a member of ASME, USA.